The Statistical Fingerprints of Quantum Gravity

by:

Mohammad H. Ansari

A thesis
presented to the University of Waterloo
in fulfilment of the
thesis requirement for the degree of
Doctor of Philosophy
in
Physics

Waterloo, Ontario, Canada, 2008

I hereby declare that I am the sole author of this thesis. This is a true copy of the thesis, including any required final revisions, as accepted by my examiners.

I understand that my thesis may be made electronically available to the public.

Abstract

In this thesis some equilibrium and non-equilibrium statistical methods are implied on two different versions of non-perturbative quantum gravity.

Firstly, we report a novel statistical mechanics in which a class of evolutionary maps act on trivalent spin network in randomly chosen initial states and give rise to Self-organized Criticality. The result of continuously applying these maps indicate an expansion in the space-time area associated.

Secondly, a previously unknown statistical mechanics in quantum gravity is introduced in the framework of two dimensional Causal Dynamical Triangulations. This provides us a useful and new tools to understand this quantum gravity in terms of effective spins. This study reveals a correspondence between the statistics of Anti-ferromagnetic systems and Causal Dynamical quantum gravity. More importantly, it provides a basis for studying anti-ferromagnetic systems in a background independent way.

Thirdly, two novel properties of area operator in Loop Quantum Gravity are reported: 1) the generic degeneracy and 2) the ladder symmetry. These were not known previously for years. The first one indicates that corresponding to any eigenvalue of area operator in loop quantum gravity there exists a finite number of degenerate eigenstates. This degeneracy is shown to be one way for the explanation of black hole entropy in a microscopic way. More importantly, we reproduce Bekenstein-Hawking entropy of black hole by comparing the minimal energy of a decaying frequency from a loop quantum black hole and the extracted energy from a perturbed black hole in the highly damping mode. This consistency reveals a treasure model for describing a black hole in loop quantum gravity that does nor suffer from the restrictions of an isolated horizon. The second property indicates there exists a ladder symmetry unexpectedly in the complete spectrum of area eigenvalues. This symmetry suggests the eigenvalues of area could be classified into different evenly spaced subsets, each called a 'generation.' All generations are evenly spaced; but the gap between the levels in any every generation is unique. One application of the two new properties of area operator have been considered here for introducing a generalized picture of horizon whose area cells are not restricted to the subset considered in quantum isolated horizon theory. Instead, the area cells accepts values from the complete spectrum. Such horizon in the presence of all elements of diffeomorphism group contains a number of degrees of freedom independently from the bulk freedom whose logarithm scales with the horizon area. Note that this is not the case in quantum isolated horizon when the complete elements of diffeomorphism applies.

Finally, we use a simple statistical method in which no pre-assumption is made for the essence of the energy quanta radiated from the hole. We derive the effects of the black hole horizon fluctuations and reveal a new phenomenon called "quantum amplification effects" affecting black hole radiation. This effect causes unexpectedly a few un-blended radiance modes manifested in spectrum as discrete brightest lines. The frequency of these modes scales with the mass of black hole. This modification to Hawking's radiation indicates a window at which loop quantum gravity can be observationally tested at least for primordial black holes.

Acknowledgements

This thesis puts a formal end to my twenty two years of life as a student. I should start by acknowledging my parents who played a significant role in my education and to whom I dedicate this thesis. My father, Abdolali Ansari, is the founder of the Teachers College of Kermanshah (Daneshsaraye Aali e Kermanshah) and was the first president of this College between 1955-1980. He has taught many courses in this college mainly on Mathematics and Persian literature. My father is the first person who implanted in me the joy of mathematics by spending hours with me motivating the discovery of new proofs for geometrical theorems. His passion for discovering laws between seemingly random numbers and also in working with rulers and compasses in his way for finding systematic methods for splitting angles into several pieces are among those memories that never will be eliminated from my memories. My mother, Fatemeh, sacrificed the blossom moments of her highschool education, which could easily lead to her university studies, helping her four children through every step of their lives and educations. I warmly thank her for everything she has done for us.

My interest to Physics started in high school by the motivations I received from our young and curious physics teacher Mr. Mollanejad who was then a BSc. student of Mechanical engineering. Lateron, as an undergraduate student of physics in IUT (Isfahan University of Technology) I had the opportunity to learn the basics of modern physics from two of the best professors Drs. Mojtaba Mahzoon and Mehdi Barezi. Soon after in the University of Isfahan, I started research in theoretical physics for my Master studies. At the first year a famous researcher of particle physics joined Physics department of the University of Isfahan. My journey into the world of quantum field theory and gravity started with the courses he lectured for graduate students and this has led me to become his first student. Prof. Bijan Sheikholeslami is a known physicist for his works mostly on Sheikholeslami-Wohlert (SW or clover) action in lattice gauge theory and his 1986 paper on this so far has received over than 700 citations according SLAC SPIRES data. My last four years were the most relevant years to the contents of this thesis. During this time I enjoyed being the student of one the pioneers of the theory of Loop Quantum Gravity, Prof. Lee Smolin. Lee was the first person who welcomed me in Waterloo and the second person who became excited each time I received a new result. I also would like to thank Fotini Markopoulou for collaboration on one project which was a turning point for me on doing science throughout modeling, and all of her supports and long term discussions about her unique way of looking into quantum gravity. I also would like to thank Abhay Ashtekar, Martin Bojowald, John Brodie, Bianca Dittrich, Olaf Dreyer, Laurent Freidel, Kirill Krasnov, Etera Livine, Carlo Rovelli, Artem Stardoubusev, and Rafael Sorkin for all of discussions and email exchanges. During the course of completing the works related to this thesis I enjoyed also discussing science with my freinds Drs. Amjad Ashoorioon, Dumitro Astefanesi, Hoda Moazzen, Hamid Molavian, Tomasz Konopka, David Pullin, Ali Tabei, and Yidun Wan.

Mohammad H. Ansari
Waterloo, Canada
April 2008

To My Parents,

Fatemeh and Abdolali

Contents

List of Figures

List of Tables

List of Illustrations

Preface

This thesis consists of six chapters. Chapter 1 is the introduction, which explains some of the troubles with perturbative quantum gravity, some non-perturbative methods in quantum gravity, including Loop Quantum Gravity and Causal Dynamical Triangulations, and some answers to why 'loop' quantum gravity, and what are the reasonable statistical strategies in the non-perturbative gravity.

Chapter 2 is published in Classical and Quantum Gravity. This chapter was done in collaboration with Lee Smolin who performed by clarifying his idea of applying self-organized criticality in quantum gravity. This work reports the first signs of the emergence of space-time from Self-Organized Criticality on spin networks. We would like to thank Maya Paczuski for discussion on this.

Chapter 3 is published in Nuclear Physics B as a result of my collaboration with Fotini Markopoulou. Fotini here performed her skills in simplifying Causal Dynamical Triangulation. This work is on a novel statistical mechanics for Causal Dynamical Triangulations and its RG transformation limits. We would like to thanks Lee Smolin and Thomas Konopka for discussions.

Chapter 4 is published in Nuclear Physics B. It reveals the generic degeneracy of area states in loop quantum gravity that verifies Bekenstein-Hawking Entropy.

Chapter 5 is published in Nuclear Physics B. It introducing ladder symmetry, Modification of the black hole radiation from the area fluctuations of hole horizon.

Chapter 6 has not been submitted to journals yet on its first version. This work is dedicated to another quantum correction to the radiation of a quantum horizon through Loop Quantum Gravity and a modification on the intensity calculation.

The author based on the contents of chapter 4, 5 and 6 received ''John Brodie Prize of Creativity and Independence in Research'' in 2006 from the Perimeter Institute for Theoretical Physics.

Chapter 1

Introduction

What sort of laws shape the universe? The answer is given by understanding two things: 1) what is space-time, 2) what is the dynamics of space-time.

The first one has no unique answer. In fact, there could be many answers to it, among some of which are: metric fields, frame fields and connections, causal sets, causal sites, closed strings, topological fields, spin networks, etc. Usually any reasonable assumption for simplifying a physical system such as space-time is acceptable as long as its dynamics satisfies some physical facts. What makes a theory successful is mostly its dynamics.

So far there have been many different models for studying space-time dynamics in quantum scales; from perturbative methods to non-perturbative and also from continuum models to discrete ones.

The **traditional quantum gravity** considers a fixed background metric on space and time. Any prturbation to this background generates gravitons. Graviton is a massless particle assumed to be of spin two and represents the gravitational degrees of freedom on the background space-time. Similar to other massless gauge particles, gravitons at each point of space-time can take only two physical degrees of freedom.

According to Einstein's theory of gravity, despite other forces and fields in which some restricted symmetries such as Lorentz, or Poincare symmetries are respected, gravity respects a more general symmetry. This enters into the Equivalent Principle based on which gravitational equations must have the same form in any reference frame. In a more mathematical language, gravity is a **diffeomorphism** invariant force.[1] Because in the traditional quantum gravity a preferred background is considered on top of which there are gravitons (perturbations) jiggle around, the diffeomorphism constraint is simplified, linearized and becomes completely solvable. Therefore, this version of gravity (that does not have the full diffeomorphism because of choosing a preferred background for it) becomes a local field theory with two degrees of freedom defined at each point. The Einstein-Hilbert Lagrangian could be re-written in the language of perturbations on top of a fixed background, with or without matter inclusion. This Lagrangian is simplified and finally seen to contain the interaction of gravitational field (the perturbative field) with itself with some additional derivatives involved. A derivative is known to be of inverse length unit, therefore the coupling coefficients of such terms must be of an appropriate length dimension in order to cancel extra dimensions and keep the action dimensionless, (1). This makes this

[1] In mathematics, a diffeomorphism is a map between smooth manifolds. It is an invertible function that maps one differentiable manifold to another, such that both the function and its inverse are smooth.

theory different from other local field theories because of the serious problems such dimensionfull coefficient may cause.

One of the problems in front of accepting this theory as a candidate quantum gravity is that quantum field theory of gravity when quantized is not **renormalizable**. The reason is this theory has an *infinite* number of complicated interacting vertices. As a typical local field theory, when the momentum of a graviton that belongs to an internal loop diagram becomes arbitrarily large, the scattering amplitude diverges. This looks similar to any quantum field theory; however in theories other than gravity the divergences can be removed when the interaction coefficient is re-scaled. In other words those theories are 'renormalizable'. Renormalization means the divergences from high energy scales can be absorbed into the re-definition of original parameters appearing in the theory. In the quantum field theory of gravity, we cannot eliminate UV divergences because the gravitational coupling G appears in all interactions and carries dimension of length. In other words, the couplings in gravity are not free to be tuned.

Note that this problem of non-renormalizability does not mean that quantum mechanics is incompatible with gravity. There is room for progress within quantum field theory in lower energy scales. In fact, one can consider quantum field theory of gravity to be an '**effective' field theory** for energies well below the Planck scale of 10^{19} GeV. In an effective field theory, higher loop orders require new couplings by which the UV divergences are eliminated. For a theory of pure gravity with no matter, amazingly, the one-loop divergences cancel, as demonstrated by 't Hooft and Veltman (2). However, this is not the case in higher perturbation orders and also when matter is included, (1). Therefore, this method is not applicable for energies higher than one loop scattering patterns. For higher energies a new technique (of any kind) is required.

In addition to the non-renormalizability of quantum field theory of gravity, there are several other illnesses that are not cured yet in this theory. In the followings, a number of attempts to fix theseproblems are listed.

1. The non-renormalizability problem is due to some extra derivatives on gravitational self-interacting terms. First it was thought this problem could be cured if higher derivatives are added into the original Einsten-Hilbert action, (the terms such as R^2 etc.). This, when is calculated up to the first order of perturbation, and in the composition of matter fields inputs some additional interacting terms that potentially remove the problematic interacting terms in large N limit, (3). However, it has been noted in UV limits it produces two different types of gravitons: an unstable and massive graviton and a stable and massless one. The unstable graviton could decay into infinite number of the massless gravitons. Since it turns out the mass of the massive graviton is gauge-independent, choosing any gauge cannot eliminate the graviton mass. This violates the unitarity of scattering matrix. Details can be found in (4) and (5). One way to tackle this problem was then thought to be adding even higher derivative terms into the action, (i.e. R^3, R^4, terms.) Doing so makes this theory completely unitary; however since the action contain any number of derivatives the theory becomes highly non-local in the sense that it does not depend on space-time derivatives at all. Such a non-local theory is useless.

2. The equivalence principle restricts gravitational degrees of freedom (gravitons) to be localized at one point, instead they should be found at any finite region. The reason is that space-time at any point is flat and contains no excitation mode, therefore there could not any graviton localized at a point. In other words, it is said the degrees of freedom are non-local in general relativity. This important principle is missing in the localized field theory of gravity. The aftermath of artificially loosening the equivalence principle is that gravitons are associated with every point of the manifold individually. This localization causes over-counting the number of degrees of freedom in a manifold and finally ended up with some infinities in the scattering amplitudes as it is stated before this. Physicists tried to overcome this over-counting problem by the descretization of manifold. This could be done mathematically in several different methods. In some approaches this piecewise discretization of a manifold is naturally extracted from within other assumptions, and in some other models it is implanted the way it is assumed. This cures the over-counting problem, but definitely changes it gives up the traditional quantum theory methods and instead new approaches towards quantum gravity should be taken.

Given the difficulties of quantum field theory of gravity, physicists tried to test their chances towards a consistent quantum gravity using completely different approaches such as **string theory**.

String theorists realized that there is a link between the problem of non-renormalizability, non-unitarity and over-couting the degrees of freedom in quantum field theory of gravity in semiclassical limit. They used an alternative approach to cure these problems all together at the same time. They keep all of the traditional structure of a perturbative quantum field theory except one. They propose graviton is not associated with a point; instead the points are replaced with strings. In this way, they found the gravitational excitations could be considered as the standing wave excitations of a finite-size *closed* string.

In the low-energy limit string theory is reduced into a quantum field theory. Closed strings explain gravitons and open strings explains gauge fields. Since closed strings can be express by closed strings, it was conjectured for instance at the semi-classical limit S-matrix of gravity can be expressed by the S-matrix of non-Abelian gauge theory; a formalism called KLT. It is obvious such kind of conjectures, from which KLT is only one, are not fundamental because they do not provide the quantum field theory of gravity in its Einstein-Hilbert in a precise way.

String theory conceptually fails to satisfy some of the fundamental axioms of general relativity:

1. Due to diffeomorphism invariance the physical degrees of freedom of a space-time are only those associated with actual physical events. Diffeomorphism should produce a link between the string degrees of freedom which are gauge-dependent. However, the degrees of freedom in strings are not relational at all and therefore cannot satisfy diffeomorphism.

2. The scale at which the replacement of gravitons with strings occurs is determined by the use of the background metric that remains untouched after replacement of graviton with strings. In other words, different background metrics give rise to different string theories. These theories should be unified by **M-theory**, however

to understand M-theory one needs a better understanding of non-perturbative quantum gravity.

These typical analytic and conceptual problems suggest a non-perturbative approach towards quantum gravity as a safer candidate. However, the main obstacle is the mathematical construction of such a theory is not well-established and should be worked out by general relativity physicists. So far, a few non-perturbative candidate methods have been developed, two of which are the so-called Loop Quantum Gravity (LQG) and Causal Dynamical Triangulations (CDT).

1- Loop Quantum Gravity:

Loop Quantum Gravity is a non-perturbative canonical theory for gravity in Planck scales. However, this theory is not the first canonical approach towards general relativity. The canonical picture of gravity was known since 60's all in the form of spatial metric and their canonical conjugate extrinsic curvature variables. This traditional picture of a canonical quantum gravity turns out to be more complicated than it could guide us to a solvable theory.

In the dark ages, a bright miracle happened! Palatini rewrote gravity in terms of two conjugate variables: the gravitational **connections** and its momenta and the outcome action turned out to be quite interestingly simple! The gravitational connections are those part of gravity force responsible for parallel propagating chiral spinors. The conjugate momenta are nothing but orthonormal triads that determine the spatial Riemannian geometry.

Later on physicists understood there is a redundancy in Palatini action. The **self-dual** part of the fields are sufficient for the purpose of reconstructing general relativity! Therefore a phase space was made by the self-dual connections and their momenta. They were given some internal $SU(2)$ gauge freedom and the self-dual gauge-valued connections got a new name: '**Ashtekar-Sen variables**' denoted by $A^i_\mu(x)$, where i indexes the internal gauge components and μ does the physical space components. These variables since are $su(2)$-valued multiply with Pauli matrices in formulae. The conjugate momenta to Ashtekar-Sen variables are desitized frame fields (tetrads) $\widetilde{E}^i_\mu$ from which metric, **area**, **volume**, and the other geometrical variables are constructed.

Reformulating the general relativity in terms of this phase space of variables $(A, \widetilde{E})$ provides us with a Hamiltonian theory that turns out to be a constraint theory with gauge, diffeomorphism and Hamiltonian **constraints**. This theory manifests a specific constraint algebra that is known. The physical solutions to the constraints are supposed to be at the intersection of these constraints.

First strategy to first-quantizing the theory was to writing the wave function as a function of Ashtekar-Sen variables. However, later on it became clear that such a wave function is not normalizable.

In a different approach, and extended phase space was made by the use of **holonomies** (the exponentials of Ashtekar-Sen variables on closed line) as the variables of configuration space, and their corresponding momenta, the flux variables (the integral of E variables on 2-surfaces). This turns out to be a consistent way to quantize the theory and as a consequence the quantum theory was formed based on loop quantization of holonomies.

The quantum algebra is thus generated by holonomies of 1- dimensional curves (edges) and fluxes across 2-dimansional surfaces. The requirement of background independence surprisingly selects a unique representation of this quantum algebra on a kinematical Hilbert space. The classical constraints (gauge, diffeomorphism and Hamiltonian constraints) when promoted into **self-adjoint** operator, selects the subset of Kinematical Hilbert space that determines the 'physical' Hilbert space.

As a constraint theory, the outcome result is not seemingly time dependent. When one of the degrees of freedom is chosen to be an internal clock, the other degrees of freedom could be seen as variables that evolve with respect to the internal clock.

One-dimensional loop α are in fact the generators of holonomies. Let us denote open-loop holonomy with $U[\alpha(x_i, x_f)]$ and closed-loop holonomy with $T^0[\alpha]$:

$$U[\alpha(x_i, x_f)] = \mathcal{P}e^{\int_{x_i}^{x_f} A^i_\mu \sigma^i dx^\mu}, \qquad T^0[\alpha] = \mathrm{tr}\mathcal{P}e^{\oint_\alpha A^i_\mu \sigma^i dx^\mu}$$

where σ^i are Pauli matrices, $\mathcal{P}$ is path order symbol similar to time order symbol in quantum field theory. When the orientation of integration over loop is inverted, since $SU(2)$ group is not an oriented group, this does not change the T^0.

The key advantage of using the holonomies T^0 instead of Ashtekar-Sen variables is the fact that T^0 is gauge-invariant by definition and non-sensitive to the re-parametrization of the loop. We indicate T^0 with a closed loop without any orientation.

On the loop basis an extended phase space could be developed. The conjugate momenta of T^0 could also be defined. We need appropriate $su(2)$-valued gauge-invariant variables for **loopy momenta** as well. The simplest way to make these variables is that conjugate momenta are carried into the trace of T^0. By this we really mean $\widetilde{E}^i$ should grasp a loop at a typical point, say x^* (called base point.) When the orientation of the integration over the loop is inverted, since the matrices of $\widetilde{E}^i$ is trace-free, it does not change the loopy momenta.[2] It is standard to denote the phase space variables by $T^0,\ T^1,\ T^2,\ T^3$. These can be classify as $T^0,\ T^i$, where $i = 1, 2, 3$ where T^0 is holonomy on a loop and the other three are momenta; which are

$$T^i[\alpha] = \mathrm{tr}\ \ U\left[\alpha\left(x, x^*\right)\right] \widetilde{E}^i\left(x^*\right)\ \ |_{x=x^*}. \tag{1.1}$$

In a simple case where the internal gauge group is $U(1)$ since the fields are scalar the definition of (1.1) becomes $T^i = T^0\widetilde{E}^i$. In this definition the first term (T^0) can be factored out from all definitions of T^i and the loopy momenta will become simplified into $\widetilde{E}^i$. This means in the simple gauge group of $U(1)$, the densitized conjugate of Ashtekar-Sen variable, E^i, can play the role as the conjugate momentum of T^0 as well.

At the moment we are equipped with some gauge-invariant variables that serve to construct a good phase space for gravity. There is a pictorial way to represent the variables. T^0 can be depicted by a gray loop without any base point on it and without orientation. Loopy moments variables, T^i, will be depicted by oriented loop with a gray point on as a base point where E^i may **grasp** the loop.

These variables T^i together with T^0 respect a loop algebra. First of all, note that $\{T^0[\alpha], T^0[\beta]\} = 0$. The rest of the algebra is depicted below. The left side of the relation (1.2) indicates $\{T^j[\alpha], T^0[\beta]\}$.

[2]However, note that the orientation does make difference when the Poisson bracket of loops are calculated.

Pink color is the loop of α and green color is the loop of β. The grey point, which denotes the grasping of a momentum at a loop, here belongs to the pink loop.

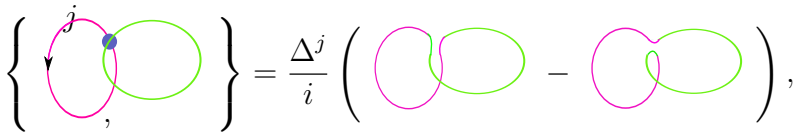

$$= \frac{\Delta^j}{i} \left(\quad - \quad \right), \tag{1.2}$$

where Δ^i is a function of two loop curves $\alpha(s)$ and $\beta(t)$, that is defined $\Delta^i[\alpha,\beta](s) \equiv \int dt\ \delta^3(\alpha(s),\beta(t))\ \dot{\beta}^i(t)$. If the base point is not at the intersection of the two loops the result is zero.

Similarly the Poisson bracket of $\{T^j[\alpha], T^k[\beta]\}$ can be evaluated. The result is

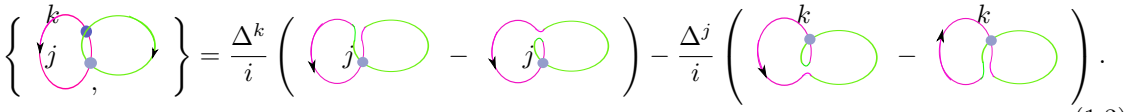

(1.3)

If either of the base points is not the intersecting points of the two momenta loops, the poisson bracket is zero. Note this algebra looks line an unusual one because the Poisson brackets of momenta do not vanish!

A gauge connection field can be represented in different representations based on the gauge irreducible representations. Depending on the representation, the loop variables take different values. Therefore the configuration space could be thought of as a labeled loop whose labels determine the *spin* of the internal gauge representation of connection fields.

The field theory of gauge fields in the continuum limits can be obtained by appropriately gluing theories associated with all possible graphs on a given manifold. Therefore, from the quantum theory of holonomies and its momenta a classical field theory may emerge whose corresponding geometry is physical.

The extended configuration space defined here was based on one dimensional loops. Different loops can be connected to one another on vertices. We can extend this configuration space structure onto the one that describes a graph Γ. This system is equivalent to lattice gauge theory on the graph Γ.

A **graph** is a collection of edges and vertices as a floating lattice. Since there is no background metric, terms like rectangular and triangular have no invariant meaning. Instead four-, and tri-valent graphs could be meaningful. When a graph becomes the basis of defining loop variables, it plays as a generator for the purpose of defining basis configuration variables. Let us now define the ingredients of these variables: an **edge** is an oriented, 1-dimensional sub-manifold with two boundary points (v_i and v_f). The two boundaries are the **vertices** of the edge. A graph is a collection of edges such that two edge do not intersect unless they meet at a vertex.

To every edge a gauge group such as $SU(2)$ is internally assigned that constructs the configuration variables of the extended phase space of edges $\mathcal{U}$. Recall the holonomy of an edge $e(v_i, v_f)$ is defined by $U[e(v_i, v_f)]$.

To each vertex in the graph a gauge group is associated with that produces an internal space for vertices $\mathcal{G}$. For instance, if there are n edges and v vertices in a graph, the edge space $\mathcal{U}$ and vertex space $\mathcal{G}$ are respectively isomorphic with $[SU(2)]^n$ and $[SU(2)]^v$.

Recall loop holonomy is gauge invariant. If the two ends of a loop are open the holonomy will no longer be gauge-invariant. Despite the inhomogeneous form of gauge transformation that Ashtekar-Sen variables indicate ($A \rightarrow gAg^{-1} + g\partial g^{-1}$), holonomies are locally gauge transformed homogeneously only on the initial and final edge points: $U \rightarrow g(v_f)Ug^{-1}(v_i)$. In other words, the space of $\mathcal{G}$ defined on vertices can internally rotate $\mathcal{U}$. Note that in a graph the edges meet one another at vertices. A gauge transformation rotate each vertex of the graph internally. Figure 1 indicates gauge rotation of a vertex at a simple triangle graph. In this picture, internal space of holonomies are depicted by the tri-framed edges since it possesses internally three degrees of freedom in $SU(2)$ group. The gauge transformation is indicated by gauge-rotating the internal space of a vertex.

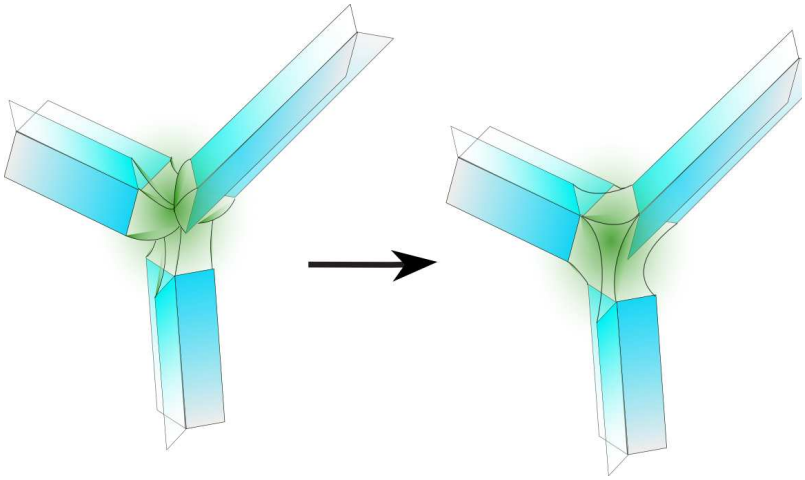

Figure 1.1: A schematic gauge-transformation on a gauged graph, where the vertices as well as the edges get internal spaces. Here the three internal components of $su(2)$-valued holonomy on an edge are indicated by the tri-framed edges. Three holonomies intersect at a vertex. The gauge transformation of the lattice is indicated by rotation on the internal $su(2)$ space of the vertex. Gauge invariant restriction accepts only those states in which the vertex is invariant after gauge transformations.

However, a gauge-invariant graph state is the state in which all the gauge-transformations are put into one equivalence class. A **gauge-invariant space** is the one in which the gauge transformation of vertices does not change a state. This space is $\mathcal{U}/\mathcal{G}$. In such a space the vertices become intertwiners between edges and they are invariant under gauge transformation. Such a gauge-invariant labeled graph is a '**spin network**'. In fact a spin network state is determined by a graph, its edge labels and its vertex intertwiners.

Let us mention what the **intertwiners** are. Consider a space made of the tensor product of some holonomy configuration spaces: $\mathcal{U}_1 \otimes \mathcal{U}_2 \otimes \cdots \otimes \mathcal{U}_k$. The space of this product determines the states of the joint vertex of these holonomies. The elements of this space are the vertex states $v^{a_1 a_2 \cdots a_k}$ in which a_i is the index associated with the holonomy space $\mathcal{U}_i$. Now consider that we gauge transform holonomies. A typical holonomy $\mathcal{U}_i$ by the tensor $R^{a_i}_{\ b_i}(\mathcal{U}_i)$. This changes the state of the vertex into $w^{b_1 b_2 \cdots b_k} = R^{b_1}_{\ a_1} R^{b_2}_{\ a_2} \cdots R^{b_k}_{\ a_k} v^{a_1 a_2 \cdots a_k}$. In the case $w = v$ the state of the vertex is an *intertwiner*. In fact, in a spin network, each vertex accepts only those states that are

intertwiners.

Diffeomorphism changes the underlying graph as well as the state, however since different states are summed over and there is no lattice spacing on the spin network structure the physical state respects the underlying diffeomorphism invariance.

Spin networks are the basis states in Loop Quantum Gravity based on which physical variables are defined. We can easily quantize the variables as long as the physical constraints are satisfied on a physical sector. From these loop variables one can indeed define the variables that make more physical sense. For instance the three-metric of a Cauchy surface is made by grasping a loop twice (recall if a loop is grasped once it makes T^i variables. Area and volume variables are made of the T^i's. One of the most important variables that can be made of the loop variables is the scalar constraint (the Hamiltonian constraint). This is the basic structure of loop quantum gravity.

Loop Quantum Gravity has been so far studied on the two basis of its canonical versions and its path integral version (**spin foam** models). In this theory the existence of a finite size area and volume arises as a consequence of quantizing area and volume operators. However, solving the dynamics of this theory is still hard!

Note that the choice of defining one dimensional loop as the basis for defining holonomies is just a matter of flavor and mathematical simplicity. There is not absolute physical reason why the configuration variables should not be defined on higher dimensional objects such as Witten's framed holonomies. Recently, Lee Smolin and his colleagues started a series of interesting researches in which instead of loops ribbons are taken into account that mimic some mathematical definitions of particles in the form of **Preon model**. This could potentially be a different way of looking into the quantization of space-time with matter as braided and twisted ribbons. However, so far they did not define the phase space variables. Moreover, the theory requires a tangle algebra that should be constructed out of the ribbon variables. This may results into a different theory that could be different from Loop Quantum Gravity with even a different name such as Ribbon Quantum Gravity.

This non-perturbative theory deserves to be taken seriously because on top of its fundamentally sophisticated assumptions, it results in some significant physics. A number of them are:

Inflation: In a spherically symmetrized manifold the theory gives rise to inflation in small scales, (9).

Singularity resolution: The big bang singularity turns out to be unexpectedly replaced by a quantum bouncing which resolves the historical problem of big bang singularity (10).

Black Hole Entropy and Its Radiation: There could be two different pictures in Loop Quantum Gravity for black holes:

1. If the Hayward's theory (44) of isolated horizon is re-written in the language of Loop Quantum Gravity it indicates that the isolated horizon carries a finite number independent degrees of freedom. Under the action of complete classes of diffeomorphism the number of physical degrees of freedom do *not* verify **Bekenstein-Hawking entropy**; however if a subset of the diffeomorphism group that differs between different locations on a black hole

horizon is taken, the required entropy is verified. (Nonetheless, there is no single reason why a subset of diffeomorphism group should be taken.) Such a classical horizon that is quantized after its definition allows a subset of area cells. This subset is not an important subset and area fluctuations of a horizon do not put any notable effect on Hawking's semi-classical radiation, (11). However, this is not the case in the second picture.

2. The meaning of a null surface is quantum world is completely different from its classical. In Hayward's Isolated Horizon theory a classical marginally trapped null surface is defined and Ahtekar,Krasnov, Baez and Corichi have quantized it. Because of the too restrictive boundary conditions they must apply, it is guaranteed that the result they derived should be completely different from the result of defining a quantum black hole by its evolutions as spin network state. In this thesis we explain how this different approach verifies the Bekenstein-Hawking black hole entropy after counting all physical degrees of freedom. Most interestingly this not only is argued to be a more physical picture that better explains the properties of a black hole in quantum world, it unexpectedly manifests the fingerprints of Loop Quantum Gravity in black hole radiation which makes Loop Quantum Gravity testable, (13), (14)!

There are also some models that has not come yet into testable results, but they are evolving rapidly at the time this thesis is written; one of these are the studies of quantum black holes initiated by Husain and Winkler, (66; 12). In this study, a quantum black hole is derived from the quantization of null expansion variable. This is a 1+1 field theory based on $u(1)$-valued connection field and scalar matter. In this direction a quantum black hole is studied from within a fully dynamical picture of gravity such that the presence of a trapped surface, a surface from which light cannot come out, and its location is derived from within the black hole state evolution. This picture may result into a concrete study of a black hole radiation in a fully dynamical treatment that may modify or alter Hawking's radiation. Note that what we study in this thesis is not affected by this forthcoming result since we consider the horizon surface fluctuation effects on the black hole radiation.

2- Causal Dynamical Triangulations:

The second non-perturbative strategy we refer to in this thesis is the so-called Causal Dynamical Triangulations (CDT).

In this approach the finiteness of a region to which gravitational degrees of freedom should be attributed is pre-assumed. It is also assumed in a Lorentzian space-time only **causal histories** contribute to the quantum gravitational path integral. On such a space-time a 'global' time-foliation is also assumed. Using these tools, the space-times appearing in the regularized path integral become a set of piecewise linear causal geometries, made out of triangles (two-simplices) whose edge lengths provide an ultraviolet cut-off.

In order to perform the summation over these causal histories a rotation to Euclidean space-times is performed. Each piecewise linear causal geometry has a continuation to Euclidean signature, but the class of Euclidean geometries included in

the path integral will only be a subclass of the total classes of Euclidean geometries. This summation turns out to be different from that of Euclidean quantum gravity in the sense that multi-branches and baby universes are not created. This model has been studied for two-simplex case as well as three- and four-simplex cases.

This model has both applications as a basis for defining spin foam models as well as the descritization of world sheets for defining non-perturbative non-critical string theory. One is interested in the limit where the lattice spacing goes to zero. There is evidence for the existence of an underlying (non-perturbativly defined) continuum quantum field theory in four dimensions and the results seem to be in qualitative agreement with recent renormalization group calculations. In two dimensions the non-perturbative quantum gravity can be solved analytically at the discretized level.

Except the theory of topological fields in which the local degrees of freedom are removed and the physical parameters are defined on the infinite boundary, other non-perturbative approaches to gravity, such as LQG and CDT, deals with many local degrees of freedom. This necessitates the existence of a 'general relativistic many body theory'. Such a complete theory does not exist yet. As a candidate a pure statistical mechanics can be worked out to understand the building blocks of space time.

One should be aware that the **statistics** of the gravitational building blocks could not be pre-assumed. One should be careful in using statistical methods because applying one even un-important assumption may brings up an avalanche of un-intentional consequences that may deeply implies bosonic or fermionic or any other statistics to gravity. This makes the statistical development of general relativity extremely instructive, creative and at the same time difficult, yet possible!

What we study in this thesis is mostly based on the statistics of LQG and CDT quantum gravity theories. In next chapter, chapter 2 we study an evolution to the spin network. One of the main problems with Loop Quantum Gravity is its semi-classical limits. In simple words, we do not know what kind of local evolution may end up with a space-time such as Schwarzschild (or any other) solutions to the Einstein's equations. In this chapter we introduce a class of evolution in a trivalent spin network that keeps the number of vertices and edges fixed and only the spin representation of edges change. Such a spin network state remains as a 'frozen spin network'. This study has been done for one specific reason and the basic motivation behind this is the idea that space-time after the initial quantum bounces evolves into the expanding state. In the expanding state there are a number of parameters that are tuned in theory. We want the expansion and the tuning of parameters become both as a result of local *evolution* and nothing else. One application to this could be potentially the emergence of Hubble parameter in cosmology by evolution. Given this, it is very interesting that there are some systems whose parameters reach critical behavior, with scale invariant correlations, without any necessity to tune the parameters from outside the system. These are typically non-equilibrium systems that reach critical behavior after evolution in real time from a random start. Among these are *self-organized critical systems*. It is then attractive to consider the idea that the critical behavior is necessary if classical space-time is to emerge from a background independent quantum theory of gravity arises from a process analogous to self-organized critical phenomena.

In chapter 3, we study the statistics of the two-simplices in 2 dimensional Causal Dynamical Triangulations. Without considering any additional assumption to those

of Causal Dynamical Triangulations we find that these blocks follow the same statistics of spin chain models. Although this statistical behavior is rather different from the model so far have been studies since here the spins are lattice dependent and the lattice is background independent.

In chapter 4, we study the area operator in Loop Quantum Gravity. Based on one unexpected result, it is shown that associated to each area eigenvalue in the complete spectrum of area operator there exists a finite number of eigenstates. This is called 'the **generic degeneracy** of area operator'. Moreover, the black hole entropy is shown to be proportional to the black hole horizon area. Under the assumption of Dreyer's conjecture the Bekenstein-Hawking entropy is verified.

In chapter 5, we show Loop Quantum Gravity admits a kind of area quantization that is characterized by three quantum numbers. We show the complete spectrum of area is the union of equidistant subsets and a universal reformulation with fewer parameters is possible. Associated with any area there is also another number that determines its degeneracy. The complete spectrum of area could be reformulated into a universal form with two parameters and more importantly it is the union of exactly equidistant subsets. This is another symmetry in the spectrum of area that is called the '**ladder symmetry**.' The spectrum of radiation due to these new properties reveals a clear discretization on a few brightest lines which cannot blend into one another due to quantum amplification effect. The most notable point is that Loop Quantum Gravity as one fundamental theory of quantum gravity is substantially testable with an observational justification if primordial black holes are ever found.

In chapter 6, a modification to the previous method of analyzing the radiance intensities is presented that makes the result one step further precise. A few of harmonic modes appear to be extremely amplified on top of Hawking radiation. They are expected to form a few observable lines with the wavelength not larger than the black hole size.

Chapter 2

Self-organized Criticality in quantum gravity

2.1 What is this about?

If you grab some sand grains in your hand and let them drop from the bottom of your fist to fall on a spot of a table, they make a sand pile. Repeating this a few times, the pile grows. It is interesting that the pile slope (the angle between the table and the sides of the sand) during the growth to any scale is practically fix at about 37 degrees; no matter how large the pile grows up. By adding more sand grains to the pile, there may appear some disordered walls on top of the pile; however accumulating more grains will causes a sudden falling of the disordered walls in the form of avalanche. This automatic process whose cause is the gravity force guarantees automatically the maintenance of the critical angle in any pile scale. This appears to be a robust phenomena and the critical angle does not depend of the scale of the pile, such that it is called a scale-invariance critical angle. This is a well-studied stochastic process called Self-organized Critical phenomena.

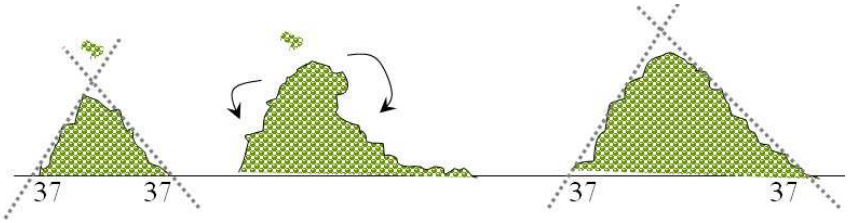

The definition of a Self-organized Critical system is mathematically well-known. Let us explain this definition in a model that describes a sand pile system computationally. Assume a grid network with a finite number of boxes, each with n sides. There are 3 laws required to approach the recognizing of Self-organized Critical phenomenon: 1) a universal constraint, 2) an evolution rule, and 3) a relaxation rule. The constraint for instance in the sand pile model is defined such that *each box cannot contain more than n sand inside*. A 'saturated box' is a box that contains n sands. The evolution rule chooses a box at random and adds one sand into it. If the constraint is satisfied the evolution is repeated. If the constraint is violated, the relaxation law applies on the box such that the box does not accept the $(n+1)$-th

sand and moreover all of its internal n sands are passed into its first neighboring boxes equally (one sand to each adjacent box).

Letting such a system to evolve, the network may manifests more than one relaxation after adding a sand to a saturated box. This is because as time goes on it is likely that two or more saturated adjacent boxes exists at a state. Once one box is relaxed, the addition of a sand into its adjacent box violates constraint there and thus another relaxation is necessary. Therefore, sometimes with addition of one sand to a saturated box a cascade of consecutive avalanches may occur in the whole network, sometimes at one spot sometimes in some different spots on the network. Note that the number of relaxations necessary to make the grid satisfying the constraint, determines the *size of avalanche*.

Sometimes, when box A relaxes its sands, the addition of a sand into its adjacent box B may make the box B over-saturated and another relaxation occurs at B and a sand is returned into A. This may go somewhere else afterwards and returns into A again and again from different locations. This way the box A may become over-saturated again and a second relaxation becomes necessary at it. If one counts the number of relaxations in a way that the repetition of relaxations in a box is not counted, one can estimate the overall area where the avalanches have affected the grid. This number determines *the area of avalanche*.

We let the network evolve by itself and in a matrix we keep recording the sizes and areas of avalanches. The distributions of each size and area of avalanche should also be recorded in a matrix. A Self-organized Critical system is recognized if a power law (scale invariant) distribution of all sizes and all areas of avalanche emerges. Moreover, at the same time the system should manifest the stability of a network-related parameter such as the number of saturated boxes at each step. This guarantees the network takes care of keeping he critical parameter stable without tuning it rom outside at any scales. In a real sand pile system the critical parameter is the critical slope of the pile sides.

2.2 Self-organized Criticality in Quantum Gravity

We study a simple model of spin network evolution motivated by the hypothesis that the emergence of classical space-time from a discrete microscopic dynamics may be a self-organized critical process. Self organized critical systems are statistical systems that naturally evolve without fine tuning to critical states in which correlation functions are scale invariant. We study several rules for evolution of *frozen spin networks* in which the spins labeling the edges evolve on a fixed graph. We find evidence for a set of rules behave analogously to sand pile models in which a critical state emerges without fine tuning, in which some correlation functions become scale invariant.

2.3 Introduction

Since the work of Wilson and others (16) it has been understood that the existence of a quantum field theory requires critical phenomena, so that there are strong correlations on scales of the Compton wavelength of the lightest particle. If this scale is to remain

fixed as the ultraviolet cutoff length is taken to zero, the couplings must be tuned to a critical point, so that the ratio of the cutoff to the scale of the physical correlation length diverges. This requires asymptotic scale invariance of the kind found in second order phase transitions.

Similar considerations apply to quantum gravity in a background independent formulation such as loop quantum gravity, or causal set models. The problem is not alleviated if the theory is shown to be finite due to there being a physical ultraviolet cutoff, as in loop quantum gravity(17). Instead, the need for a critical phenomena is even more serious as there is no background geometry. This means that away from a critical point the system may not have any phenomena that can be characterized by scales much longer than the Planck length. That is to say, the volume, measured for example, by the number of events, may become large, but there may still be no pairs of events further than a few Planck times or lengths from each other. This is seen in detail in models whose critical phenomena has been well studied, such as dynamical triangulation models(18) and Regge calculus(19). Away from possible critical points, the average distance between two nodes or points need not grow as the number of events (or the total space-time volume) grows. Instead, one sees that for typical couplings, statistical measures of the dimension, such as the Hausdorff dimension, can go to infinity or zero.

In equilibrium statistical mechanical systems, critical phenomena of the kind required for a system to exhibit a large hierarchy of scales is only found on renormalization group trajectories that flow to ultraviolet fixed points of the renormalization group. It typically requires a fine tuning of many couplings to put the system on a physical renormalization group trajectory. This may be seen to be generally problematic when the system under study is not a laboratory experiment, but is conjectured to be a theory that is both fundamental and cosmological, for in this case who is to do the fine tuning required for our macroscopic world to emerge?

Given this, it is very interesting that there are some systems whose parameters reach critical behavior, with scale invariant correlations, without any necessity to tune the parameters from outside the system. These are typically non-equilibrium systems, which reach critical behavior after evolution in real time from a random start. Among these are self-organized critical systems studied by (20; 21; 22).

It is then attractive to consider the idea that the critical behavior necessary if classical space-time is to emerge from a background independent quantum theory of gravity arises from a process analogous to self-organized critical phenomena. This idea was proposed earlier(23), where it was proposed that the low energy limit of quantum gravity might be analogous to a system evolving to a self-organized critical behavior such as directed percolation. This idea was then studied in some detail by Borissov and Gupta (28) in the case of a certain simplification of loop quantum gravity. In this simplification, the graph on which a spin network basis state is defined does not evolve, rather the spin labels evolve on a fixed graph. Such rules define a class of theories we call *frozen spin network theories.* Moreover, the identities that impose gauge invariance at vertices are not imposed as conditions on states, instead the dynamics is chosen so that the system evolves to gauge invariant states.

Borissov and Gupta in (28) did not find a set of evolution rules which are self-organized critical. Here we study a new set of evolution rules, and show evidence that at least one of them is self-organized critical.

Before going on we note that our results have one severe limitation. We work here not with quantum gravity per se, but with the classical statistical mechanics of spin networks. The evolution rules we study are stochastic rather than quantum mechanical; they are described by real probabilities rather than complex amplitudes. Whether the considerations of self-organized critical systems can apply to critical phenomena in quantum systems is presently unknown, to our knowledge there is as yet no example of quantum self-organized critical phenomena. Nor can we naively apply the method of Euclidean continuation as is done in conventional quantum field theory, by means of which quantum amplitudes are related to statistical mechanical problems. The reason is that in quantum gravity there is no preferred time coordinate by means of which the Euclideanization can be done.

To make this thesis self contained for interested readers in both quantum gravity and statistical physics, we give very brief introductions to spin network states in section 2 [1] and to self-organized criticality in section 3. In section 4 we suggest two different classes of propagation rules for frozen spin networks. The first class is based on choosing an edge at random and changing its color by a constant value and then making the network gauge invariant. In this class we generalize a model which was studied for one special propagation rule in (28). Some of the rules in this class were studied and it was seen that none of them exhibited self-organized criticality. The second class is based on choosing a vertex at random among all vertices of a trivalent spin network and changing the colors of its three incident edges by a constant even value. We do find a rule in this class that exhibits power law behavior, which is suggestive of self-organized critical

systems.

Section 5 presents some of the results of a numerical study we carried out which provides evidence that members of this second class of rules exhibit self-organized criticality. This is followed by our conclusions.

2.4 Spin network states

For the purposes of this thesis a spin network is a combinatorial labeled graph. It consists of a graph γ, which consists of a finite number of oriented edges $e_1, e_2, \cdots$ incident at vertices $v_1, v_2, \cdots$. The edges are labeled by the irreducible representation of a Lie group, G. In the case of canonical quantum gravity in $3+1$ dimensions, $G = SU(2)$, so that the labels on edges are spins. The *color* of an edge is defined as twice the spin, $c_i = 2j_i$.

In this thesis we will consider only trivalent spin networks which may be embedded in a plane. Dual to such an imbedded trivalent spin network is a triangulation of a region of space(24). The length of a side in the triangulated network is proportional to the color of its dual edge in the spin network, $2l_{side} = l_{Planck} \cdot c_{edge}$ (25). The triangle inequalities hence provide constraints on the lengths of the sides of a triangle. Therefore there is a constraint on the colors of incident edges at a vertex. The constraint is called *the gauge-invariance constraint* because it also corresponds to the spin network states being gauge invariant, in the sense that they are solutions to

[1] Those readers wanting a more detailed introduction to loop quantum gravity are encouraged to look at (17).

Gauss's law(17)[2]. It can be shown that the constraint on a vertex is:

$$a + b \geq c, \quad a + c \geq b, \quad b + c \geq a; \tag{2.1}$$

$$a + b + c = even. \tag{2.2}$$

where a ,b and c are the positive integer colors of three incident edges at a vertex.

In loop quantum gravity, spin network states evolve by the application of local evolution rules, which apply to a single node or a small number of neighboring nodes(17). In the dual picture, these involve a small number of neighboring triangles (24). The evolution rules have been derived in both a Hamiltonian and path integral framework and come in several versions. Here we study a class of rules which are greatly simplified from those studied in the literature. We keep one key feature of the rules derived by quantization of the classical theory, which is that they involve the modification of a spin network state by the addition or subtraction of a small loop of non-Abelian flux. This corresponds to the fact that the Einstein equations are first order in the curvature of the space-time connection. The addition or subtraction of a loop of electric flux corresponds precisely to the multiplication of the state by a small Wilson loop of the spacetime connection.

In the exact forms of dynamics of LQG, the loop of space-time connection is multiplied by operators in the space-time metric, which have the effect of gluing the loop to the graph representing a state in a way that preserves gauge invariance (represented in the dual picture by the triangle inequalities.) Thus, the effect of the dynamics is to evolve the graphs from gauge invariant configurations to other gauge invariant configurations which differ by the addition or subtraction of a loop of flux.

Here we propose a two step dynamical process which has the same effect. The first step is to simply add or subtract loops of flux. As we will see, this can result in a state in which the triangle inequalities are not satisfied. The second step is to adjust the labels on nearby triangles so as to ensure that the result satisfies the triangle inequalities. Thus, gauge invariance is achieved only in the end; it comes as a result of a relaxation process which involves the addition or subtraction of more loops of flux. This gives rise to avalanches of moves, whose statistics gives rise to scale invariant dynamics.

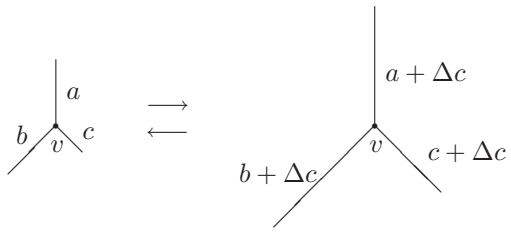

Figure 2.1: The dynamics of quantum gravity is represented by the addition or subtraction of loops of flux, corresponding to the fact that the Einstein equations are linear in the curvature of the spacetime connection. a, b and c are the colors of the edges incident at the vertex v and Δc is a positive or negative integer.

[2]In the case of nodes with valence higher than three, the implication of Gauss's law is more complicated. Each vertex v_i of the spin network is labeled by an invariant, in the product of the representations of the edges incident on it.

2.5 Self-organized criticality

A self-organized critical (SOC) system is one which has critical, that is scale invariant behavior, without fine tuning of parameters. The earliest example of such a system is the sandpile of Bak, Tang and Wiesenfeld(20). Since then, many such systems have been studied, including models of phenomena as diverse as biological evolution, earthquakes, astrophysical phenomena and economics(21).

One way that SOC systems are identified is by measuring the distribution in space and time of events in the system's evolution, and looking for power law behavior. A set of events which is contiguous in both time and space is called an *avalanche*. Self-organized criticality (SOC) occurs when the distribution of the sizes of avalanche follows a power law(20; 21; 22):

$$P(s) = s^{-\alpha} \tag{2.3}$$

where α, s and $P(s)$ are a positive constant, the size of avalanche, and the distribution of a size of avalanche, consecutively. Because the distribution is power law rather than exponential, there is no preferred scale that characterizes the avalanches. There is no largest avalanche, and no typical size for an avalanche. Hence we can say that the system exhibits the same structure over all scales.

2.6 Evolution rules for frozen spin networks

Our aim is to find evolution rules that realize SOC in 2d planar trivalent spin networks. For simplicity we consider frozen spin networks, which are ones for which the labels change but the underlying graph remains fixed[3]. In this context we may still attempt to mimic the basic features of the Hamiltonian constraint of quantum gravity such as the fact that the dynamics consists of terms which add elementary loops of flux to the original graph.

We begin by constructing a fixed triangulated triangle graph on which we will define and study evolution of the labels (Figure 2.6).

We then construct the dual spin network by connecting the centers of each triangle to the centers of the adjacent triangles. The result is a trivalent spin network, with boundary given by the dual of the segments of the edges of the original triangle.

The evolution rules we will invent are designed to be analogous to the rules by which a sandpile model evolves. First, sand is randomly dropped onto the pile. The pile is in equilibrium so long as the slope of the pile is not too much. If a new piece of sand causes the slope to exceed that value, the sand flows, till a new equilibrium is established. Thus the evolution rules have four steps: 1) drop sand randomly, 2) check to see if the slopes are too much, 3) if so move sand locally until all slopes are reduced below the condition for equilibrium. 4) Go back to step one.

We may consider an analogous set of rules for color to evolve on a graph. The height of the pile is analogous to the color. The constraint of a real sand pile model that the side slope not to exceed a certain value here in our model is replaced by the maintenance of gauge invariance at each node. Thus, the rules we will consider also have four steps: 1) add or subtract colors to randomly chosen edges. 2) check to see

[3]There is a limited sense in which the topology of our graphs can change, which is when edges have length zero. When one edge of a triangle is zero, gauge invariance requires the other two edges are equal. The triangle then can be considered to have disappeared.

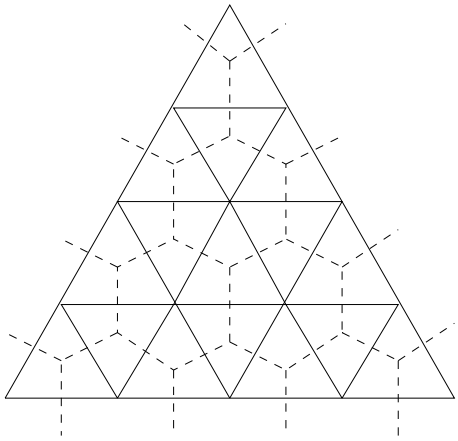

Figure 2.2: Frozen spin network (dashed network) and its dual, the triangulated triangle (solid lines). This lattice was picked only because we want to restrict ourselves into the tri-valent vertices. However, note that what we have chosen as a base spin network is nothing but a 3-valent labeled graph. There is no lattice spacing and no restriction on the lattice sides except what comes about from within gauge invariance. Note that we could potentially work with higher-valent graphs but in those graphs the gauge invariance takes a different form that makes it rather difficult to easily define it the same way it is defined in a triangular lattice.

if the gauge invariance condition is satisfied at all nodes. 3) if it is not, then move the colors at edges adjacent to non-gauge invariant nodes around, till gauge invariance is restored. 4) go back to step one.

The process by which sand redistributes itself on the pile till equilibrium is re-established is called an *avalanche*. The size of an avalanche is the number of moves it takes to restore stability. When a pile has reached a self-organized critical state many slopes are just at the value below that which causes sand to flow downwards. Once this state is reached the distribution of sizes of avalanches becomes scale invariant.

By analogy, the process by which colors re-arrange themselves on the graph may also be called an avalanche. If the network reaches a critical state, many nodes will be in a state where one more addition of a color value causes gauge invariance to be satisfied. This means that the dual triangle is degenerate, so that the triangle inequality is just barely satisfied. We seek rules such that, once a sufficient number of nodes are in such a critical state, the distribution of sizes of avalanches become scale invariant.

We may consider rules in which the color added $\triangle c$ to a vertex is always even or always odd. The difference between them is as follows. Adding an odd color to an edge, say $\triangle c = \pm 1$, will always cause the gauge invariance condition (2.2) to be violated. But if we add (or subtract) even colors, the situation is more complicated, as gauge invariance at the adjacent nodes will sometimes be satisfied and sometimes be violated. This is analogous to the case of a sandpile in which a new piece of sand sometimes will and sometimes will not increase the slope to a value where an avalanche starts. We found by numerical simulation that critical phenomena can occur in the latter case in which the changes are even. The case in which the changes are odd does not seem to evolve analogously to a sandpile model.

In the case that three incident edges at a vertex have the particular colors which make one of the three conditions of (2.1) saturated we call the vertex a *flat vertex*. If

the initial edge that has accepted $\triangle c$ is the one with the largest color value, adding $\triangle c = +2$ to it will violate gauge invariance. If the initial edge has the smallest color value, subtracting $\triangle c = -2$ from it will violate gauge invariance. A vertex such as this, where gauge invariance is violated (or the triangle relation fails for the dual triangle), will be called a *GNI*, for gauge, non-invariant vertex.

Models of this type fall into two classes according to whether the random changes are made at edges or nodes. In the first class, we choose *an edge* at random and change its color by an adding or subtracting Δc. In the second class we choose *a vertex* at random and change the colours of all the three edges of it by adding or subtracting Δc. We can think of the latter case as one in which closed loops of dual flux are added around each node, in rough analogy with the evolution rules in loop quantum gravity and spin foam models.

2.6.1 Random edge models

The evolution of spin network[4] can be defined as changing the colour of one edge, chosen at random, by $\triangle c = \pm 2$ and checking the conditions (2.1,2.2) at all vertices. The propagation rule for recovering the possible violation of the gauge conditions can be defined in different ways. The following are examples of possible propagation rules for this class of models.

I. In the case that adding colour +2 to the initial edge produces a GNI-vertex at its ends, the propagation rule on the vertex can be chosen to be:

   - adding $\triangle c = +2$ to one of the two less-coloured edges, or
   - adding $\triangle c = +2$ to both of the less-coloured edges, or
   - passing the added colour +2 from the initial edge to one of the two less-coloured edges.

II. In the case that subtracting colour -2 from the initial edge produces a GNI-vertex, the propagation rule can be chosen to be:

   - subtracting $\triangle c = -2$ from the largest edges, or
   - adding $\triangle c = +2$ to one of the less-coloured edges, or
   - adding $\triangle c = +2$ to both of the less coloured-edges, or
   - passing the added colour -2 from the initial edge to one of the other two edges.

In either case, we construct a model in which we:

- initialize a 2d spin network with random but gauge-invariant colours on its edges.
- choose an edge at random. and change its colour by adding (subtracting) to (from) a constant value of colour $\triangle c$.
- check gauge invariance condition (2.1,2.2) from the very first vertex to the last vertex.

[4]The spin network can be a planar or a closed network. By a closed spin network we mean a network in which there is no boundary in that and by walking on edges we will return to the initial point. For example a tetrahedron with 4 vertices and 6 edges can be thought of as a simple closed spin network.

- propagate $\triangle c$ from a GNI-vertex to other vertices by a propagation rule until the whole network becomes gauge invariant again.
- store the number of updated edges as the size of avalanche.
- repeat these steps a large number of times in order to see the behavior of spin network in a long time.

Borissov and Gupta (28) studied a particular propagation rule on a 2d planar spin network. The model has one parameter, which is a probability, p. The evolution rule is as follows. A vertex is chosen randomly. The edge with biggest colour among the three incident edges at a vertex is then evolved. The colour of that edge is increased by +2 with probability p or decreased, by -2, with probability $1 - p$. Similarly, if the arbitrary edge is the smallest one the colour -2 is subtracted from the edge with probability p or the colour +2 is added to that with probability $1 - p$.

They report that the rule, for different values of p, produces an exponential distribution of avalanches $P(s) \sim e^{-s/\sigma}$, where σ is the decay constant.[5] This evolution does not exhibit SOC on a 2d planar spin network. This means the process of the recovery of gauge invariance under the special propagation rule they have proposed, is not self-similar.

We have studied some of the above propagation rules for open 2 dimensional planar spin networks. In none of these cases did the distribution of avalanche show scale invariant behavior.

We also studied various rules for colours evolving on closed graphs including a tetrahedron and a network like a Bucky ball with 60 vertices and 90 edges. We did not see evidence of scale invariant behavior for any closed network we studied. We suspect that a closed system is less likely to exhibit scale invariant behavior because the flux cannot leave the system. (For a good review of the role of boundary in sandpile model refer to (32)). An SOC system is typically an open system, with a flow of energy or matter through it. It is the flow of energy or matter through the system that drives the self-organization of the system.

In order to understand these models, it is useful to consider the graphical representation shown in Figure 2.6.1. In the figure, we associate each of three axes with the colour on an edge incident to a given node.

The triangle inequalities (2.1) divide the 3d colour space into two different regions. All gauge-invariant vertices are located inside or on the boundary of a pyramid bounded by three surfaces, which are given by the equations,

$$a + b = c, \quad a + c = b, \quad b + c = a; \tag{2.4}$$

where a, b and c are the colours of the three incident edges on a vertex. We call the three boundaries *sheets of flatness*. These correspond to flat triangles. We call the region a *gauge invariant pyramid* [6].

For a sandpile to be in a critical state, a fixed fraction of the steps between sites must be at the critical value such that the addition of one grain of sand will cause an avalanche of shifts of grains. The flat triangles play the same role in this model, they are the triangles whose next evolution, by the addition or subtraction of loops of

[5] They report that σ reaches a maximum value when the probability p becomes close to 0.4.

[6] Note that not all of the points inside the pyramid are gauge invariant because a colour-point (which represents the colour condition of a vertex) should also satisfy (2.2)

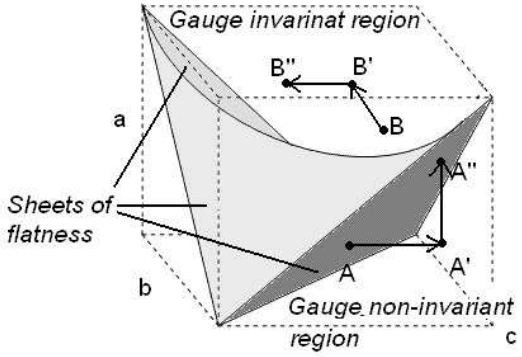

Figure 2.3: *3d colour space of each vertex.* All colour-points inside the pyramid satisfy the conditions (2.1, 2.2). Point A represents a flat vertex whose evolution kicks it out of the gauge invariant pyramid (A') and using a propagation rule can make it flat again. (A'')

flux, is likely to lead to gauge-non-invariant configurations. Hence in a critical state there must be a fixed fraction of such flat triangles. We will see that this expectation is satisfied when we find a set of rules that generates scale invariant distributions of avalanches.

In Borissov and Gupta's model the vertices whose colour-points are inside the gauge invariant pyramid (and are not flat) always are modified by the addition of positive colours. By adding a positive colour to one of the edges of such a vertex, its colour-point goes farther away from the origin of the colour space. Roughly speaking, in this situation the probability of finding the new colour-point on one of the sheets of flatness decreases. Therefore the probability of producing a flat vertex by a non-flat vertex is not high. In the simulation of the model it is clear that as time goes on, only small number of avalanches happen and for this reason the distribution of small size avalanches grows faster than larger ones. Thus the model does not exhibit a power law distribution of avalanches.[7]

2.6.2 Random vertex models

We now consider a different class of models, in which the evolution proceeds by adding or subtracting colour simultaneously on all edges incident to a single vertex. We call these *random vertex models.*

The motivation for these models comes from looking at Figure 2.6.1. We see that if we subtract colour from all three edges of a gauge invariant vertex (like B), the new point will be closer to one of the sheets of flatness. We then define a class of evolution rules based on choosing nodes rather than edges at random. In this class of rules, we will subtract the colour -2 from *all* three edges incident on the chosen node.

The result can be to violate the gauge condition at that node and/or at adjacent nodes. To recover gauge invariance we need to define a propagation rule. One of the possible candidates is add $+2$ to all the three incident edges at the GNI-vertex. We call this simple rule the *triangle propagation rule* because it adds three equal colours

[7]The fraction of flat triangles is related to the fact that those vertices which become flat initially remain on the sheet of flatness and after a while no more colour-points join the sheets.

to a trivalent vertex.

To specify the rule we have to give an ordering to the nodes. In our simulations, we use a simple ordering, left to right and top to bottom. We sweep the graph, checking the gauge invariance condition (2.1,2.2) at each node. When we find a GNI we act with the triangle propagation rule, by adding +2 to the colours on the edges incident to that node. When the checking is done once for all of the vertices, the sweep is repeated because new GNI-vertices may have been produced in the first sweep. We continue to repeat the propagation rule until all vertices become gauge invariant.

For example, consider the following network:

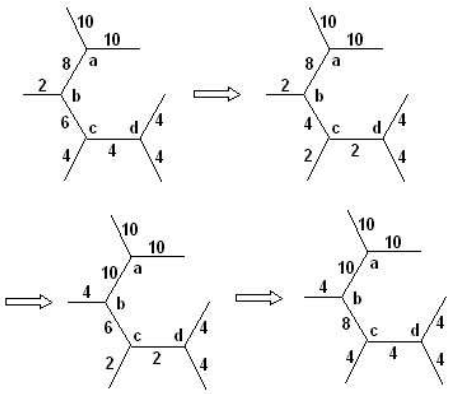

The first diagram shows a simple network. In the second step, it has been evolved by subtracting -2 from each edge incident to the vertex c. We then sweep the graph, from top to bottom and from left to right. Vertex c remains gauge invariant but b is not gauge invariant, so we act by adding +2 to each of its incident edges. But this makes c a GNI-vertex. In the fourth step, +2 has been added to the edges incident to the vertex c. Doing so, this new network becomes gauge invariant. The number of steps in the avalanche in this evolution is 2 because two vertices were updated in order to make the network gauge invariant.

Let's summarize the random vertex class:

- Initialize the spin network by assigning random colours to its edges, requiring only that gauge invariance is satisfied at each node.
- Choose a vertex at random.
- Subtract a triangle of -2 from the three edges of the initial vertex.
- Check the gauge condition (2.1,2.2) at all vertices, by sweeping through the nodes according to some fixed rule. Fix each GNI-node by adding a triangle of +2 colour to each edge of its dual triangle.
- Continue till the graph is again gauge invariant. Count the number of updated vertices. This is the size of the avalanche.
- Go back to the second step of the algorithm and repeat.

2.7 Results

We now report on the simulation of the rule just described, which did lead to scale invariant behavior.

We did the simulation for a 2d planar spin network with 570 edges and 361 vertices. For the initial start we assigned random even numbers between 10 to 30 to each edge, requiring only that the graph be gauge invariant initially. Using the rules just described, we evolved the spin network labels for ten million steps. The result is shown in Figure 2.7.

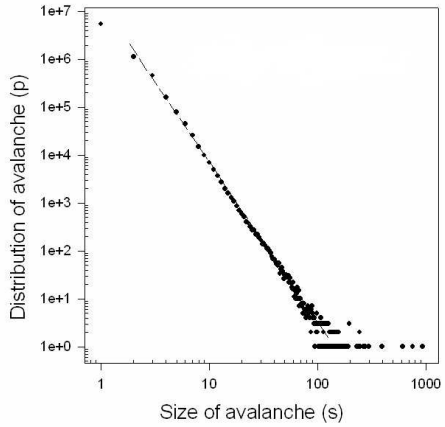

Figure 2.4: The log-log plot of the distribution of avalanche in a 2d planar spin network.

To completely define the evolution rule we mention:

- The nodes were always swept the same way, from left to right and up to down.
- It happens often that the colour on an edge is reduced to 0. The rules act on such edges as on the others, with the one exception that the -2 rule is never applied to a node when one of its edges is 0, as that would lead to an edge with a negative colour. However the triangle propagation rule acts on triangles with one or more edges zero as on other triangles. For example, a triangle with colours $(0, 18, 18)$ is gauge invariant, and so is skipped by the triangle propagation rule. But a triangle labeled $(0, 2, 4)$ is fixed, by adding $+2$ to each edge. The result is $(2, 4, 6)$, which is gauge invariant.

The distribution of the size of avalanches in a loglog scale behaves, to a good extent, linearly. Thus the dynamics of the triangle propagation rule on the spin network follows a power law and exhibits Abelian self-organized critical behavior. The relation between the distribution of avalanche and the size of avalanche is:

$$P(s) = s^{-3.3} \tag{2.5}$$

to a good accuracy.

In a SOC model usually both area and size of avalanches are checked to behave power-law distributions. Area is the number of sites involved in an avalanche, no matter how many times they topple. In other word, the area is where the avalanche is taking place, and usually for larger lattices one finds larger areas, because it has a

lattice dependent cut-off in its power-law distribution. If this distribution instead of being power-law is exponential, the avalanches do not expand in space and basically it does not matter if one takes a small or large lattice, as long as this is bigger than the maximum area that an exponential distribution is likely to give in finite samples (30).

To ensure this, we provide a typical plot of the distribution of area of avalanches. Figure 2.7 indicates the power-law behavior of area to a good accuracy in its distribution. Therefore, the macroscopic emerging of avalanches in space can be observed during this evolution of spin network. In other word, the avalanches do not resemble of some local resonances in a few nodes.

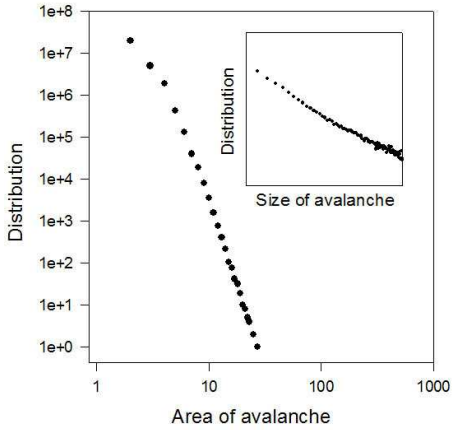

Figure 2.5: A typical log-log plot of the distribution of the area of avalanche and its corresponding log-log distribution of the size of avalanche.

In each time step of the evolution, we recorded the average of colours of the network and the fraction of the flat triangles, which are the cause of avalanche. In Figure 2.7 we see that the fraction of the number of flat vertices (or their dual triangles) is maintained about 0.3 during the simulation, while in Figure 2.7 we see how the average colour in the spin network fluctuate in time.

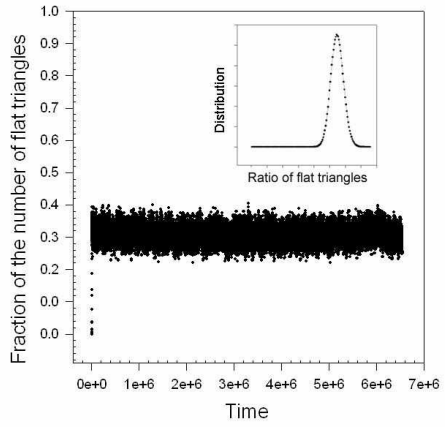

Figure 2.6: The fraction of flat triangles in time.

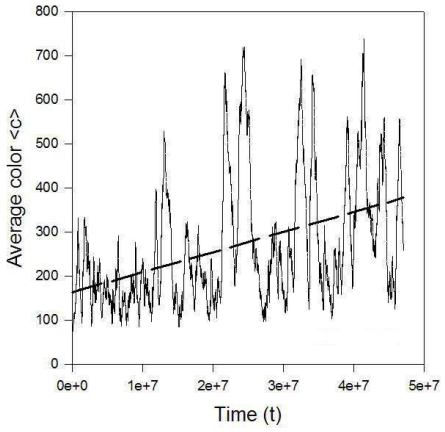

Figure 2.7: The average colour of the spin network in time in fifty million iterations.

As colour is proportional to length, Figure 2.7 exhibits a universe, described by our 2d planar spin network, expanding in time. The model, this is an example[8] of self-organization not to an attractor state, but to an asymptote, on which the average radius has a constant rate of inflation (expansion), is critical, and exhibits avalanches of activity with power-law distributed sizes. This example demonstrates that self-organized critical behavior occurs in a larger class of systems than so far considered: systems not driven to an attractive fixed point, but, e.g., an asymptote, may also display self-organized criticality.

Finally, it is instructive to see how the evolution rule studied here affects the dual geometry, expressed in terms of the triangulation. In the Figure 2.7 we follow a piece of a dual spin network, as it evolves. We see the evolution is irregular in both time and space. Nevertheless, when averaged over large times and distances, a scale invariant behavior emerges.

2.8 Conclusions

We have proposed a propagation rule for colours to evolve on a 2d planar open spin network, which appears to exhibit self-organized critical behavior.

It appears that with a special choice of evolution rule, the dynamics evolves the system to a dynamical equilibrium state, within which the behavior of the system appears to be scale invariant.

This work is a step in the investigation of the hypothesis that the emergence of our classical world from a discrete quantum geometry is analogous to a self-organized critical process. Among the further steps are 1) the study of models in which the underlying graphs themselves evolve by local rules, analogous to those studied here, 2) the study of other correlation functions, including those that would be interpreted as propagation amplitudes for matter and gravitational degrees of freedom, and 3) an increase in the valence, from three to four valent graphs, which is expected to correspond to the dynamics of geometry in 3+1 dimensions, and 4) the demonstration that self-organized critical phenomena exists for quantum evolution and not just for

[8]For another example see (33) and (34).

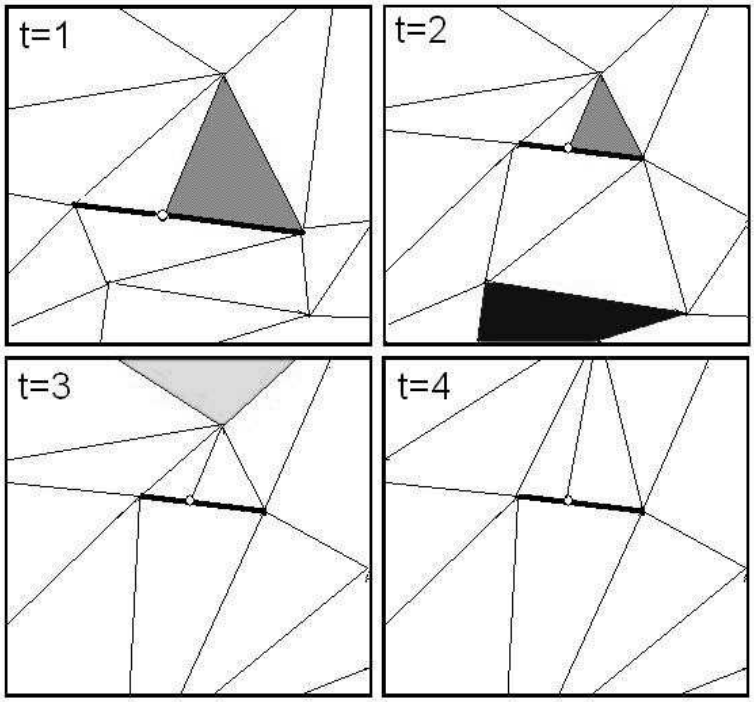

Figure 2.8: A few steps in the evolution of a part of a dual triangulation. The thick line (included a vertex in the middle) represents a flat triangle. At t=2, a triangle of colour -2 is added to the shaded triangle, shrinking its sides. The triangle inequalities are violated on some neighboring triangles and these are resolved by addition of a triangle of colour +2 to them. At t=3 we then iterate the procedure subtracting 2 from the edges of the black triangle and at t=4 we do the same to the bright gray one.

ordinary statistical systems.

Chapter 3

Statistical formalism for Causal Dynamical Triangulations

3.1 What is this about?

How a realistic universe can be constructed out of little space-time building blocks? Why the universe has 4 dimensions as how we experience?

Causal Dynamical Triangulations (CDT) is a model that claims it answers these questions. The construction of space-time out of geometrical building blocks has a long history. In all the previous models, people could not answer the main questions such as what asked above and some other questions such as the non-zero cosmological constant.

The triangulation of space time has been tried out so far in two main directions: 1) a triangulation called 'Dynamical Triangulations' in which the sides and angles of the building blocks are fixed and the interior region of a building block is completely flat; and 2) a triangulation called 'Regge calculus', in which the sides of the building blocks are subject to change. Each one of the two has some advantages but neither one is a complete model.

Let us discuss some of the problems within the Dynamical Triangulations. In this model, an Euclidean manifold is taken. The topology of the building blocks and the global space are both assumed. For instance, to build up a universe of three dimensions, tetrahedra are utilized. The tetrahedra are glued together from their sides with the hope that a three spatial piecewise manifold can be constructed out of them. However, this turns out to be problematic.

One of the problems is this may create a branch or a baby universe that may pop out of an extensive manifold. Such structures can increase the global dimension of the outcome space-time even up to infinity, thus is not a realistic universe. It is easier to imagine this in two dimensions. Assume we want to create a planar surface out of triangles. The sides of 6 triangles, all joint at one vertex, produce a planar surface. We can add more than 6 triangles to the vertex and as a result a curved surface is made. The main question is how one, who sits on the vertex, can find a local law that guarantees closing the composition of the triangles at the vertex such that a side of the last triangle is glued to a side of the first one. If this is not satisfied, a spiral of triangles continues around the vertex into infinity rounds that makes the vertex a singularity. These types of triangulations should be modified such that these

problematic structures are banned from being created. One of the modified models is Causal Dynamical Triangulations or CDT.

In CDT, we start off with the Lorentzian building blocks whose sides are both time- and space-like. The construction is now ruled strongly by causality in the presence of a preferred and external direction of time. This, when gives rise to a space-time, generates a finite dimensional space-time without any branch or baby universe. This has been so far checked to be correct in three and four dimensions. Therefore, from this point of view, Causal Dynamical Triangulations is the only successful model of general relativity that describes why does the universe we live in has only dimensions.

Despite all of the successes of CDT, this model suffers from some problems such as its violation of diffeomorphism invariance. In other words, it is not acceptable in general relativity that a preferred direction of time is pre-assumed. Therefore, a modifications to CDT is necessary. For this purpose, we need to understand this model is a less complicated approach than the original calculations. In the followings, we try to understand what is the statistics of the building blocks without pre-assuming whether they are boson, femion or any other objects. In fact, we derive the statistics of the triangles from within general relativity. Moreover, we try to understand what kind of restrictions causality applies on the critical exponents of the model. A similarity with a background independent anti-ferromagnetic system is derived and it is discussed how the universe can does a phase transition from a stable phase into other phases with different geometry.

3.2 Statistical formalism for Causal Dynamical Triangulations

We rewrite the 1+1 Causal Dynamical Triangulations model as a spin system and thus provide a new method of solution of the model.

3.3 Introduction

The failure of perturbative approaches to quantum gravity has motivated theorists to study non-perturbative quantization of gravity. These seek a consistent quantum dynamics on the set of all Lorentzian spacetime geometries.

One such approach which has led to very interesting results is the causal dynamical triangulation (CDT) approach(35; 36). In the interest of understanding why this approach leads to non-trivial results, in this thesis we study a reformulation of it as a spin system. The basic idea is that causal structure is coded into the values of a set of spins, in such a way that causal relations are expressed as constraints on the allowed spin configurations. This makes possible a new method of studying the model which is complementary to that used in the original thesis. In this thesis we study only the $1 + 1$ dimensional model(35), but we believe the method described here generalizes to higher dimensions and can include matter.

In the next section, we review the CDT model in $1+1$ dimensions and the solution to it given by Ambjorn and Loll in (35). In section 3, we reformulate the CDT model as a spin system, which we call the statistical model. In section 4, we show how to solve the model by a procedure made natural by the translation of the model into a spin

system. In section 5, we discuss the application to the model of the renormalization group, after which we close with a brief discussion of what we learned about quantum Lorentzian geometry from the translation to a spin system.

3.4 Definition of the model

In this section, we review Causal Dynamical Triangulations, as defined in (35).

Causal Dynamical Triangulations is arrived at by a discretization of the path integral for quantum general relativity in $1+1$ dimensions. In 1+1 dimensions, the continuum Einstein action is

$$S[g] = \Lambda \int \sqrt{-g}\, dA, \tag{3.1}$$

where $g = det\,(g_{ab})$, and $a, b = 0, 1$. dA is the element of area and Λ is the cosmological constant. The metric g_{ab} represents the geometry of space-time.

We define the amplitude to evolve from an initial geometry, which is a circle of length l_0, to a final geometry, a circle of length l_t, formally by

$$\mathcal{A}[l_0, l_t] = \int d\mu[g_{ab}] e^{iS[g]}, \tag{3.2}$$

where the sum is over geometries with fixed topology $S^1 \times [0, 1]$, $d\mu[g_{ab}]$ is the measure and the boundaries of the histories are two circles of lengths l_0 and l_t.

We now discretize this path integral. A given history is represented by a set of t spacelike circles (or rings), which are labeled $S_{(i)}$. These are considered time slices in some fixed gauge (40). Each ring has l_i vertices, connected by edges which are assumed to be of length unity in Planck units. It is required that every time-slice has at least one edge.

The vertices of two adjacent loops are connected by a set of timelike edges of length-squared $-a^2$. These define the causal structure of the discrete history and are chosen so that the surface is broken up into triangles. To ensure this, the leftmost future vertex of a vertex i-th of $S_{(t)}$ is the rightmost future vertex of the vertex $(i+1)$-th of the same ring. A triangle has one space-like edge, which sits on one of the space-like edges of $S_{(t)}$ and two timelike edges, which connect two vertices of $S_{(t)}$ to either one vertex of $S_{(t+1)}$ ("up" triangle), or two vertices of $S_{(t-1)}$ ("down" triangle). Each history is then a piecewise flat Lorentzian geometry. In each triangle $g = -1$, and the action becomes $S = \lambda A$, where A is the summation of the areas of triangles. The area of each Lorentzian triangle is $\frac{\sqrt{5}}{2}a^2$ (39). Therefore, the action of a time-slice consisting of n triangles is $S = \lambda n \frac{\sqrt{5}}{2} a^2$. We absorb the factor of $\frac{\sqrt{5}}{2}$ in λ and the action becomes $S = \lambda n a^2$.

The path integral amplitude for the propagation from geometry l_1 and l_2 is the sum

$$\mathcal{A}[l_0, l_t] = \sum_{\text{histories}} e^{i\lambda A}, \tag{3.3}$$

over all such piecewise flat manifolds defined in this way with initial and final circles fixed. Note that the cosmological constant Λ is replaced by the "bare" cosmological constant λ. Note also that topology change is excluded by the requirement that each history have topology $S^1 \times [0, 1]$.

In summary, the following are key assumptions of the model:

1. *Fixed topology*: the topology of the boundaries and interpolating spacelike slices is S^1 and each history is $S^1 \times [0,1]$. Each slice has length ≥ 1.
2. *The amplitudes are given by a path integral*: the amplitude of propagation from the initial ring to the final ring is given by the sum over all interpolating histories.
3. *Histories are triangulations*: the leftmost future vertex of a vertex i-th of $S_{(t)}$ is the rightmost future vertex of vertex $(i+1)$-th of $S_{(t)}$.

3.4.1 Review of the generating function method

In this subsection we review briefly the method of solution of the problem given in (35).

Let there be l_t vertices in $S_{(t)}$ and l_{t+1} vertices in $S_{(t+1)}$. If k_i vertices of $S_{(t+1)}$ are in the future of the vertex i of $S_{(t)}$ then, because of condition 3, the total number of vertices of $S_{(t+1)}$ is $l_{t+1} = \sum_{i=1}^{l_t} (k_i - 1)$. The two spatial rings are connected by $\sum_{i=1}^{l_t} k_i$ triangles; l_t of which are "up" and l_{t+1} are "down".

To propagate from l_0 to l_1 in one time-slice, the action is $S = \lambda a^2 \sum_{i=1}^{l_t} k_i$ and the amplitude is

$$G(\lambda, l_0, l_1; \Delta t = 1) = \frac{1}{l_0} \sum_{\{k_1, \ldots, k_{l_0}\}} e^{i\lambda a^2 \sum_{i=1}^{l_0} k_i}. \tag{3.4}$$

Generally, if we mark the vertices of the initial ring, the amplitude becomes

$$G_*(\lambda, l_0, l_t; \Delta t = t) = l_0 G(\lambda, l_0, l_t; \Delta t = t), \tag{3.5}$$

where the G_* denotes that the vertices of the initial ring are marked. If we mark the vertices of the final loop, the amplitude becomes

$$G_*^*(\lambda, l_0, l_t; \Delta t = t) = l_0 l_t G(\lambda, l_0, l_t; \Delta t = t). \tag{3.6}$$

Using the conditions 2 and 3, the corresponding amplitude between times $t = 0$ and $t = 2$ can be written as:

$$G(\lambda, l_0, l_2; \Delta t = 2) = \sum_{l_1=1}^{\infty} G(\lambda, l_0, l_1, \Delta t = 1)\, l_1 G(\lambda, l_1, l_2, \Delta t = 1). \tag{3.7}$$

With marked initial vertices, the amplitude is:

$$G_*(\lambda, l_0, l_2; \Delta t = 2) = \sum_{l_1=1}^{\infty} G_*(\lambda, l_0, l_1, \Delta t = 1)\, G_*(\lambda, l_1, l_2, \Delta t = 1). \tag{3.8}$$

Thus, we are able to write the amplitude of evolution from $t = 0$ to $t = t$ with l_0 initial vertices and l_t final vertices as:

$$G_*(\lambda, l_0, l_t; \Delta t = t) = \sum_{l_1=1}^{\infty} G_*(\lambda, l_0, l_1, \Delta t = 1)\, G_*(\lambda, l_1, l_t, \Delta t = t - 1). \tag{3.9}$$

To solve equation (3.9), we Laplace transform it,

$$G_*\left(x,y,\Delta t=t\right)\equiv\sum_{k,l=1}^{\infty}x^l y^k G_*\left(\lambda,k,l;\Delta t=t\right), \tag{3.10}$$

with the definitions $g:=e^{i\lambda a^2}$, $x:=e^{i\lambda_0 a}$ and $y:=e^{i\lambda_t a}$ in which λ_0 and λ_t are the cosmological constant on the initial and final boundaries respectively. Using the Laplace transformation (3.10) on equation (3.9), we obtain the one-time-step G_*:

$$G_*\left(x,y,g,\Delta t=1\right)=\frac{g^2xy}{\left(1-gx\right)\left(1-gx-gy\right)}. \tag{3.11}$$

The amplitude in terms of $g^m x^n y^p$ defines the region of convergence $|g|\leq 1/2$, $|x|\leq 1$ and $|y|\leq 1$. The iterative relation on the Laplace transformed amplitude is then

$$G_*\left(x,y,g,\Delta t\right)=\frac{gx}{1-gx}G_*\left(\frac{g}{1-gx},y,g;\Delta t-1\right). \tag{3.12}$$

Ambjorn and Loll in (35) showed that the iterative relation can be written in a simpler way:

$$G_*\left(x,y,g,t\right)=\frac{F^{2t}\left(1-F^2\right)^2xy}{\left(A_t-B_tx\right)\left(A_t-B_t\left(x+y\right)+C_txy\right)}, \tag{3.13}$$

$$F=\frac{1-\sqrt{1-4g^2}}{2g},\quad A_t=1-F^{2t+2},\quad B_t=F\left(1-F^{2t}\right),\quad C_t=F^2\left(1-F^{2t-2}\right).$$

The corresponding equations for the Laplace transformed amplitudes are:

$$G_*\left(x,y,g,\Delta t=t\right)=x\frac{d}{dx}G\left(x,y,g,\Delta t=t\right), \tag{3.14}$$

$$G^*_*\left(x,y,g,\Delta t=t\right)=y\frac{d}{dy}G_*\left(x,y,g,\Delta t=t\right). \tag{3.15}$$

The asymmetry between x and y in the expression (3.11) is due to the marking of the initial ring. If we also had marked the final ring, the corresponding generating function would be obtained from $G_*\left(x,y,g;\Delta t=1\right)$ by acting with $y\frac{d}{dy}$ (which is equivalent of multiplying $G_*\left(l_0,l_1,g,\Delta t\right)$ by l_1):

$$G^*_*\left(x,y,g;\Delta t=1\right)=\frac{g^2xy}{\left(1-gx-gy\right)^2}. \tag{3.16}$$

The corresponding generating function $G^*_*\left(x,y,g;\Delta t=t\right)$ is obtained from $G_*\left(x,y,g;\Delta t=t\right)$ by acting with $y\frac{d}{dy}$,

$$G^*_*\left(x,y,g;\Delta t=t\right)=\frac{F^{2t}\left(1-F^2\right)^2xy}{\left(A_t-B_t\left(x+y\right)+C_txy\right)^2}. \tag{3.17}$$

In the continuum limit we expect that the bare propagators are subject to a wave-function renormalization. However, all coupling constants with positive mass dimension undergo an additive renormalization, while the partition function undergoes a

multiplicative wave-function renormalization (38). The only non-trivial continuum limit of eq. (3.13) is obtained when $|F| \to 1$, so $F = e^{i\alpha}$ for $\alpha \in \mathbf{R}$. The singular Green's function can be cured by multiplying it by a cut-off dependent factor (38). This limit is equivalent to $|g| = \frac{1}{2cos\alpha}$. Thus, from the convergence condition, we find $g = \pm 1/2$ (at $\alpha = 0, \pi$).

3.5 The dual statistical model

We now recast the 1+1-dimensional Causal Dynamical Triangulations model as a spin system with certain constraints on their configurations and couplings, reflecting the geometric properties of the CDT.[1]

We proceed as follows. Each triangle i will be regarded as a spin σ_i. We associate to each down triangle (with two vertices on $S_{(t)}$ and one on $S_{(t-1)}$) an up spin and to each up triangle (with two vertex on $S_{(t)}$ and one on $S_{(t+1)}$) a down spin. Spins can take two possible values, $\sigma_+ = gx$ when they come from an up triangle, and $\sigma_- = gy$ when they correspond to a down triangle. The spins will live on a trivalent lattice and we find it convenient to graphically denote the two states of a spin as:

$$\sigma_i := \begin{cases} \sigma_+ = gx, & \text{ 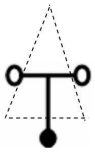 } \quad \text{“spin down”}, \\ \\ \sigma_- = gy, & \text{ 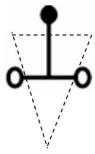 } \quad \text{“spin up”}. \end{cases} \tag{3.18}$$

The dashed line represents the triangle dual to each spin. Each spin has one black head and two white head, which are dual to one spacelike edge and two timelike edges, respectively.

Gluing two triangles along a common edge defines a spin-spin interaction. The CDT weighing of the triangulations means there are two kinds of interactions: gluing two triangles along their space-like edges gives a spin-spin interaction of strength J_S, while a gluing of two timelike edges corresponds to coupling J_T as follows:

$$J := \begin{cases} J_S & = \frac{1}{xy}, & \text{spacelike} \\ J_T & = 1, & \text{timelike.} \end{cases} \tag{3.19}$$

No gluing of a timelike to a spacelike edge is allowed. We have incorporated these couplings to the graphical notation (3.18): the interaction between two black heads of two spins occurs with the spin-spin interaction coupling J_S, and the interaction between two white heads does with a J_T coupling.[2]

In an ordinary spin system, the values of spins are not related to the structure of the lattice. The lattice is fixed while the values of the spins on the nodes vary.

[1] Another statistical mechanical approach to the CDT model is developed in (37)”

[2] Sometimes in this thesis we call J_T coupling the “white interaction” because of the coupling it provides between two white heads, and J_S coupling the “black interaction” because of the coupling it provides between two black heads.

However, in a model of gravity we do not have any pre-assigned lattice, since the space-time is completely dynamical. In our formalism space-time is created by the configurations of the spins.

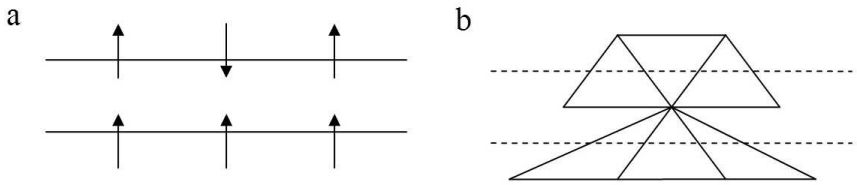

Figure 3.1: a) An arbitrary spin configuration and b) the dual geometry

Let us look at a simple example to explain how the spins relate to the causal structure and geometry. In Figure 3.5(a), we see a lattice consisting of two rows with a certain number of spins. In an ordinary spin system without an external field, the spins fluctuate independently of the lattice. However, in our model, the spins define the causal structure of the resulting geometry. Following the rules just described, Figure 3.5(a) is interpreted as a dual geometry, shown in Fig. 1(b). We see from Figure 3.5(b) that the spins in Fig. 1(a) define a geometry that does not satisfy the causality constraints of CDT. The dual space-time is not causal as there are vertices in the second slice that have no past in the initial slice.

We will impose constraints on the dual spin system so that all spin configurations have dual CDT histories:

1. *Causality constraint:* Each up spin in row t ($t < t_{final}$) must be coupled to a down spin in row $t+1$, with coupling J_S.
2. *Non-degeneracy constraint:* Every row has at least one spin.

A spin system that satisfies these constraints is dual to a history of the CDT model. [3]

It is instructive to give an example of a spin configuration that does satisfy the causality constraints. The triangulation

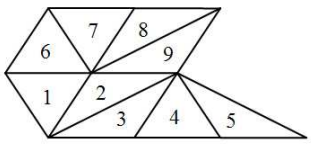

(3.20)

in the dual spin system is:

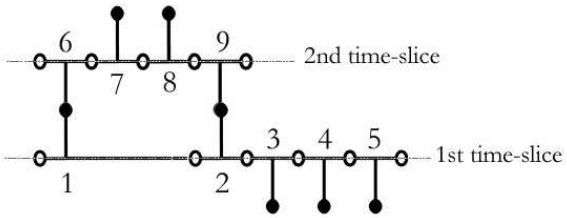

(3.21)

[3]From the point of view of statistical physics, the present model is analogous to a "diluted" 2 dimensional classical Ising model because the number of spins in each time-slice can vary (see, for example, (41)).

The amplitude of this history is:

$$A = (\sigma_1 J_S \sigma_6)\ J_T\ \sigma_7\ J_T\ \sigma_8\ J_T\ (\sigma_9 J_S \sigma_2)\ J_T\ \sigma_3\ J_T\ \sigma_4\ J_T\ \sigma_5 = g^9 x^4 y^2. \qquad (3.22)$$

Note that the dual spin system can be read as a history somewhat analogous to a Feynman diagram. The history of (3.21) begins with three initial black circles, and ends with two final black circles. In between there are two moments of discrete time, given by the rows of J_T couplings. There are no unpaired black or white circles, except for the initial and final black ones (recall that we have cylindrical boundary conditions on the boundary white ones).[4]

Next, we use this definition of the model to count the 2d CDT histories.

3.6 Computing CDT amplitudes using the dual spin system

We now want to calculate the 1+1 CDT path integral amplitude from a given initial ring to a given final ring, using the dual spin system. Here, the evolution amplitude is given by a correlation function between the spins of the boundary rows.

We will find it convenient to introduce a notion of effective spins, which allows us to sum the causal histories.

3.6.1 Single-row configurations

We will illustrate the spin system solution by first calculating the CDT amplitude for a single row of spins. This means all spin configurations on rows containing from one to infinite number of spins, subject to the causality and non-degeneracy constraints.

In fact, for one row, we only have the non-degeneracy constraint, which we impose using what we call "the box". A box is two spins with opposite orientations, with one J_T coupling. This is denoted by

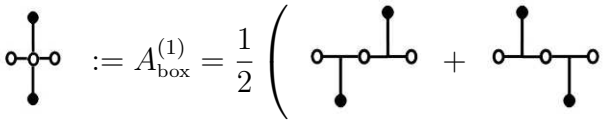

$$:= A^{(1)}_{\text{box}} = \frac{1}{2}\left(\quad + \quad \right) = g^2 xy. \qquad (3.23)$$

The superindex $^{(1)}$ is a reminder that we are working with one-row configurations. The geometric constraint is equivalent to requiring that each row must contain *at least one box*.

For a single row of spins, there are no J_S couplings and we have simply the combinatorics of spins attached to a box. In a row of N spins, two of them have to make a box, and are no longer free to be up or down[5], hence,

$$A^{(1)}_N = c_N A^{(1)}_{box} \left(\sum_{i=1,2} \sigma_i \right)^{N-2}, \qquad (3.24)$$

where c_N is the number of ways of choosing two consecutive marked spins (the box) among N spins, $c_N = \frac{2}{N}\binom{N}{N-2} = N-1$.

[4] An example of the spacetime structure with equal intermediate rings can be thought of as the tower of Pizza (from above of which Galilei did his famous gravitational experiment).

[5] Since the spins are located on a closed chain, the amplitude is not sensitive to locations of spins. On the other hand since the free black heads on the initial and final rings are marked, different location of A_{box} among spins is counted as a different configurations.

For example, for $N = 4$:

$A^{(1)}_{N=4} =$ 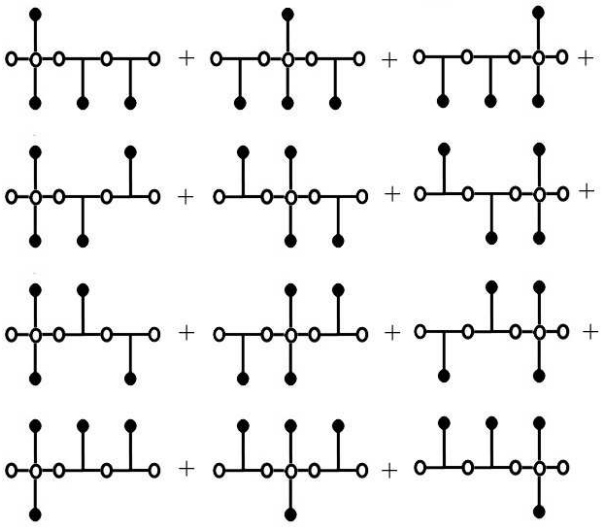

$$= 3A^{(1)}_{\text{box}} \left(\sum_{i=1,2} \sigma_i \right)^2 = 3 \left(g^2 xy \right) (gx + gy)^2 . \tag{3.25}$$

This amplitude is actually the Laplace transformed amplitude, similar to a Greens function. In the dual triangulation, the Laplace inverse transform of the above is the amplitude to go from an initial ring of length l_0 to a final ring of length l_1. So we have to add up all Laplace transformed amplitudes for different ring lengths (spin number and configurations) to derive the Green's function.

The single-slice amplitude, $A^{(1)}$, is

$$A^{(1)} = \sum_{N=2}^{\infty} A^{(1)}_N = A^{(1)}_{\text{box}} + g^2 xy \sum_{N=3}^{\infty} (N-1)\, g^{N-2} (x+y)^{N-2} . \tag{3.26}$$

To perform the sum, we redefine $n = N - 2$ to obtain:

$$\begin{aligned} A^{(1)} &= g^2 xy \left[1 + \sum_{n=1}^{\infty} (n+1)\, g^n (x+y)^n \right] \\ &= g^2 xy \sum_{n=0}^{\infty} (n+1)\, g^n (x+y)^n . \end{aligned} \tag{3.27}$$

We now define the quantity $A := g\,(x+y)$, so that the above equation can be rewritten as

$$A^{(1)} = g^2 xy \sum_{n=0}^{\infty} (n+1)\, A^n . \tag{3.28}$$

For $|A| \leq 1$, eq. (3.28) sums to the same result of (3.16):

$$A^{(1)} = \frac{g^2 xy}{(1-A)^2} = \frac{g^2 xy}{(1-gx-gy)^2} . \tag{3.29}$$

Non-marked vertex amplitude

Comparing the amplitude (3.29) with the results of (35), we see our result is symmetric on x and y since both our up and down spins are marked. To derive the exact result of Ambjorn and Loll in (35) we need unmarked up spins.

We can illustrate this for $N = 4$:

$A^{(1)}_{*N=4} =$

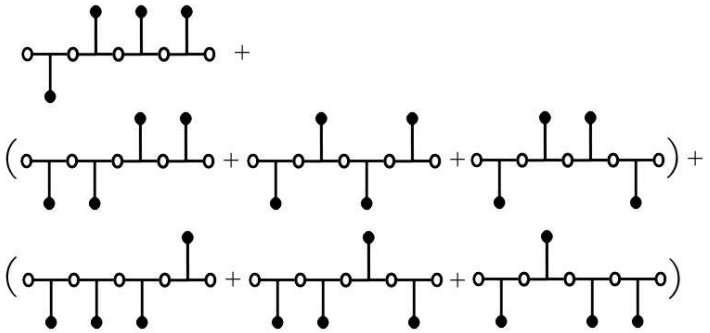

$$= g^4 xy\left(y^2 + 3xy + 3x^2\right). \tag{3.30}$$

Since the top black circles are not distinguished, we have only one term with 3 up spins. For two up spins there are three terms, for the possible permutations of the two marked down spins, etc.

Summing over all spins, we find the unmarked amplitude $A^{(1)}_*$ for one row to be:

$A^{(1)}_* =$

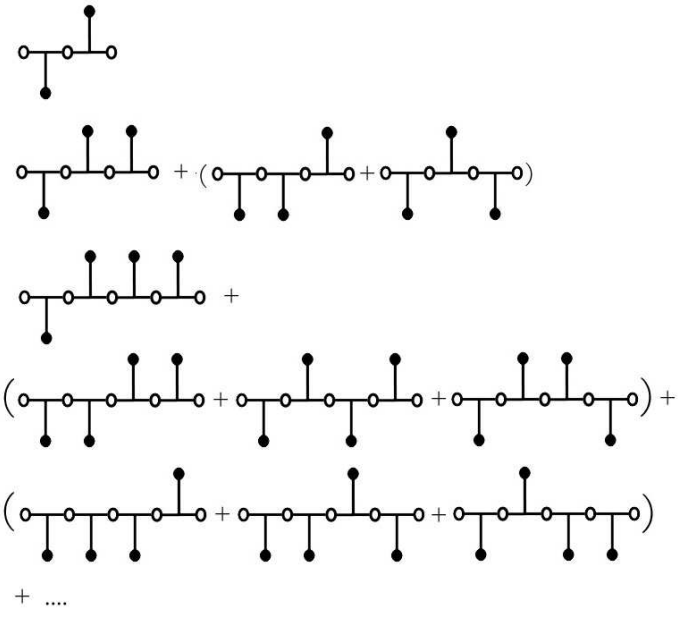

$$= g^2 xy + g^2 xy\,(gy + 2gx) + g^4 xy\left(y^2 + 3xy + 3x^2\right) + \ldots. \tag{3.31}$$

To sum the infinite series we use a simple trick. We add and subtract $1 + gx + g^2x^2 +$

$g^3x^3 + \ldots$ from the amplitude (3.31) to find

$$\begin{aligned} A_*^{(1)} &= \Big(1 + gx\left(1 + gy + g^2y^2 + \ldots\right) + g^2x^2\left(1 + gy + g^2y^2 + \ldots\right)^2 + \ldots\Big) \\ &\quad - \left(1 + gx + g^2x^2 + g^3x^3 + \ldots\right) \\ &= \frac{g^2xy}{(1-gx)\,(1-gx-gy)}, \end{aligned} \tag{3.32}$$

which is the same result of the unmarked one-step transfer matrix amplitude (3.11). It is easy to see that using the eq. (3.15),

$$A^{(1)} = y\frac{d}{dy}A_*^{(1)}. \tag{3.33}$$

In fact $A^{(t)}(x, y, g)$ (the corresponding amplitude of marked initial and final spins in t slices) is exactly equivalent to the $G_*^*(x, y, g, t)$ solution of the generating function method.

3.6.2 Two-row configurations: the effective spin $\Sigma^{(2)}$

Our solution of the CDT departs from the transfer matrix method of (35) when more than one row is considered. For a spin configuration of n rows of spins, we will introduce an effective spin $\Sigma^{(n)}$ which makes the n rows of spins σ_i a single row of these effective spins. Once the appropriate form of the effective spin has been found the remaining calculation is very straightforward. [6]

The form of the effective spin $\Sigma^{(n)}$ is different for odd or even n. We start with the 2-row effective spin $\Sigma^{(2)}$. This effective spin has the form

$\Sigma^{(2)} =$ 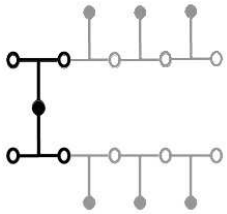 (3.34)

where the gray spins denote rows with spins from zero to infinity so that the above diagram is

$$\Sigma^{(2)} = (gx)\;\; J_S\,(gy) \sum_{l_0=0}^{\infty} (gx)^{l_0} \sum_{l_1=0}^{\infty} (gy)^{l_1} \tag{3.35}$$

$$= \frac{g^2}{(1-gx)\,(1-gy)} = \frac{g^2}{(1-\sigma_+)\,(1-\sigma_-)}. \tag{3.36}$$

Note that the solid black part of $\Sigma^{(2)}$ is the implementation of the causality constraint for two rows.

To calculate the two-row amplitude $A^{(2)}$, we first need $A^{(2)}_{box}$. The diagram of $A^{(2)}_{box}$ differs from $\Sigma^{(2)}$ in that in $\Sigma^{(2)}$ the number of the gray spins run from zero to infinity

[6] Let us remind that any horizontal sequence of black heads make a time-slice as well as any horizontal sequence of white heads.

while in $A^{(2)}_{box}$ they run from one to infinity. In other words, the presence of at least one up spin in the final row and one down spin in the initial row is guaranteed. However, the end row spins are distinguishable and have to be counted separately. We thus easily find the amplitude for $A^{(2)}_{box}$ to be:

$$A^{(2)}_{box} = (gx)\, J_S\,(gy) \sum_{l_0=1}^{\infty} l_0\,(gx)^{l_0} \sum_{l_1=1}^{\infty} l_1\,(gy)^{l_1} = \frac{g^4 xy}{(1-\sigma_-)^2\,(1-\sigma_+)^2}. \tag{3.37}$$

The amplitude $A^{(2)}$ is obtained from all possible configurations of effective spins attached to one $A^{(2)}_{box}$. Since the spins are marked, as in the amplitude of the one-row case, the position of $A^{(2)}_{box}$ has to be taken into account. The final result is:

$$A^{(2)} = A^{(2)}_{box} \sum_{N=0}^{\infty} (N+1)\left(\Sigma^{(2)}\right)^N = \frac{A^{(2)}_{box}}{\left(1-\Sigma^{(2)}\right)^2}. \tag{3.38}$$

3.6.3 The odd and even effective spins

We can now generalize the method we used to count one- and two-row Green's functions to the general case. We shall find it useful to consider separately the cases of even and odd numbers of slices. Since there is no interaction between a white and a black head, we can divide interactions and cover all black interactions by defining the notion of effective spin, and white-interact them along their common time-slice (-slices).

Note that, in the one-row case, there were two values of spin σ, up and down. In the two-row case, there is only one type of effective spin. This generalizes: even-row configurations can be mapped to single-row with one type of effective spin, while odd-row configurations need two-valued effective spins.

Odd effective spins

It is instructive to find the effective spin for three rows first. One can see that all three-row configurations can be constructed from these two building blocks:

$$\Sigma^{(3)} := \begin{cases} \Sigma^{(3)}_+ = \frac{g^2}{1-\sigma_+}, & \text{ 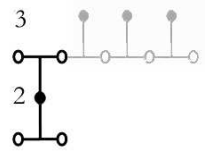 } \quad \text{“three-row effective up spin”} \\ \Sigma^{(3)}_- = \frac{g^2}{1-\sigma_-}, & \text{ 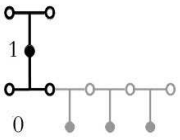 } \quad \text{“three-row effective down spin”}. \end{cases} \tag{3.39}$$

The labels 0, 1, 2 and 3 on the black heads denote the order of the rows, from initial, 0, to final, 3. There are two different sequences of σ_i spins in each one of the effective spins. $\Sigma^{(3)}_+$ has a sequence of σ_+ spins in row 3, while $\Sigma^{(3)}_-$ has a sequence of σ_- spins in row 1. Again, the number of gray spins varies from one to infinity.

$\Sigma_-^{(3)}$ and $\Sigma_+^{(3)}$ can white-interact by their common white heads. In fact, any the connection between the initial slice (the zeroth row) and the final slice (the 3rd row) occurs if and only if at lease one $\Sigma_-^{(3)}$ white-interacts with at least one $\Sigma_+^{(3)}$. This minimal interaction makes $A_{box}^{(3)}$.

We evaluate $A_{box}^{(3)}$ as previously. We need at least one $\Sigma_+^{(3)}$ and one $\Sigma_-^{(3)}$ in each configuration. The initial and final loops all spins are marked and thus it matters which one of the gray spins we convert to a black spin (whose presence is necessary in A_{box}). Thus, like (3.23) we have:

$$\begin{aligned} A_{box}^{(3)} &= \frac{1}{2}\left(g^2\sum_{l_0=1}^{\infty} l_0\,(gx)^{l_0}\right) J_T \left(g^2\sum_{l_3=1}^{\infty} l_3\,(gy)^{l_3}\right) \\ &+ \frac{1}{2}\left(g^2\sum_{l_3=1}^{\infty} l_3\,(gy)^{l_3}\right) J_T \left(g^2\sum_{l_0=1}^{\infty} l_0\,(gx)^{l_0}\right) \\ &= \frac{g^6 xy}{(1-\sigma_-)^2\,(1-\sigma_+)^2} \\ &= g^2 A_{box}^{(2)}. \end{aligned} \tag{3.40}$$

The three-row amplitude is now easily derived from the possible configurations of N effective spins on a single $A_{box}^{(3)}$:

$$A^{(3)} = A_{box}^{(3)}\sum_{N=0}^{\infty}(N+1)\left(\Sigma_+^{(3)}+\Sigma_-^{(3)}\right)^N = \frac{A_{box}^{(3)}}{\left(1-\Sigma_+^{(3)}-\Sigma_-^{(3)}\right)^2}. \tag{3.41}$$

Generalizing this, it is straightforward to check that, for odd-row configurations, $\Sigma_\pm^{(j)}$, $A_{box}^{(j)}$ and amplitude $A^{(j)}$ are:

$$\Sigma_-^{(j)} = \frac{g^2}{1-\Sigma_-^{(j-2)}}, \qquad \Sigma_+^{(j)} = \frac{g^2}{1-\Sigma_+^{(j-2)}}, \tag{3.42}$$

$$A_{box}^{(j)} = g^2 A_{box}^{(j-1)}, \tag{3.43}$$

$$A^{(j)} = \frac{A_{box}^{(j)}}{\left(1-\Sigma_+^{(j)}-\Sigma_-^{(j)}\right)^2}, \tag{3.44}$$

where $j = 1, 3, 5\ldots$.

Even effective spins

To find a generalized formula for even rows, it is useful to study first the case of four rows.

The easiest way to calculate the corresponding effective spin in four rows is by comparing it with the two rows. We take the two components of $\Sigma^{(3)}$ as the new fundamental spins so that $\Sigma^{(4)}$ has the same form as $\Sigma^{(2)}$ (3.34), but with the $\Sigma_\pm^{(3)}$

replacing the $\sigma_{\pm}$:

$$\Sigma^{(4)} = \frac{g^2}{\left(1-\Sigma_+^{(3)}\right)\left(1-\Sigma_-^{(3)}\right)}. \tag{3.45}$$

We can now calculate $A_{box}^{(4)}$. Diagrammatically, it is

$A_{box}^{(4)} =$ 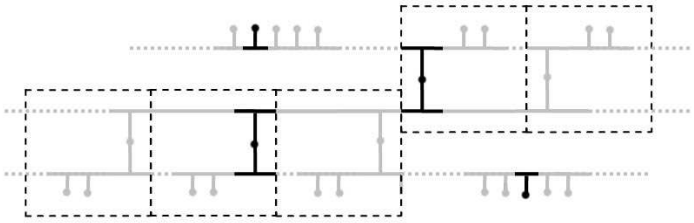

Each box represents a $\Sigma^{(3)}$ spin and the number of boxes ranges from zero to infinite. In the $A_{box}^{(4)}$ diagram, we should guarantee the existence of at least two "**I**" shapes for the two intermediate slices. One of them is located inside one of the bottom row of boxes and the other one inside one of the top ones. In the above diagram they were indicated in black colour. In addition to these two "**I**" shapes, we must also guarantee the existence of at least one $\Sigma_-^{(1)}$ (i.e. σ_-) in the initial time-slice and one $\Sigma_+^{(1)}$ (i.e. σ_+) in the final time-slice, in order to connect initial and final rings with the least number of connections between slices. How can we choose the $\Sigma_-^{(1)}$ and $\Sigma_+^{(1)}$ spins? A suggestion is that they are chosen among the other gray $\Sigma^{(1)}$ spins inside the boxes. Although, the suggestion is problematic because, in general, the two $\Sigma^{(1)}$ spins may appear inside two boxes that are different than the previously guaranteed ones. Therefore the existence of such boxes, which support the two $\Sigma^{(1)}$ spins, should be guaranteed first. The existence of the box requires the existence of its "**I**" shape part. Turning on more gray "**I**" shapes, does not meet the initial motivation of defining the notion of A_{box}, which was any necessary connection between the initial and final rings such that at every ring the existence of only *one spin* is guaranteed (due to non-degeneracy constraint).

Another suggestion for supporting the existence of these two $\Sigma^{(1)}$ spins is that some $\Sigma^{(1)}$ spins live independently (with respect to boxes) on the initial and final rings and among them the existence of one up and one down ones is guaranteed. The idea is acceptable since it meets the condition of the least number of guaranteed spins among the most arbitrary configuration of connections between the initial and final rings (which is 6 in this case).

Therefore the weight of $A_{box}^{(4)}$ can be generally written:

$$\begin{aligned} A_{box}^{(4)} &= g^6 xy \left[\sum_{M=1}^{\infty} M\left(\sigma_+\right)^M \cdot \sum_{N=1}^{\infty} N\left(\sigma_-\right)^N \cdot \sum_{L=1}^{\infty} L\left(\Sigma_+^{(3)}\right)^L \cdot \sum_{K=1}^{\infty} K\left(\Sigma_-^{(3)}\right)^K \right] \\ &= \frac{g^6 xy}{\left(1-\sigma_+\right)^2\left(1-\sigma_-\right)^2\left(1-\Sigma_+^{(3)}\right)^2\left(1-\Sigma_-^{(3)}\right)^2}. \end{aligned} \tag{3.46}$$

The final amplitude then is:

$$A^{(4)} = A^{(4)}_{box} \sum_{N=0}^{\infty} (N+1) \left(\Sigma^{(4)}\right)^N = \frac{A^{(4)}_{box}}{\left(1-\Sigma^{(4)}\right)^2}. \tag{3.47}$$

Similarly, for the general even-j rows, the effective spin, $A^{(j)}_{box}$ and general amplitude $A^{(j)}$ are:

$$\Sigma^{(j)} = \frac{g^2}{\left(1-\Sigma^{(j-1)}_{+}\right)\left(1-\Sigma^{(j-1)}_{-}\right)}, \tag{3.48}$$

$$A^{(j)}_{box} = \frac{g^{2(j-1)}xy}{\prod_{i=1}^{j-1}\left(1-\Sigma^{(i)}_{+}\right)^2\left(1-\Sigma^{(i)}_{-}\right)^2}, \tag{3.49}$$

$$A^{(j)} = \frac{A^{(j)}_{box}}{\left(1-\Sigma^{(j)}\right)^2}, \tag{3.50}$$

where $j = 2, 4, 6 \ldots$.

3.7 Renormalization Group

Our aim in this section is to study the continuum limit of the statistical model we defined. This is the limit in which the number of rows goes to infinity. We do this by deriving a fine-grained correlation function and searching for critical behavior in which the Green's functions scale. This is straightforward because the method we have used to solve the model already involves defining and summing effective spin degrees of freedom.

It is important to note that the definition of effective spins which then live on a one-dimensional chain, key to our solution, works for 1+1 CDT because the space-like and time-like couplings scale differently and there is no coupling between time-like and space-like edges.

We denote the effective spin in the continuum limit by $\Sigma^{(\infty)}$. In this limit, there is only one component for the effective spin. Also, there is no difference between even and odd slices.[7] The effective spin weighs:

$$\Sigma^{(\infty)} = \cfrac{g^2}{1-\cfrac{g^2}{1-\cfrac{g^2}{1-\cfrac{g^2}{1-\ddots}}}} = \frac{1-\sqrt{1-4g^2}}{2}. \tag{3.51}$$

We now can apply a renormalization group transformation, acting on a chain of infinite-row effective spins. In the continuum limit, it is not necessary to consider the $A^{(\infty)}_{box}$ since it is only one of the effective spins and the system is big enough to consist of many effective spins. With this simplification, the amplitude of a chain with N spins is

$$A^{(\infty)}_N \simeq \Sigma^{(\infty)}_1 \Sigma^{(\infty)}_2 \Sigma^{(\infty)}_3 \cdots \Sigma^{(\infty)}_N. \tag{3.52}$$

[7] Using the equation (3.48) for the only component of the effective spin, we see the spin is invariant under the transformation $\Sigma^{(\infty)} = \frac{g^2}{1-\Sigma^{(\infty)}}$. Therefore in the continuum limit, there is no difference between odd and even effective spins.

Rescaling of the Green's function of the amplitude of gravity happens when the critical exponent of dimensional rescaling factor is one (35). We start fine-graining the above amplitude to

$$A^{(\infty)}_{\frac{N}{2}} \simeq \Sigma^{(\infty)}_1 \Sigma^{(\infty)}_3 \Sigma^{(\infty)}_5 \cdots \Sigma^{(\infty)}_{\frac{N}{2}}. \tag{3.53}$$

The renormalization group provides us with a specific parameter value with which the amplitude is conformally invariant. This occurs when three of finer spins are conformally equivalent to the resealed amplitude of two coarser spins:

$$\Sigma'^{(\infty)}_1 \Sigma'^{(\infty)}_3 = 2\ \Sigma^{(\infty)}_1 \Sigma^{(\infty)}_2 \Sigma^{(\infty)}_3, \tag{3.54}$$

where 2 is the dimensional rescaling factor.

Substituting equation (3.51) in (3.54) we obtain

$$\left(\frac{1-\sqrt{1-4g'^2}}{2}\right)^2 = 2\ \left(\frac{1-\sqrt{1-4g^2}}{2}\right)^3.$$

We now see that g' and g have a non-linear relation:

$$g' = \pm\frac{1}{2}\sqrt{1-\left(1-\left(1-\sqrt{1-4g^2}\right)^{\frac{3}{2}}\right)^2} =: \pm f\left(g\right), \tag{3.55}$$

or, graphically, [8]

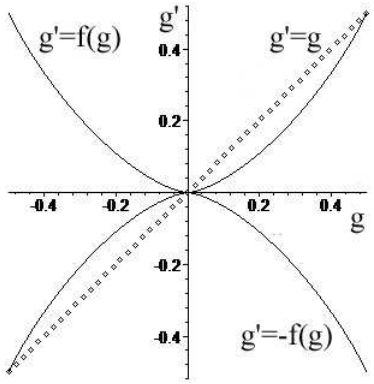

We can iterate this coarse-graining to produce a coarser one-dimensional chain. One can see that, after a few iterations, the triangular coefficients approach the fixed points $g = 0$ and $g = \pm\frac{1}{2}$. This result agrees with the continuum limit of the Causal Dynamical Triangulation model(35).

Inserting $\Sigma^{(\infty)}$ in equations (3.49) and (3.50), we find that

$$A^{(\infty)}_{box} = \lim_{j\to\infty} \frac{g^{2(j-1)}xy}{\left[\left(1-\sigma^-\right)\left(1-\sigma^+\right)\left(1-\Sigma^{(3)-}\right)\left(1-\Sigma^{(3)+}\right)\ldots\left(1-\Sigma^{(j-1)-}\right)\left(1-\Sigma^{(j-1)+}\right)\right]^2} \tag{3.56}$$

[8] There is also another possible relation $g' = \pm\frac{1}{2}\sqrt{1-\left(1+\left(1-\sqrt{1-4g^2}\right)^{\frac{3}{2}}\right)^2}$, whose fixed point is at $g = 0$.

and, therefore, the amplitude in the continuum limit is:

$$\begin{aligned} A^{(\infty)} &= \frac{A_{box}^{(\infty)}}{\left(1-\Sigma^{(\infty)}\right)^2} \\ &= \frac{4A_{box}^{(\infty)}}{\left(1+\sqrt{1-4g^2}\right)^2}. \end{aligned} \tag{3.57}$$

The denominator in the region of convergence (where $|g| \leq 0.5$, $|x| \leq 1$ and $|y| \leq 1$) is always positive and non-zero.

Note that the denominator of equation (3.56) is an infinite product of terms, each term defined recursively from the previous terms. Since the limit of the effective spins is $\Sigma^{(\infty)}$, we can approximate $A_{box}^{(\infty)}$ with its limit:

$$A_{box}^{(\infty)} \leq \lim_{j\to\infty} \frac{g^{2(j-1)}xy}{\left(1-\Sigma^{(\infty)}\right)^{4(j-1)}}. \tag{3.58}$$

3.8 Discussion

In this thesis we constructed a spin system with constraints that provides a dual description of the 1+1 Causal Dynamical Triangulation model of (35). By inventing a notion of effective spins, we were able to solve the model. We should emphasize that the fact the model is solvable is not new, and the solution we find is completely equivalent to that of the original thesis of Ambjorn and Loll (35). However, the dual spin model gives an alternative way of understanding what it means to define a sum or path integral over causal structures. As such, we expect it may be useful in higher dimensions and when matter is included.

In closing we make a few observations that may be useful for future work in this direction.

- Our effective spins are quite different from the ones used in coarse-graining of standard spin systems. Here the effective spins really carry out the sum over spin lattices necessary in a quantum gravity model.
- There is an analogy between curvature and the Hamiltonian of an antiferromagnetic spin system. The reason is that a triangulated 2d flat spacetime corresponds to the case in which the triangles in each time slice alternate between up and down triangles. In the dual spin system this is a configuration in which up spins alternate with down spins. Also, the causality conditions require that the spins alternate between up and down in the time-like direction. Hence, if the ground state of the gravity theory for small cosmological constant is locally approximated by flat spacetime, this will correspond to a configuration of spins which alternates in both the space and time directions. This suggests that the ground state of the gravity system should resemble the ground state of a two-dimensional antiferromagnetic system. Whether this generalizes in higher dimensions will be investigated in future work.
- In the CDT model, a Euclidean continuation is made which maps the quantum gravity system in 1+1 dimensions to a classical statistical system in 2 dimensions.

We note that it may be possible instead to use the method described here to map the quantum gravity system to a one-dimensional quantum spin chain and solve it directly as a quantum mechanical system.

Chapter 4

Generic degeneracy in loop quantum gravity

4.1 What is this about?

The idea of Isolated and Dynamical Horizon theory was first worked out by Heyward in 1994, (44). He derived the complete definition of a marginally null surface that is trapped on a black hole horizon. A few years later, using Hayward's completed results, Ashtekar and his colleagues re-wrote the same theory in the language of Ashtekar-Sen variables, (11). This work in its classical approach does not add anything into what has been known before then.

However, some interesting results come up when they quantized Heyward's isolated horizon theory by the use of principles of loop quantum gravity. Before this development Rovelli has argued that a black hole entropy should be proportional with its horizon area. Lee Smolin linked loop quantum gravity to topological field theory and argued that a black hole should be described by a Chern Simon's action. Later on, Krasnov based on that idea argued the derivation of a black hole entropy from the counting of puncture states. Ashtekar, Krasnov, Baez and Corichi based on the quantization of Hayward's isolated horizon theory, later on, claim that they have found a way to describe the entropy of black hole microscopically, (45).

Today it is known that the justification of black hole entropy by a quantum isolated horizon becomes possible only and only if the horizon area cells of a black hole are '*assumed*' to be distinguishable from one another. Why? There is no concrete reason for this. Some experts say there is a straightforward response to the question of why the punctures are distinguishable, which is that they are distinguished by their connections to a spin network outside of the surface. If that state is complicated enough it can serve to distinguish the punctures where the graph ends. This argument has a main obstacle: in Loop Quantum Gravity one counts those black hole states which can interact with the outside world, whence the entropy refers to the microstates of the boundary itself. If the network outside of the surface is changed such that the links of two punctures A and B are swapped, the two systems A and B become indistinguishable again. As a consequence, the external states affects the number of horizon degrees of freedom. By induction, this can be extended into all of the punctures residing on the horizon.

The second restriction of a quantum isolated horizon is that one begins with a

suitably restricted sector of general relativity and then carries out quantization. This is nothing but an effective description of a quantum black hole and should not be taken too seriously. For thermodynamic considerations involving large black holes, effective descriptions seems to be adequate, but it is important to note that an isolated horizon provides an entropy that matches semi-classical one by over-counting the physical degrees of freedom.

Some experts explain the distinguishablity of punctures by assuming a conjecture on the action of isolated horizon. Since an isolated horizon in Ashtekar-Sen variable language is described by the Chern-Simons action, a 'sequence' of punctures on a horizon explains the wave function of the horizon. Being a sequence, the punctures are ordered and this make them distinguishable. However, as it is clear, there is no absolute physical reason why should one restricts the wave functions into a sequence of punctures instead of a set of punctures in which there is no generic order.

In summary, if the entropy of an isolated horizon is determined only by counting the number of degrees of freedom that '*reside on the horizon*' the distinguishability of the punctures cannot be linked to the external network and its complication! In fact, if this is done, again by any change in the external states the horizon entropy becomes affected and reduced. If all of the physical diffeomorphism invariant degrees of freedom are counted, what an isolated horizon is left with is an entropy that is proportional maximally to $\sqrt{A}$ and no more.

In general, the problem of describing a black hole entropy by microstates if is not justified, it is a failure for a quantum gravity. We describe here is that loop quantum gravity is enriched with another argument of black hole entropy description that does not suffer from the diffeomorphism violation problem.

In this work, we reveals an internal degeneracy that provides the Bekenstein-Hawking entropy for a black hole. This is the only correct entropy reported for a black hole that is described microscopically within loop quantum gravity without any pre-assumption for the distinguishability of the area cells. The area operator in its form of definition in loop quantum gravity contains a degeneracy that is enough for the purpose of determining a black hole entropy. Since the area eigenstates are insensitive to the completely tangential edges residing on the horizon, these edges provides a complete distinguishability of the area cells.

In this picture, the complete spectrum of area is used. This way of looking into a black hole that contains the complete spectrum of area, it seems that any surface contains an entropy proportional to the surface area. Although an entropy-like number is associated with any surface, this reveals that the difference between a black hole horizon and other random cauchy surfaces is not in their kinematical entropy. Black hole as is known is a dynamical entity. According to the second thermodynamics law of black hole this number should be non-decreasing. This important property recognizes a black hole horizon from a random cauchy surface. When in the course of time it is seen a surface evolves such that its entropy-like number in all time is non-decreasing that surface could be a candidate for being a black hole horizon. This is very interesting picture because the new approach towards understanding a quantum black hole via the evolution of spin network although is not a complete model from its dynamical view, this is a treasure model that links cryptography and one way quantum information flow problems directly into loop quantum gravity.

During the last two years after introducing this new picture, this picture has been

taken into some research group attention: including the Tokyo group of Tanaka and Tamaki who are working on the definition of a black hole via the complete spectrum of area, the Madrid group of Diaz-Polo and Fernandes-Borja who are working on Black hole radiations, the canadian group of Freidel and Ryan who are working on Spin Foam Model, as well as the group of Koster, Bunnlund and DeBenedictis who are working on higher genus horizon, and some others.

Let us summarize:

1. The area operator and its eigenvalues and eigenstates are known for years since 1994 in Smolin and Rovelli's works (59) and later on in its full spectrum form by Ashtekar, Lewandowski (60) and separately by Rovelli and Ferrittelli (70).

2. The degeneracy we report here is heavily certain and is a fact behind the definition of the area operator. It is valid as long as the complete spectrum of area in loop quantum gravity is valid.

3. Isolated horizon theory cannot justify a black hole entropy without over-counting the degrees of freedom.

4. We report Bekenstein-Hawking entropy of black hole after removing all (and not only a few) of non-physical degrees of freedom. The justification is heavily certain.

5. This opens a new school of thought about defining a quantum black hole. The idea this justification proposes is why not we try to understand a quantum black hole from the evolution of spin network states, instead of recognizing it via the evolution of the classical manifold underlying the spin network. Quantum world is different from a Classical one and the definition of localization and semi-causality being of a black hole in these two worlds are drastically different.

4.2 Generic degeneracy in loop quantum gravity

Without imposing the trapping boundary conditions and only from within the very definition of area it is shown that the loop quantization of area manifests an unexpected degeneracy in area eigenvalues. This could lead to a deeper understanding of the microscopic description of a quantum black hole. If a certain number of semi-classically expected properties of black holes are imposed on a quantum surface its entropy coincides with the Bekenstein-Hawking entropy.

4.3 Introduction

In the early works on black holes in loop quantum gravity (42), it was first understood that a black hole entropy can be derived from the internal boundary of space without imposing any boundary condition. The underlying details of this picture was later on recovered when the definition of a marginally trapped surface (43) was rewritten in the Ashtekar-Sen variables and this definition was extended into a quantum sector (45). Such a surface after quantization contains a finite number of degrees of freedom and consequently carries an entropy that coincides with the Bekenstein-Hawking

black hole entropy, [1]. In this thesis by the use of the same setting similar to the one of original works by Rovelli (42), we show that area operator acting on a typical inhomogeneous surface state manifests a degeneracy that here is worked out in both SO(3) and SU(2) group representations. This degeneracy exhibits a scale invariant correlation with area with the same exponent in both groups. However, this is not the only degeneracy an area eigenvalue is left with. Recently it was understood in (14) that the complete spectrum of area can be re-classified into different equidistant subsets. This symmetry (the so-called ladder symmetry) increases the total degeneracy such that the degeneracy of a large area eigenvalues becomes proportional to its area exponentially. Moreover, we present the derivation of the Bekenstein-Hawking expression for the entropy of a Schwarzschild black hole of large surface area by the use of Dreyer's conjecture (47) that the minimal area of a hole in its dominant configuration should be identified with the emissive quanta from a perturbed black hole in highly damping mode. This motivates a rather different picture of a quantum horizon whose precise dynamical definition perhaps should be looked at from within a spin foam model, (48).

In loop quantization approach to quantum gravity the kinematical state space is taken to be L^2(connections on SU(2) bundle). For any graph with finitely many edges and vertices embedded in a spatial manifold, the space of connections is $\mathrm{SU}(2)^n$ (or alternatively $\mathrm{SO}(3)^n$) where n is the number of edges. In fact, a connection on a graph tells us how to parallel transport information along each edge of that graph. The canonical conjugate of this connection field represents the quantum geometry of space. The space of physical states is obtained by imposing constraints: the gauge-invariance, the diffeomorphism invariance, and the invariance under time evolution.

Given a graph and a surface in space, the area operator is supposed to be the quantum analog of the usual classical formula for the area of S. This operator only cares about the points where the graph intersects the surface. A subset of surface states which has no node residing on the surface was originally considered by Smolin and Rovelli where they derived their eigenvalues in (59). Later on, all possible states of a surface were considered and the complete spectrum of area eigenvalues were found from different approaches, (50). From the calculation, it was uncovered that those edges which are completely tangential to the surface do not contribute in the surface area, albeit the tangent vectors of crossing edges do contribute in it.

An edge with respect to an underlying surface falls into two classes. It may

- cross the surface at one intersecting point and bend at the surface on the point to induce a tangent vector on the surface, or
- reside completely tangential to the surface.

A spin network with respect to three different surfaces S_1, S_2, and S_3 is shown in Figure (4.1). The quantum state of surface S_3 contains the bulk edges j_u and j_d and their tangent vector j_{u+d} at their joint node. Note that the quantum states corresponding to the surfaces S_1 and S_2 contain the edges of equal spins on both sides without bending at these surfaces.

The area eigenvalue associated with a typical quantum state $\langle j_u, j_{u+d}, j_d, j_t|$ is $a = m_{j_u, j_{u+d}, j_d}\ a_o$,

[1] Recently a different approach towards this entropy from the use of quantum information theory techniques in Loop Quantum Gravity has also been developed in (46).

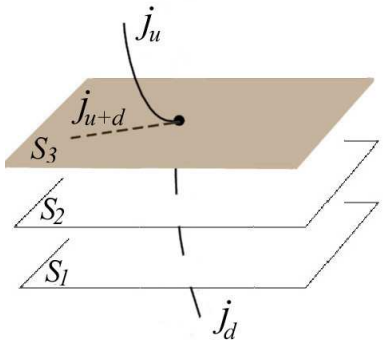

Figure 4.1: The position of a surface relative to spin network.

$$m_{j_u,j_{u+d},j_d} = \sqrt{2f(j_u) + 2f(j_d) - f(j_{u+d})}, \tag{4.1}$$

where $f(x) = x(x+1)$ and $a_o := 4\pi\gamma\ell_{\rm P}^2$. The parameter γ is a dimensionless parameter called the Barbero-Immirzi parameter (51) and $\ell_{\rm P}$ is the Planck's length $\sqrt{\hbar G/c^3}$. Moreover, the tangent vector accepts a finite number of quantum values from the following spectrum:

$$j_{u+d} \in \{|j_u - j_d|, |j_u - j_d| + 1, \ldots, j_u + j_d\}. \tag{4.2}$$

The tangent vector at a node is a spin between the sum and difference of crossing edges at the node and resembles the total vector of two quantum angular momenta (i.e. spin and orbital angular momenta) in the Hydrogen atom. This pictorially is shown in Fig. (4.2) where the case (a) indicates $j_{u+d} = j_u + j_d$ and the case (c) indicates $j_{u+d} = |j_u - j_d|$. The case (b) in Figure (4.2) shows an intermediate value for the tangent vector between the maximum and minimum.

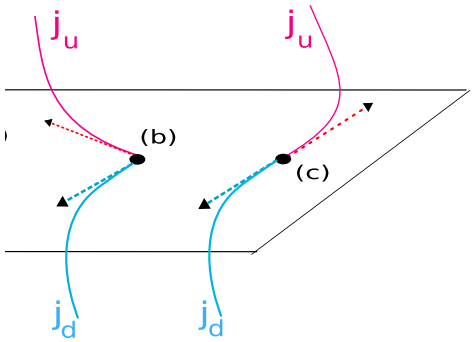

Figure 4.2: Different components of the tangent vector of the upper and lower spins on the surface. The dashed arrows in blue and red colours corresponds to the edges in the lower and upper side.

Let us now describe a subset of eigenstate that was reported first by Smolin and Rovelli as the area eigenstates in (59). At a vertex if neither one of the upper and lower edges bends at the surface, the tangent vector becomes zero. In the lack of the completely tangential edges at the vertex, due to the gauge invariance, the upper and lower spins must be equal. The quantum of area in this case becomes $a =$

$2a_o\sqrt{j(j+1)}$. Therefore, the subset includes only those states with puncturing edges without bending at it.

Consider now a closed surface that divides space into two disjoint subsets of interior and exterior regions. Since such a surface has no boundary a few additional vertices are needed in order to close its corresponding spin network. This makes unwanted contributions to the action of the area operator via the constraints:

$$\sum_\alpha j_u^{(\alpha)} \in \mathrm{Z}^+, \quad \sum_\alpha j_d^{(\alpha)} \in \mathrm{Z}^+, \tag{4.3}$$

where α indicates the vertices of the graph. Note that these constraints are trivially satisfied in the SO(3) representation of the spin network states, because the spins are already in pairs (integer numbers). However, in $SU(2)$ group representations some spin network states are excluded by (4.3).

4.4 Generic degeneracy

For a given j_u and j_d a set of eigenvalues is generated from a minimum value (where $j_{u+d} = j_u + j_d$) to a maximum value (where $j_{u+d} = |j_u - j_d|$) by (5.8). Changing either j_u or j_d, a different finite set of area eigenvalues is generated whose elements may or may not coincide with the elements of other set of area eigenvalues. Generating area eigenvalues from different eigenstates indicates that the spectrum of eigenvalues becomes denser in larger area. All of the eigenvalues are unexpectedly degenerate. In fact *there exist a finite set of eigenstates that correspond to every area eigenvalue.*

Let us consider the first four area eigenvalues in SO(3) group as samples. These are $a_{\min} = \sqrt{2}a_o$, $a_2 = 2a_o$, $a_3 = \sqrt{6}a_o$, and $a_4 = 2\sqrt{2}a_o$, respectively. Note this a_4 is the minimal eigenvalue of the subset that was first discovered as the spectrum of area eigenvalues by integer spins. This area has been considered many times in the literature as the minimal area cell in the dominant configuration of a black hole horizon (i.e. see (42; 45; 46; 47)); however it is the double of the minimal area eigenvalue $a_{\min}$ in the complete spectrum of (5.8).

The table (4.1) shows the detail of area states corresponding to these four area eigenvalues.

area	j_u	j_{u+d}	j_d	area	j_u	j_{u+d}	j_d	area	j_u	j_{u+d}	j_d
$a_{\min}$	0	1	1	a_3	0	2	2	a_4	1	0	1
$a_{\min}$	1	1	0	a_3	1	1	1	a_4	1	4	3
$a_{\min}$	1	2	1	a_3	2	2	0	a_4	3	4	1
a_2	2	4	2	a_3	2	5	3	a_4	3	7	4
a_2	2	3	1	a_3	3	5	2	a_4	4	7	3
a_2	1	3	2	a_3	3	6	3	a_4	4	8	4

Table 4.1: The eigenstates corresponding to the first four SO(3) eigenvalues.

The three states corresponding to the minimal area are: 1) the state with the upper spin one edge crossing the surface and bending at it on the point. Such an edge induces all of its spin to the surface at the point. However a completely tangential edge is necessary to lie on the surface and ends at that point in order to make this state gauge invariant off the surface. 2) The state with lower spin one edge similar to the previous state. 3) The state with the upper and lower spins one edges bending at

the surface such that their tangent vector come along each other in the same direction. This tangent vector could also connect to other completely tangential excitations on the surface.

In SU(2) group the eigenstates of the first six eigenvalues are tabulated in the table (4.2). These eigenvalues are: $a_{\min} = \frac{\sqrt{3}}{2}a_o$, $a_2 = a_o$, $a_3 = \frac{\sqrt{7}}{2}a_o$, $a_4 = \sqrt{2}a_o$, $a_5 = \frac{\sqrt{11}}{2}a_o$, and $a_6 = \sqrt{3}a_o$. Note that the sixth eigenvalue is in fact the minimal area applied in the literature so far for the purpose of black hole entropy calculation in this group.

area	j_u	j_{u+d}	j_d	area	j_u	j_{u+d}	j_d	area	j_u	j_{u+d}	j_d
$a_{\min}$	0	$\frac{1}{2}$	$\frac{1}{2}$	a_4	0	1	1	a_6	$\frac{1}{2}$	0	$\frac{1}{2}$
$a_{\min}$	$\frac{1}{2}$	$\frac{1}{2}$	0	a_4	1	1	0	a_6	$\frac{1}{2}$	2	$\frac{3}{2}$
a_2	$\frac{1}{2}$	1	$\frac{1}{2}$	a_4	1	2	1	a_6	$\frac{3}{2}$	2	$\frac{1}{2}$
a_3	$\frac{1}{2}$	$\frac{3}{2}$	1	a_5	1	$\frac{5}{2}$	$\frac{3}{2}$	a_6	$\frac{3}{2}$	3	$\frac{3}{2}$
a_3	1	$\frac{3}{2}$	$\frac{3}{2}$	a_5	$\frac{3}{2}$	$\frac{5}{2}$	1				

Table 4.2: The eigenstates corresponding to the first six SU(2)-valued spin networks.

The minimal area in this group is degenerate in the two states each with a crossing spin one-half edge bending at the surface. In these states there must be at least one completely tangential edges of spin one-half connecting to the intersecting point.

Note that in the degenerate eigenvalues we investigated here, which are the first a hundred levels, there is only one state that exceptionally does not appear as a degenerate state and that is the state with area a_2 in SU(2) group. In this state the upper and lower edges of spins one-half connect at a vertex and bend at the surface along the same direction.

We counted the number of the degeneracy g for different eigenvalues in scatterplots and the area and its degeneracy appeared to be correlated in Figure 4.3. These scatterplots indicates the results in SU(2) and SO(3) group representations of spin networks separately in the log-log graphs.

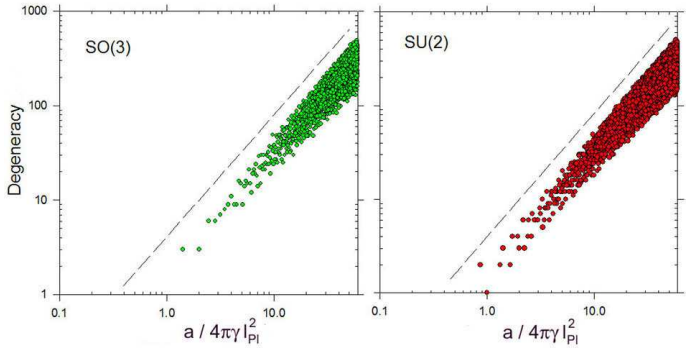

Figure 4.3: The scatterplot of correlation between the area eigenvalues and the degeneracies of their corresponding eigenstates.

The eigenvalue degeneracy grows roughly as a power-law but with increasing scatter, namely

$$g(a) \approx \left(\frac{a}{a_o}\right)^{\alpha+\epsilon}, \tag{4.4}$$

where $\alpha = 0.96$ with the scatter uncertainty $\epsilon = \pm 0.03$.

This particular degeneracy is scale invariant and robust, however we will show in this thesis this is not the only degeneracy of eigenvalues.

For the purpose of further clarifications, we plot the minimal area levels and their corresponding degeneracy separately in Figure (4.4).

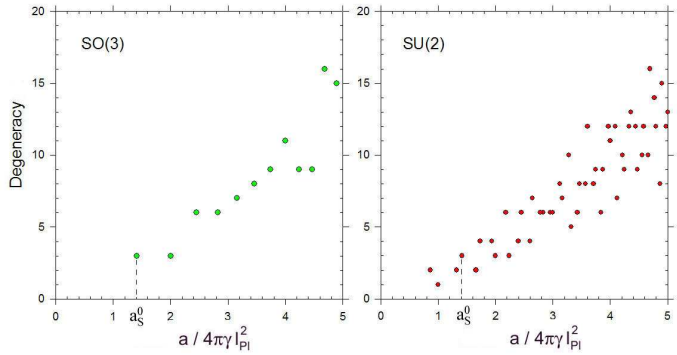

Figure 4.4: The scatterplot of a few first area level degeneracies.

In fact it is obvious that we do not need two different plots for the SO(3) and SU(2) groups because the spectrum of area in the SO(3) group is contained in the SU(2) group degeneracy graph. For instance, in Figure (4.4) we named the minimal area in the SO(3) group by a_o^S and showed this area is the fourth level in the SU(2) group. More importantly this is the reason why the exponent of the power law (4.4) in the both group representation is the same.

Recently the complete spectrum of area was proved to be the union of equidistant spectra, (14). Each one of the subsets possesses a gap between levels equal to $a_o\chi\sqrt{\zeta}$. In SO(3) group ζ is any square-free number $\{1, 2, 3, 5, \cdots\}$ and the group characteristic parameter is $\chi := \sqrt{2}$; and in SU(2) group ζ is the discriminant of any positive definite form $\{3, 4, 7, 8, 11, \cdots\}$ and the group characteristic parameter is $\chi := 1/2$. In other words, the complete spectrum reformulates into $a_n(\zeta) = a_0\chi\sqrt{\zeta}n$ for $\forall\ n \in \mathbb{N}$. Fixing ζ a generation of evenly spaced numbers is singled out. The parameter ζ is therefore called the generational number.

Based on this classification, one can re-classify the generic degeneracy of area levels into the generations. Plots (a-e) in Figure (4.5) indicates this classification in the first five generation. Plot (f) compares the degeneracy of the first level of different generations.

Note that in any generation the area of higher levels can be decomposed precisely into smaller fractions of the same generation (without approximation) namely, $a_n = na_1 = (n-2)a_1 + a_2 = \cdots$. Let us consider for instance the configuration na_1. Each one of these area cells is degenerate. However, the states corresponding to the eigenvalue in different regions of the surface are distinguishable because by definition various number of completely tangential edges with various spins could be connected to each vertex without changing the area and the geometric configurations. Therefore, the degeneracy of the area eigenvalue a_n is in fact $\Omega_n = g_n + g_{n-1}g_1 + \cdots + (g_1)^n$. Obviously the dominant term in the sum belongs to the configuration with maximum number of the area cell a_1.

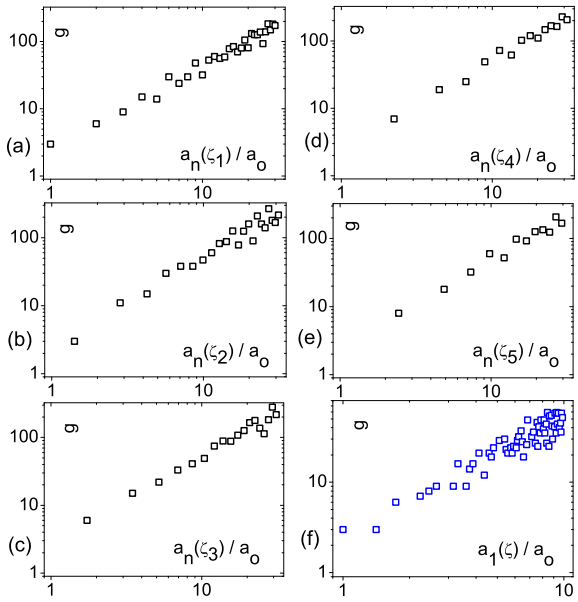

Figure 4.5: The generic degeneracy of figure (4.3) classified into generation in SO(3) group case.

4.5 Entropy

Consider a surface S of a large area A. This area is the sum of quanta in different configurations. In the dominant configuration it contains the maximum number (N) of minimal degenerate area cell; $A \approx N a_{\min}$, where $N \gg 1$. Let us now consider a surface that is a black hole horizon. By the use of the Einstein's equation for a collapsing star from a non-spherical state all radiatable perturbations to the surface are shown to be radiated away such that at the late stage the hole is left only with its monopoles. Now imagine the initial deformation is located in a certain region of the horizon. The future evolution of the field from that point depends on the exact spin network state of that location, which includes the states of completely tangential excitations. The state evolves under the action of a Hamiltonian and is expected to radiate away energy from the event horizon. Therefore, in the quantum states of a black hole the complete information of spin network states makes regions distinguishable from each other, although they may appear with the same area. Having defined the dominant configuration for the surface, the degeneracy of this configuration is therefore $\Omega(A) = g(a_{\min})^N$. Consequently, the dominant entropy associated to the underlying surface is proportional to $N \ln g(a_{\min})$ or equivalently

$$S = A \ \ln g(a_{\min})/a_{\min}. \tag{4.5}$$

It is instructive to compare this result with the result coming out of the Isolated Horizon picture. In that picture the hole separates the space manifold into two sections, namely a horizon boundary and the outer space. Gauge degrees of freedom are still considered to be redundant in the bulk states but they become physical

degrees on the boundary. The reason is that the kinematical Hilbert space of space includes the Hilbert spaces of the horizon $\mathcal{H}_s$ and the bulk $\mathcal{H}_b$. The reduction of gauge degrees of freedom from this space takes place only in the bulk partition because $\{\mathcal{H}_s \otimes \mathcal{H}_b\}/SU(2) \sim \mathcal{H}_s \otimes \{\mathcal{H}_b/SU(2)\}$. This means the horizon Hilbert space accepts the gauge transformation redundancies as the physical states. An edge of spin j puncturing the boundary produces $2j+1$ physical states on the surface. By assuming that different area cells on the horizon are distinguishable the dominant configuration is the one with a maximum number of the minimal area $a_{\min}^{(\text{punc})}$ (the area of spin $j_{\min}$ puncture). Consequently, black hole entropy becomes $S = A \ln(2j_{\min} + 1)/a_{\min}^{(\text{punc})}$. Note that, as it was mentioned above, the minimal quantum of area in this calculation is not the minimal area in the complete spectrum of area.

Now the question is what reason caused this subset of area to be considered as the basis for representing the geometry of a horizon? The easy answer to this question is that at the time this study was done the complete spectrum of area was not known. Rovelli in his original work on black hole entropy (42) fairly mentions this result is restricted to the known area at the time of publishing that paper and that a complete spectrum of area was not known then.

However, there is a more sophisticated and physical answer to this. As soon as one assumes a black hole horizon as the internal boundary of space, the contribution of the boundary to the gravity action of the space becomes the Chern-Simons action, [2]. When this space is quantized the geometry of this boundary, in principle, is described by a set (and not a sequence) of punctures. As it was mentioned above, the gauge degrees of freedom on this boundary become physical. Regardless of the group representation that suits the boundary fields (which could be either SU(2) or U(1)), since the internal spin network states in this approach are removed out, the boundary is left only with a subset quanta (those which puncture the boundary).

However, beyond postulations and assumptions there is no physical reason to outlaw considering the spin network states in the interior region of a black hole. Indeed, the black hole interior may be in an infinite number of states. For instance, the black hole interior may be given by a Kruskal extension so that on the other side of the hole there is another universe. The inclusion of these states in fact allows the horizon to be quantized via the complete spectrum of area. However, the number of those internal states cannot affect the interaction of the hole with its surroundings. From the exterior, the hole is completely determined by the properties of its surface. Thus, the entropy relevant for the thermodynamical description of the thermal interaction of the hole with its surroundings is determined by the states of the quantum gravitational field on the black hole surface.

In principle, depending on the Hamiltonian operator that maps the physical Hilbert space of the interior region of a closed surface into itself, the surface may evolve and its area may increase, decrease or become unchanged in the course of time. In the case of black hole, the time evolution map is responsible for its non-decreasing area character and turning the kinematic entropy we reported here into a physical non-decreasing entropy, (73). This motivates a picture of a more quantum black hole in which the quantization of space occurs prior to the definition of the black hole sector. Here we restrict the results into only the kinematical ones and disregard arguing about the

[2] This is also true in any BF theory action. More precisely nothing enters into this surface term from the special character of gravity as a constrained BF theory.

dynamics. Of course one way to start the definition of such a horizon perhaps is possible through a spin foam model, (for review of different models see (48)).

A non-rotating spherical black hole 'reacts' to any perturbation by some complex frequencies called *quasinormal modes*. This makes a black hole horizon state different from a random surface. The imaginary part of the modes is the frequency at which the perturbation is damped. The real part is the frequency at which a quantum of energy is emitted from the black hole or is absorbed into it.

For large damping, i.e. large imaginary frequency, the real part of the frequency approaches to the non-zero value $0.04371235/M$. Crutial for our argument is an observation made by Hod. He remarked that the constant real part of the quasinormal frequencies is nothing but $\ln 3/8\pi$, (**?**).

When the perturbation is damped very quickly, the response of the black hole are the emission of the quantum of energy $\Delta M = M_{\rm Pl}^2 \ln 3/8\pi M$, (53). Since the quanta of energy and area are proportional to each other $\Delta M = \Delta A$ $(c^4/32\pi G^2 M)$, the exchanging area from the black hole is $\Delta A = 4 \ln 3 \ \ell_{\rm P}^2$.

Following Dreyer's conjecture (47) for identifying the classical perturbation of a black hole horizon in highly damping mode with the transition between the two natural configurations, it can be assumed $\Delta A = a_{\rm min}$. From this equivalence the entropy of a black hole in Planck's area unit becomes

$$S = A \ln g_1(\zeta_{\rm min})/4 \ln 3 \ \ell_P^2 \tag{4.6}$$

in *any* group representation.

Unexpectedly in SO(3) group, since the degeneracy of the minimal area is three, the two logarithms from the numerator and denominator of (4.6) are canceled out and the Bekenstein-Hawking entropy is verified. This lets us to calculate the Barbero-Immirzi parameter by the size of minimal area. This minimal area in this picture is a half times smaller than the minimal area on a boundary. The reason is that here we do not restrict the horizon to be a boundary of space and the internal spin network exists and connects to the horizon surface. The Barbero-Immirzi parameter becomes tuned here to the value $\gamma = \frac{\ln 3}{\pi\sqrt{2}}$. This value is the double of what has been reported using Dreyer's result in a boundary picture of horizon.

In SU(2) group, since the degeneracy of the minimal area is two and using equation (4.6) the semi-classical result does not hold. This indicates that the two groups $SU(2)$ and $SO(3)$ do not act similar when gravity is quantized, despite the fact the two groups are equivalent in classical gravity.

In summary, we reported that the complete spectrum of area possesses eigenvalue degeneracy. This degeneracy with respect to area in both group representations is power law with increasing scatter. However since the complete spectrum of area is the union of different equidistant subsets, the total degeneracy of a large eigenvalue becomes proportional exponentially to its area. The black hole entropy relevant for the thermodynamical interaction of a black hole with its exterior region is the number of the quantum microstates of the horizon which are distinguishable from the exterior of the hole. We have obtained that the entropy is proportional to the area. Moreover we derived the exact form of the Bekenstein-Hawking formula when the minimal area is considered to be the quantum of area emitted from the hole in its highly damping mode.

Chapter 5

Spectroscopy of a canonically quantized horizon

5.1 What is this about?

Considering the quantum definition of a black hole via spin network as a new approach in loop quantum gravity that is described in this thesis, we can define a quantum black hole in two ways: 1) introducing a black hole Hamiltonian by the use of quantum information theory methods such as one way information flow evolution methods, 2) deriving the black hole transition amplitude using spin foam methods.

The area cells in loop quantum gravity are generically degenerate. Here, we report another symmetry in the definition of area operator, the so-called 'ladder symmetry.' According to this symmetry the complete spectrum of area, although becomes denser in larger area, it can be produced by overlapping some equidistant ladder spectra on top of one another. These ladders should have the gaps between the levels proportional to square-free numbers in the group representation that describes Bekenestein-Hawking entropy.

In black holes the quantum of area and energy are proportional. When an area cell decays from a black hole, this affects the entropy of black hole and thus its radiation spectrum. Based on the ladder symmetry, an interesting effect appears in the fluctuations of a horizon, the so-called 'quantum amplification effect.' According to this effect, when a quantum of energy decays from a black hole if the frequency of the decay is proportional to the gap between area ladders, the probability of the decay increases extremely higher than other decays. Therefore the spectrum of a black hole radiation should be sharp on these frequencies and among them a few of the harmonic frequencies that belong to the ladders with minimal ladder gaps, are the most brightest lines. These lines are unblended and narrow enough to be observed. We describe this new effect that is completely due to the viability of loop quantum gravity in the following pages of the thesis.

5.2 Spectroscopy of a canonically quantized horizon

Deviations from Hawking's thermal black hole spectrum, observable for macroscopic black holes, are derived from a model of a quantum horizon in loop quantum gravity. These arise from additional area eigenstates present in quantum surfaces excluded by

the classical isolated horizon boundary conditions. The complete spectrum of area unexpectedly exhibits evenly spaced symmetry. This leads to an enhancement of some spectral lines on top of the thermal spectrum. This can imprint characteristic features into the spectra of black hole systems. It most notably gives the signature of quantum gravity observability in radiation from primordial black holes, and makes it possible to test Loop Quantum Gravity with black holes well above Planck scale.

5.3 Introduction

Most astrophysicists agree that black holes exist and radiate. So far three types of black hole radiations have been investigated: (*i*) the Hawking radiation, (*ii*) the gravitational radiation, and (*iii*) the X-ray emission from the infalling materials into a black hole. In this thesis, the quantum geometry of the horizon is, under certain assumption, shown to imply revision of the first type of black hole radiation.

The Hawking radiation is known semi-classically to be continuous. However, the Hawking quanta of energy are not able to hover at a fixed distance from the horizon since the geometry of the horizon has to fluctuate, once quantum gravitational effects are included. Thus, one suspects a modification of the radiation when quantum geometrical effects are properly taken into account. Any transition between two horizon area states can affect the radiation pattern of the black hole. The quantum fluctuations of horizon may either modify, alter or even obviate the semiclassical spectrum, (54; 55).

Bekenstein and Mukhanov in (85) studied a simple model of the quantum gravity of the horizon in which area is equally spaced. They found no continuous thermal spectrum but instead that black holes radiate into discrete frequencies. The natural width of the spectrum lines turns out to be smaller than the energy gap between two consecutive lines. Thus, their simple model predicts a falsifiable discrete pattern of *equidistant* lines which are unblended. This result is not completely in contradiction with Hawking prediction of an effectively continuous thermal spectrum of black hole using semiclassical method, since the discrete line intensities are enveloped in Hawking radiation intensity pattern.

More recently, it has been possible to study the quantum geometry of horizons using precise methods in loop quantum gravity. In this non-perturbative canonical approach, the quantum geometry is determined by geometrical observable operators. Canonical quantization of geometry supports the discreteness of quantum area.[1] This theory does not reproduce equally spaced area, instead the quanta become denser in larger values, (59; 60). Having defined a black hole horizon as an internal *boundary* of space (11), only a subset of area eigenvalues contribute to identifying the horizon area. In fact, this subset contains the area associated to the edges puncturing the boundary. This subset is not evenly spaced and it turns out that the area fluctuations of such a horizon do not imprint quantum gravitational characteristics on black hole radiation, (61).

Nonetheless, restricting the quanta of horizon area to the subset of punctures is based on a non-trivial gauge-fixing of the horizon degrees of freedom. This is sufficient for the purpose of black hole entropy calculation since it results to the residence of

[1] A summary of emergent aspects of non-stringy quantum gravity theories can be found in (57), (58), and the references therein.

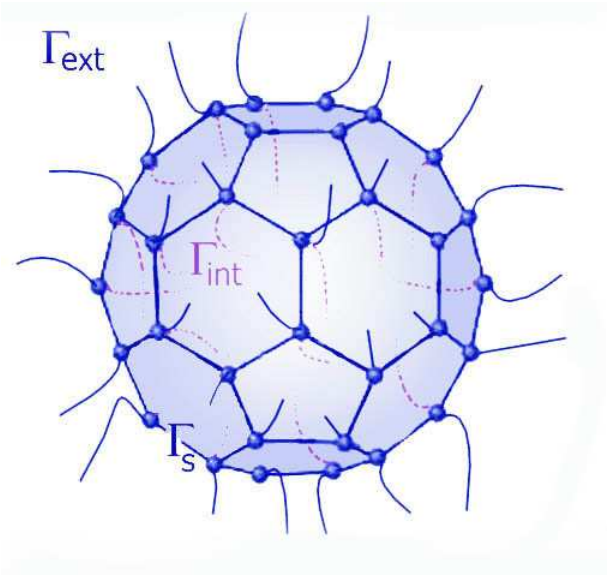

Figure 5.1: A quantized black hole

a finite number of degrees of freedom on the horizon, independently from the bulk. Such a quantization, while is too restrictive, leaves some physical ambiguities. For instance, in classical general relativity spacetime metric field does not *end* at a black hole horizon, instead it extends through the black hole. In fact, a quantum black hole in a space manifold, instead of being the reason for termination of quantum space, partitions it into three subgraphs: 1) the partition that reside outside of horizon, Γ_{ext}, 2) the partition that reside inside of the horizon, Γ_{int}, and 3) the partition that lies on the horizon 2-surface, Γ_{s}. On the horizon surface some vertices and completely tangential edges reside. The spin network states associated to a partition that consists of the vertices lying on the horizon are called *horizon spin network states*. These states determine the whole quantum geometry of the underlying horizon, Fig (5.1). Under some simplifications, the spin network state associated to a spherical symmetric structure has been worked out in (62). The quanta of such a horizon area is chosen from the complete spectrum. It reproduces the Bekenstein-Hawking entropy (13). Moreover, in this thesis it is shown that such a black hole exhibits unexpectedly a macroscopic effect in the black hole radiation.

The aim of this thesis is two fold:

1. Firstly, in section (5.5) an unexpected symmetry in the complete spectrum of area is descried. In fact, this spectrum can be decomposed into a several *evenly* spaced sets, each with individual gap between levels. This leads to a reduced formula of area eigenvalues. In $SU(2)$ version of Loop Quantum Gravity the gaps scale as the square roots of 'square-free' numbers. In $SO(3)$ version, they are the square roots of the discriminants of all possible quadratic positive definite forms.

2. Secondly, in section (5.9) it is discussed that having applied the complete spectrum of area, a black hole radiates quantum mechanically a continuous spectrum. But the existence of the symmetry within the area spectrum results to a phe-

nomenon called the *quantum amplification effect*. This generates several distinct bright lines in radiance spectrum. It gives the signature of quantum gravity observability in radiation from primordial black holes. Moreover, it challenges the isolated horizon picture conjecture, while makes it possible to test loop quantum gravity with black hole radiation well above Planck scale.

Before these, some of the attempts to discovering the signature of quantum gravity in a black hole radiation are reviewed.

5.4 Some theories

Firstly, a model of quantum gravity that predicts macroscopic effects on black hole radiation is reviewed. Afterwards the attempts within Loop Quantum Gravity are illustrated.

5.4.1 A quantum geometry and black hole radiation

A sector of spacetime may collapse and settles down to a stationary state in which the zeroth law of black hole mechanics is satisfied; the surface gravity is constant over the event horizon of the sector. The sector is called black hole. The ADM mass of a neutral non-rotating black hole non-trivially depends on the black hole horizon area. This is the first thermodynamic law of black holes,

$$A = \frac{16\pi G^2}{c^4} M^2. \tag{5.1}$$

Steven Hawking uncovered that quantum field theory in black hole curved spacetime leads to particle creation effect at the horizon, thus black hole radiates. The original derivations of this radiation was made of particle propagating into the black hole, the radiation is independent of the notion of particle, (64). The sum of the black hole entropy plus the matter entropy outside the black hole never decreases, $S_{\text{outside}} + S_{\text{black Hole}} \geq 0$. This is the generalized second thermodynamic law of black hole. This law holds even during quantum evaporation of the black hole via Hawking radiation, when a negative energy flux across the horizon decreases of area. Although, the way a black hole loses mass during the thermal radiation implicitly must involve quantum gravitational assumptions.

Jacob Bekenstein and Venceslav Mukhanov postulated a rough theory of quantum gravity in which the horizon area of a black hole is quantized in uniformly spaced tiny fractions of the Planck length scale,

$$A = \alpha n \ \ell_{\text{P}}^2, \tag{5.2}$$

where n is a natural number, and ℓ_{P} is Planck length, $\sqrt{\hbar G/c^3} \sim 1.6 \times 10^{-35}$m, which is drastically small.

Semiclassically, the discreteness of the quantum values of a horizon area leads to the discreteness of black hole mass. If a black hole is defined as a quantum system in thermodynamical equilibrium, the radiation is analogous to quantum mechanical instability that leads to quantum decays. Having the energy levels of a non-rotating neutral black hole, the transitions between neighboring energy levels causes quantum

decay. A discrete mass spectrum implies the discreteness of mass emissions. From (5.2) and (5.1) the quanta of energy are

$$\delta M = \frac{\alpha \delta n}{32\pi M} M_{\rm P}, \tag{5.3}$$

where $M_{\rm P}$ is the Planck mass, $\sqrt{\hbar c/G} \sim 2.2 \times 10^{-8}$ kg.

Under the assumption that the the change in the mass of a large black hole during the quantum emissions is negligible, $\delta M \ll M$, and by the use of (5.3), the frequencies of emissive quanta turn out to be integers multiplied by a minimal frequency. The minimum frequency is called *the fundamental frequency* ϖ,

$$\varpi = \frac{\alpha c^3}{32\pi G M}. \tag{5.4}$$

Other emissive frequencies are *harmonics* ω_n, which are proportional to this fundamental frequency by an integer n, $\omega_n = n\varpi$.

Under the assumption of uniform matrix elements of quantum transitions between near levels, the intensities of the spectral lines were worked out in (85). The outcome turns out to be enveloped by the Hawking radiation intensity, whilst the allowed frequencies are discrete and equidistant. Moreover, it turns out that the thermal broadening of the lines are smaller than the gap between any two consecutive harmonics.

From the model three major conclusion come about, (*i*) there should be no lines with wavelength of the order of the black hole size or larger, (*ii*) the black hole radiance spectrum must be clearly discrete and the lines do not overlap, (*iii*) the radiance pattern is a *uniformly spaced* discrete lines.

Nonetheless, there has not been any justification for this evenly spaced area from within the very quantum gravitational theories. In the next sections we consider a version of quantum gravity whose roots are within the so-called loop quantum gravity.

5.4.2 A quantum geometry and isolated horizon radiation

The first suggestion to describe a black hole as a 2-surface boundary of space manifold in Loop Quantum Gravity was proposed by Krill Krasnov in (65). Carlo Rovelli based on the picture discussed the black hole entropy in (82). Afterwards, by the developments of the isolated horizon theory the bounded sector was more precisely defined in a series of works, (11).

A black hole is a classical concept and its definition is highly non-local, because one has to know the information of the entire spacetime manifold $(\Sigma, g_{\mu\nu})$, in order to find the entire causal past of the future null infinity. A black hole is a sector of manifold that does not intersect with the entire past of the future null infinity. However, this definition is not well-suited for the purpose of identifying a black hole region in a non-perturbative canonical quantized space. In fact, a more local criteria must be installed on such a theory.

A classical isolated horizon is defined by a set of boundary conditions of a sector of spacetime Δ, which mimics the essential local structure of a static event horizon. Assuming the black hole sector to be $S^2 \times \mathbb{R}$, these boundary conditions are necessary to verify the black hole thermodynamic laws from the sector: 1) the Einstein equations hold at the sector, 2) the sector is null, 3) the sector is equipped with a preferred

foliation by 2-spheres transverse to its null normal l^a; the second null normal to S_Δ is n^a with $l^a n_a = -1$, 4) the sector is non-rotating, 5) l^a is twist-, shear-, and expansion-free geodesic; n^a is twist- and shear-free with negative expansion $\theta_{(n)}$, 6) $\theta_{(n)}$ is constant over each foliated shell S_Δ, 7) the flux densities of electric and magnetic fields are uniform through each S_Δ.

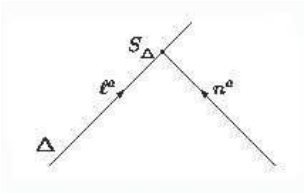

Figure 5.2: The black hole sector Δ, its two null normals and its preferred foliation S_Δ.

On the other hand, it is known that general relativity can be written in terms of gauge field. For this aim, a trivial $SU(2)$ bundle is assumed over the space 3-manifold. For each positive real number γ, a phase space ${}^\gamma\Pi$ is assumed to exist. This phase space consists of the configuration fields, the connection fields ${}^\gamma A_a^i$ (1-form), and the canonical momenta, the fields ${}^\gamma\tilde{\Sigma}_{ab\ i}$ of density weight one (2-form). $i = 1, 2, 3$ the gauge degrees of freedom and $a = 1, 2, 3$ the spatial degrees of freedom. The curvature of the connection field is a 2-form field ${}^\gamma F_{ab}^i$. The Einstein equations for any γ is verified.

The so-called 'triad fields' ${}^\gamma E_i^a$ are defined via the momentum fields $\tilde{E}_i^a := \gamma\varepsilon^{abc}\,{}^\gamma\tilde{\Sigma}_{bc\ i}$, where ε^{abc} is Levi-Civita ε^{abc} of density weight one. From the triads the 3-metric variables q^{ab} are defined, ${}^\gamma\tilde{E}_i^a\,{}^\gamma\tilde{E}^{bi} = qq^{ab}$. Also, the triad fields define area of a 2-surface. Since the area of a 2-surface is $\int_S \sqrt{q}d^2x$, given the relation between the momenta and the 3-metric, the area can be redefined as $\int_S d^2x\sqrt{{}^\gamma E_i^a n_a\ {}^\gamma E_i^b n_b}$, a functional of momenta, where n_a is the normal to the surface.

In this language, a neutral stationary black hole in the manifold is the problem of adding a boundary with special boundary condition to the theory. The black hole sector is Δ where it is foliated by $S^2 \times \mathbb{R}$. The boundary of the sector, S_Δ, must satisfy the above mentioned conditions of an isolated horizon. In the gauge language of gravity, there is a way to define two null vectors of desired properties $l^1 n_a = -1$, $l^a l_a = n^a n_a = 0$ by the use of triad momentum conjugate fields ${}^\gamma\tilde{\Sigma}_{ab\ i}$. Having the two null vectors the following conditions must be imposed further in order to make a quasi-local black hole:

Area-fixing: the manifold momenta must admit a *fixed* value of area a on the shell.

Gauge-fixing: the pullback $\overleftarrow{{}^\gamma A_a^i}$ of the bulk connection fields to the shell S_Δ are the $U(1)$ connection fields ${}^\gamma W_a$, up to a constant. For this aim, a $U(1)$ sub-bundle is selected at the shell S_Δ. By fixing a unit vector r^i at every point of the shell, the connection field on the sub-bundle will be $u(1)$-valued ${}^\gamma W_a$.

Boundary condition: the pullback $\overleftarrow{{}^\gamma\Sigma_{ab\ i}}$ of the bulk momenta to the shell S_Δ are completely determined by the curvature ${}^\gamma F_{ab} = \partial_a\,{}^\gamma W_b - \partial_b\,{}^\gamma W_a$. The relation between these two turns to be ${}^\gamma F_{ab} = -(2\pi\gamma/a)\,\overleftarrow{{}^\gamma\Sigma_{ab\ i}} r^i$.

The field equations: at the sector the equations of motion hold.

The contribution of the boundary in the gravitational action is the addition of a $U(1)$ Chern-Simons action term of the gauge fields ${}^{\gamma}W_a$. Such an action is invariant under the following transformations: 1) $SU(2)$ gauge transformation, those reduce to $U(1)$ transformation on S_Δ and identity on the infinity, 2) spatial diffeomorphism, those reduce to tangent transformation on the shell and the identity at the infinity, 3) time evolution between the fixed horizon and infinity with lapse going to zero at the horizon and a constant at the infinity, 4) phase space transformation between different γ-sectors ${}^{\gamma}\Pi$ and ${}^{\gamma'}\Pi$.[2]

Such a classical horizon does not carry independent degrees of freedom due to the existence of the strong boundary condition. However, the quantum version is different.

To quantize the theory, a graph is embedded into the manifold and the connection fields are generalized into $su(2)$-valued holonomies along the paths of the graph. Two Hilbert spaces are obtained, the one of the bulk $\mathcal{H}_{\rm bulk}$ and the one of the boundary $\mathcal{H}_{\rm boundary}$. The boundary Hilbert space is defined on the Chern-Simons charged points, namely 'punctures' of the surface. The bulk Hilbert space has a basis by *spin networks* in the spatial 3-manifold with 'loose ends' at the charge points of the internal boundary. [3]

Consider a spin network state in the bulk Hilbert space. In this wave function, the edges of the spin network are labeled by the irreducible representation of the holonomies (the so-called 'spins'), the vertices are intertwiners, the punctures by a vector $|m\rangle$ in the representation of the incident edge. If the spin of the incident edge to the puncture is j, there exist $2j+1$ different copies of puncture states, $m \in \{-j, -j+1, \cdots, j-1, j\}$.

Notice that each puncture is a place where and edge ends at the surface and thus it carries the area eigenvalue corresponding to the edge.

The surface Hilbert space $\mathcal{H}_{\rm boundary}$ contains $u(1)$-valued connection fields. The geometry of the surface is flat except at the punctures, where there are conical singularities. All different horizon wave functions corresponding to one edge of spin j produce the same horizon area, because the area eigenvalues only depend on j. Carlo Rovelli and Lee Smolin verified this area first by the use of loop operators in (59). They found that the spectrum of area associated to an edge is 'almost' equidistant in large scales. The area of a puncture depends on the irreducible dimension of the puncturing edge. In fact, these eigenvalues of area were those were discovered first. An edge of spin j generates the area $a_j = 8\pi\gamma\ell_{\rm P}^2\sqrt{j(j+1)}$ on the boundary. These eigenvalues depend only on one quantum number, j.

Having $2j+1$ different copies assigned to the same area, the horizon wave functions are degenerate, thus black hole gets non-zero entropy. The entropy is proportional to the surface area and since the surface is assumed to be of fixed area, the entropy of an isolated horizon meet the second thermodynamic law of black hole, it is non-decreasing. Therefore, the entropy is physical.

[2] In the quantum version, the quantum phase space ${}^{\gamma}\Pi$ is unitarily *inequivalent* to the one of another quantum phase space ${}^{\gamma'}\Pi$.

[3] Quantization of a black hole has not been understood yet. There are several models for this purpose. Among them those are acceptable that do not make serious contradictions with the certain classical properties of a horizon. Let us consider non-perturbative context of quantum gravity. One of the recent model introduces a quantum black hole based on the action of 'expansion operator' on a the quantum state of a mixture of geometry and matter, (66). There is another model based on causal dynamical triangulation. The causal dynamical triangulation is a non-perturbative quantum gravity analytically worked out in two dimensions in (68), statistically in (69), as well as numerically in higher dimensions. A black hole could be defined in this model, (67).

Later on Abhay Ashtekar and Jerzy Lewandowski derived the complete spectrum of area operator in (60). The spectrum that Rovelli and Smolin have discovered was a subset of the complete spectrum of area. The complete spectrum is also discrete, although the eigenvalues approaches to a continuum in large eigenvalues. This spectrum is described in section (5.4.3).

The gravitational fields about a black hole are not stable because they interact with 'non-stationary' matter fields. Only about such a shell, from the Einstein equation the decreasing of mass by ΔE corresponds to the decreasing of area by ΔA such that $\Delta A = 32\pi G^2 E \Delta E$. This correlation describes the transitions between two macroscopically stable states after mass perturbation. A quantum jumping down an area level corresponds to emission of one (or some) quantum of area. In both $SU(2)$ and $SO(3)$ versions of loop quantum gravity small values of spin j produces the quantum of area proportional to a number within the interval $[j, j+1]$. At large j the area make it approximately proportional to j. Therefore, a transitions from a high level into a low level does not coincide with the transitions from a higher level into that high level. In other words, one-puncture decays produces an effectively continuous radiance spectrum at high frequencies.

However, since the relation (5.3) is classical, it does not guarantee the occurrence of only one-puncture transmissions. A quantum black hole may also radiate a multi-puncture decay in its low damped quasinormal modes. A multi-puncture decay is an emission in which a set of punctures simultaneously undergo area shrinking in one go and produce one quantum of energy. For instance, consider a black hole made of three patches of area, two of which correspond to punctures of spin 1/2 and the third one to a spin 1. The overall horizon area is $A_1 = 8\pi\gamma(\sqrt{2}+\sqrt{3})\ell_P^2$. This black hole may decay into a geometrical configuration with two punctures of spin 1. In this case the horizon area is shrunk into $A_2 = 8\pi\gamma(2\sqrt{2})\ell_P^2$. According to (5.3) the emitted energy is proportional to $8\pi\gamma(\sqrt{3}-\sqrt{2})\ell_P^2$ by a constant, which is even smaller than the minimal single-puncture decay ($8\pi\gamma\sqrt{2}\ell_P^2$). Such a typical multi-puncture emissions can take almost any value and fill the continuous spectrum in all ranges of energy.

Since the puncture quantum of area is not uniformly spaced, the area fluctuations produces a continuous spectrum of emissive frequencies. While such a prediction satisfies the Hawking pattern of radiation, since the populations of all frequencies are uniform, there is no notable quantization effect in the black hole radiation, (61). In the next section, a different picture of black hole is reviewed and its radiance pattern is analyzed.[4]

5.4.3 A quantum geometry and spin network horizon radiation

In this section a new picture of a black hole is explained and the quantum effects on its radiation is described in the rest of the thesis.

In brief, deriving the entropy of an isolated horizon depends on fixing a gauge of the connections fields. More precisely, in the presence of such a classical boundary-like horizon in the underlying manifold, the $su(2)$-valued connection fields of the bulk are gauge-fixed into $u(1)$-valued connections on the boundary and thus the punctures take additional degree of freedom independent from those of the bulk. This assumption is too restrictive. In such a quantum surface many quanta of horizon area are

[4]Beside these two possible pictures of a horizon in loop quantum geometry, there exists also a third one that was proposed by Livine and Terno in (46).

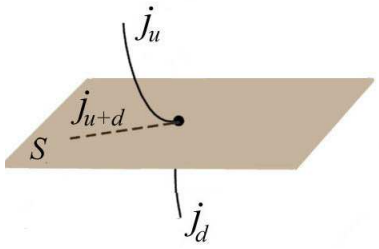

Figure 5.3: Two incident edges at a vertex residing on S.

excluded by the classical isolated horizon boundary conditions. However, considering the complete spectrum of area eigenvalues as the possible horizon area, provides the same entropy that is expected on black hole horizon, while it gives a different picture of a black hole, a more quantum picture.

There have been some attempts to define a black hole as a partition of spin network state. For instance, Martin Bojowald in (62) tried to see a spherically symmetric black hole state as a spin network state. In this picture, a black hole horizon is defined by studying the properties of an infalling spin network states associated to a 2-surface through the black hole. In this picture, instead of considering the evolution of the underlying surface and quantizing the manifold afterwards, the quantum state evolves itself independently. In fact, the behavior of the quantum surface in time can narrow the definition of appropriate dynamics of black hole.

Let us consider a quantum surface associated to a surface S in a 3-manifold Σ. This surface divides the manifold into two disjoint open sets $\Sigma_{\rm up}$ and $\Sigma_{\rm down}$ such that $\Sigma = \Sigma_{\rm up} \cup S \cup \Sigma_{\rm down}$ with $\Sigma_{\rm up} \cap \Sigma_{\rm down} = \emptyset$, Figure (5.3). Thus, the imbedding graph Γ in the presence of underlying 2-surface S is split into three subgraphs: (i) $\Gamma_{\rm up}$, which is completely in one side of S in the 3-manifold, (ii) $\Gamma_{\rm down}$, which is completely in the other side of S, and (iii) $\Gamma_{\rm s}$, which lies on S. $\Gamma_{\rm s}$ consists of some residing vertices $\{v^\alpha\}$ on S as well as some tangential edge lying entirely on the horizon surface S.

Consider a typical spin network state corresponding to a residing vertex on an underlying surface S, i.e. the one in figure (5.3). This state intertwines the bulk edges of external and internal sub-graphs, and the edges of $\Gamma_{\rm s}$. The set of all such spin networks produces a partition of spin network states called the *quantum surface states*. This state is isolated within the near-surface region. The quantum geometrical state of the surface is determined by these spin network states. A bulk edge relative to S falls into three categories: either (a) it bends tangentially at the point at which the edge crosses the surface S, or (b) it intersects the surface at a point without bending at the surface, or (c) it lies completely tangential to the surface. The edges which are completely tangential to S, the so-called 'analytical edges', do not belong to the bulk edges, instead they belong to the quantum surface S.

In both the isolated horizon picture and the black hole spin network a quantum state is associated with the horizon. But in the latter one horizon is defined classically not quantum mechanically. The continuum surface undergoes evolution and a static Hilbert space is associated with the classically evolving surfaces at each time frame. In other words, the quantum state of horizon *follows* what the underlying surface *rules*. The quantization procedure of gauge-fixing prior to the quantization is not a trivial method of quantization. In fact, in the case of quantum spacetime such a

quantization causes some ambiguities:

- The black hole sector is identified classically and remains exactly the same after quantization, without considering any uncertainty on black hole radius and its intrinsic geometry.
- The spin networks end at the black hole horizon, which contradicts with the classical definition of black hole. In classical general relativity, the metric fields extend through the horizon.
- No tunneling effect is allowed throughout the horizon.

To overcome the problems, one can treat the quantum horizon as an evolving quantum surface which undergoes its quantum evolution. The evolution is only expected to verify the classical results only at the classical limits. Such a quantum black hole is a partition of spin network, whose boundary determines its quantum horizon. However, it is not so easy to define a surface without reference to a background metric or other fields. One surface that *can* be defined in a background-independent manner is a black hole horizon. This is a property that distinguishes horizons from most other surfaces. The final state of this partition should not be influenced by the initial states of the rest of the rest of the world. The initial state of this partition should influence the final states of the rest of the rest of the world. Moreover, the entropy associated to the vertices residing on the horizon remains fixed. Also it is expected that the quantum sector gets non-expanding volume, as well as horizon area. This make it possible to make this definition of black hole more realistic because it the black hole be less hidden from a quantum system closer to the horizon, (**?**).

What is the entropy of such a quantum black hole? Considering a typical spin network state like the one of the figure (5.3), the action of area operator on this state generates an area eigenvalue. It turns out that an area eigenvalue corresponds to a *finite* number of different eigenstates. In fact, $su(2)$-valued quantum states of a surface of certain area are degenerate state. The degeneracy is such that the entropy of the surface is proportional to the surface area and in the case of black holes quantum surface the entropy verifies the Bekenstein-Hawking entropy, (13). This entropy is not necessarily non-decreasing in the course of time, unless it is fixed by the defining the appropriate evolution of horizon quantum surface states, (73).[5]

The complete eigenvalues of area operator on a typical spin network state was first studied in (60) and a few months later the results were verified by the use of recoupling theory in (70). In fact, the area of a spin network is the outcome of linking the two sides of the surface. Let the up and down edges of the vertex α get the spin $j_u^{(\alpha)}$ and $j_d^{(\alpha)}$, respectively. The two edges may bend tangentially at the underlying 2-surface at their joint intersecting vertex. The overall tangent vector induced from them on the surface take the spin $j_{u+d}^{(\alpha)}$. The spin j_{u+d} take discrete values and bounded to the following values

$$j_{u+d}^{(\alpha)} \in \{j_u^{(\alpha)} + j_d^{(\alpha)}, j_u^{(\alpha)} + j_d^{(\alpha)} - 1, \cdots, |j_u^{(\alpha)} - j_d^{(\alpha)}| + 1, |j_u^{(\alpha)} - j_d^{(\alpha)}|\}. \tag{5.5}$$

[5]The question why a horizon carries physical entropy whilst a random surface does not, is subtle and still not understood fully. This is not only a property of canonical quantization of spacetime. For instance, in the causal dynamical triangulation, which is another non-perturbative approach to quantum gravity (72), for the purpose of obtaining a 1+1 global geometry (a 2-surface) by triangular building blocks, the two components of the blocks can be respected as up and down spins with respect to an external time field, (69). If one coarse-grain a 'spin' by ignoring the interior of some randomly selected region of the surface, one will obtain an entropy-like number. However, this number will not have the properties we normally associate with entropy.

The action of area operator on a typical area state corresponding to incident edges at a residing vertex on S entangles the external and internal edge. Let us for simplicity define the colour numbers corresponding to the three spins, $p := 2j_u^{(\alpha)}$, $q := 2j_d^{(\alpha)}$, and $r := 2j_{u+d}^{(\alpha)}$. The area squared operator acting on the trivalent state $\langle p, q, r|$ entangles two sides of the underlying surface (the shaded and unshaded sides),

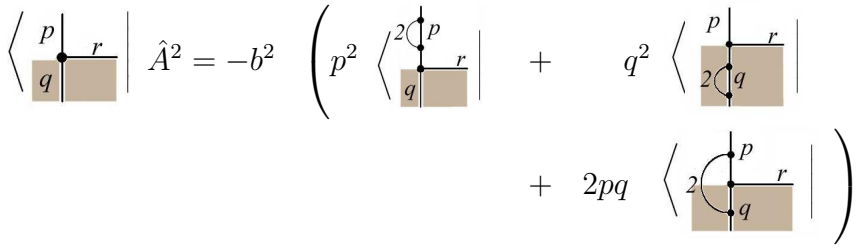

(5.6)

where $b := 8\pi\gamma\ell_P^2$. Using the reduction formulae of recoupling theory, the grasped states are identical to the original state,

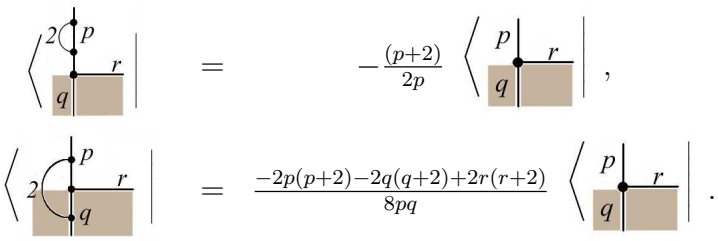

(5.7)

Substituting (5.7) in (5.6) the squared area operator acting on $\langle p, q, r|$ turns out to become an eigenstate relation non-trivially. Thus, the trivalent area state $\langle p, q, r|$ is the eigenstate of the operator. Finally, the area eigenvalues corresponding to the cell α turns out to be $a^{(\alpha)} = (4\pi\gamma)\, m^{(\alpha)}_{j_u, j_d, j_{u+d}}\, \ell_{\mathrm{P}}^2$, where

$$m^{(\alpha)}_{j_u, j_d, j_{u+d}} = \sqrt{2j_u^{(\alpha)}(j_u^{(\alpha)}+1) + 2j_d^{(\alpha)}(j_d^{(\alpha)}+1) - j_{u+d}^{(\alpha)}(j_{u+d}^{(\alpha)}+1)}. \tag{5.8}$$

A Schwarzschild black hole horizon belongs to the class of surfaces that has no boundary, $\partial S = \emptyset$ and divides the 3-manifold Σ into two disjoint sets Σ_{internal} and Σ_{external} such that $\Sigma = \Sigma_{\text{internal}} \cup S \cup \Sigma_{\text{external}}$ with $\Sigma_{\text{internal}} \cap \Sigma_{\text{external}} = \emptyset$. Thus, the graph Γ in the presence of a black hole is split into three graphs Γ_{external}, Γ_{internal}, and Γ_{s}. Notice that the corresponding states to a compact closed surface can only gauge transform into another compact closed state. Therefore, a *subspace* of gauge invariant states those correspond to the compact closed surfaces are allowed to gauge transform into each other. Thus, further restrictions are imposed on this class of quantum states, (60). The quantum states of a compact closed underlying geometry yields to those that satisfy the two conditions on the side bulk edge spins: $\sum_\alpha j_u^{(\alpha)} \in \mathbb{Z}^+$ and $\sum_\alpha j_d^{(\alpha)} \in \mathbb{Z}^+$. However, due to the existence of sum in these conditions, the spin of the majority of bulk edges in the near-horizon region are left unconditional. In other words, the conditioned trivalent states among all ingredient states of whole surface state is one or a few.

The quantum surface that is associated to a black hole horizon semi-classically determines the quantum decays of energy from the black hole. This definition is only restricted to the case of black holes and does not hold in any random surface. In the

rest of the thesis the spectroscopy of the decays is illustrated. Before it, in the next part, an important symmetry within the eigenvalues are area operator is uncovered.

5.5 Ladder Symmetry

In this part, by the use of number theory a significant property of the area eigenvalues is uncovered. Having known the complete spectrum of area symmetry (5.8) a reduced formula is written. As a consequence, the complete spectrum of area eigenvalues in both group $SU(2)$ and $SO(3)$ representations can be split into the mixtures of equidistant numbers. This lead to the quantum amplification effect, which is described in next part.

5.6 SO(3) area and Square-free numbers

In $SO(3)$ group representation, the spins are positive integers. Evaluating $\frac{1}{2}\left(m_{j_u,j_d,j_{u+d}}\right)^2$, if all repetitions of numbers (degeneracies) are identified, the whole *Natural* numbers are reproduced. This is proved in the Appendix (A).

As an immediate consequence, there exists a irreducible formula for the eigenvalues of area which depends only on one integer number. The irreducible formula of the complete area eigenvalues is

$$a_n = 4\pi\gamma\ell_P^2\chi\ \sqrt{n}, \tag{5.9}$$

where $\chi = \sqrt{2}$ and $n \in \mathbb{N}$.

In fact the eigenvalues of area operator in the original formula (5.8) that depends on three variables j_u, j_d, j_{u+d} is a reducible representation of the set. If degeneracies are identified the irreducible formula (5.9) appears.

Any integer is the multiplication of a 'square-free' number and a square number.[6] By definition, an integer is said to be square-free, if its prime decomposition contains no repeated factors. For example, 30 is square free since its prime decomposition $2 \times 3 \times 5$ contains no repeated factors. Consider the natural number $2^5 \times 3^8$. This number can be rewritten in the form $(2) \times (2^2 \times 3^4)^2$. The first part is a square-free number and the second one is a square number.

Having this decomposition of natural numbers, consider the sequence of numbers containing the same square-free factor multiplied by all squared numbers. For example the sequence $\{$ 3, 12, 27, 48, 75, 108, 147, $\cdots\}$, which is in fact $3 \times n^2$ for $n \in \mathbb{N}$. This sequence can be written in the form $3 \times \{1, 4, 9, 16, 25, 36, 49, \cdots\}$, or briefly $3\mathbb{N}^2$. Such a sequence of numbers is called a squared set. The square-free number 3 based on which the sequence $3\mathbb{N}^2$ is produced is the *representative* of the squared set $3\mathbb{N}^2$. We indicate the representative with the symbol ζ and its corresponding square generation with $\zeta\mathbb{N}^2$.

Obviously, taking square root from the elements of a squared generation, say $\zeta\mathbb{N}^2$, an equidistant sequence of numbers is produced, $\sqrt{\zeta}\mathbb{N}$. This evenly spaced set of numbers is called a '*generation.*' In fact, by doing this we decompose the set of numbers $\sqrt{n}$ into $\sqrt{\zeta}m$ for integer n and m and square-free ζ. Consequently, the

[6] The proof is in Appendix (A).

formula (5.8) is performed into the following reducible but important form:

$$a_n(\zeta) = (4\pi\gamma\ell_{\rm P}^2\chi)\ n\sqrt{\zeta}, \tag{5.10}$$

where $\chi = \sqrt{2}\ n \in \mathbb{N}$, and $\zeta \in \mathbb{A}$ for $\mathbb{A}$ stands the set of square-free numbers. The list some of the square-free numbers are given in Table (A.1) of Appendix (A).

What is special about this final formula is that it represents clearly that a generation with representative ζ gets evenly spaced area eigenvalues.

A curious reader is encouraged to read more details in the Appendix (A).

5.7 The SU(2) area and positive definite quadratic forms

In $SU(2)$ group representation, evaluating $4\left(m_{j_u,j_d,j_{u+d}}\right)^2$ from (5.8) produces the congruent numbers unto 0 or 3 mod 4. The proof is in the Appendix (B). These numbers are the page numbers of a book that is printed out only at the pages that come after each two leaves of sheets by face, 3, 4, 7, 8, 11, 12, 15, 16, 19, 20, etc. These numbers are also called *the Skew Amenable numbers*, (74).

Since the Skew Amenable number cannot be fitted into a formula with one variable. Instead, it can be fitted into the combination of these two sets: $(4\pi\gamma\ell_{\rm P}^2\chi)\ \sqrt{4n}$ and $(4\pi\gamma\ell_{\rm P}^2\chi)\ \sqrt{4n+3}$, where $\chi = 1/2$ and $n \in \mathbb{N}$. It can be proven that any skew amenable number b' can be written in terms of $b \times n^2$ for $n \in \mathbb{N}$. The numbers b are the elements of a subset of Skew Amenable numbers, the subset $\mathbb{B}$, that contains the discriminants of every positive definite quadratic forms.[7]

Henceforth, the complete spectrum of area eigenvalues $m_{j_u,j_d,j_{u+d}}$ is equivalent to the family of the generations $\{(\sqrt{\zeta}/2)\mathbb{N}\}$, where $\zeta \in B$. Area eigenvalues, instead of being determined by three quantum numbers j_u, j_d, and j_{u+d}, can be performed by two as

$$a_n(\zeta) = \left(4\pi\gamma\ell_{\rm P}^2\chi\right)\ n\sqrt{\zeta}, \tag{5.11}$$

where $n \in \mathbb{N}$ and $\chi = 1/2$. The list of some of the discriminants is given in Table B.1) of Appendix (B).

A curious reader is encouraged to read more details in the Appendix (B).

5.8 Summary of Ladder Symmetry

Remarkably the area eigenvalues in a reduced form in both group representations $SU(2)$ and $SO(3)$ are performed into one formula. In the above two subsections it was justified that the complete spectrum of area operator indeed can be specified by two indices n and ζ, instead of three indices j_u, j_d, and j_{u+d},

$$a_n(\zeta) = \left(4\pi\gamma\ell_{\rm P}^2\chi\ \right)\ n\sqrt{\zeta}, \tag{5.12}$$

where $n \in \mathbb{N}$. In $SO(3)$ representation, $\zeta \in \mathbb{A}$ and $\chi = \sqrt{2}$. In $SU(2)$ representation, $\zeta \in \mathbb{B}$ and $\chi = 1/2$. χ is the *group characteristic parameter* and ζ is the *generation representative*. Therefore, in both group representations, the area eigenvalues exhibit equally spaced symmetry which make one of the original labels redundant.

[7] For proofs refer to the Appendix (B).

Having defined the area eigenvalues, the following Lemmas can be easily investigated:

► **Lemma 1**: *Having two eigenvalues $a_1 \in \sqrt{\zeta_1}\mathbb{N}$, and $a_2 \in \sqrt{\zeta_2}\mathbb{N}$, where $\zeta_1 \neq \zeta_2$, for any choice of the eigenvalues in the corresponding generations these two eigenvalues are not equal, $a_1 \neq a_2$.* ◄

► **Lemma 2**: *Having two eigenvalues $a_1 \in \sqrt{\zeta_1}\mathbb{N}$, and $a_2 \in \sqrt{\zeta_2}\mathbb{N}$, where $\zeta_1, \zeta_2 \in \mathbb{A}$ (or $\mathbb{B}$) and $\zeta_1 \neq \zeta_2$, there in no eigenvalue in any generation that is equal to $a_1 \pm a_2$.* ◄

5.9 Radiation

In this part, based on the results of the section 5.5, the spectroscopy of a quantum black hole is worked out.

Let us briefly overview the rest of this Part. The quantum fluctuation of the horizon area of a Schwarzschild black hole may occurs at the state associated to one or more than one of the horizon area cell. Since in the complete spectrum of area the gap between consecutive eigenvalues decreases in larger eigenvalues, effectively a continuous set of radiance frequencies are expected. Considering the result of Part (I), in which the complete spectrum of area is uncovered to exhibits evenly spacing symmetry if it is classified into some subsets (the so-called 'generations'). Consider a transition from an upper area level, which belongs to the generation ζ_1, into a lower area level, which belongs to the generation ζ_2. While there is nothing special with transition between two levels of two different generations, the radiance intensities of a set of frequencies which correspond to the transition within a generation ($\zeta_1 = \zeta_2 =: \zeta$) get highly amplified. The reason is that within a generation of quantum area a typical transition can occur from many different levels. For instance, a quantum jump of the scale of the double of the gap between a generation can be initiated from the third, fourth, fifth, up to the maximum levels. These quanta are all different copies of the same energy that a black hole may radiate. In fact, quantum amplification results into discrimination between the spectral line intensities. Such emissions are unblended and amenable to possible observation in primordial black holes.

Considering the symmetry of area each one of the generations justifies the equidistant ansatz (5.2) separately after replacing $\alpha = 4\pi\gamma\chi\sqrt{\zeta}$. The fundamental frequencies which are emitted by quantum jump inside a generation ζ is

$$\varpi(\zeta) = \frac{\gamma c^3}{8GM}\chi\sqrt{\zeta}. \tag{5.13}$$

Let us name $\omega_o := c^3/8GM$ *the frequency scale factor* and is of the order of $10^{16}/M_{kg}$ (eV). For instance the frequency scale corresponding to a black hole of mass $M \sim 10^{12}$ kg is of the order of 10 keV and thus the harmonics are of order $10\sqrt{\zeta}n$ keV, though these lines are not of the same intensities. In fact, the intensity is suppressed as the gap between the levels of a generation grows. This because of the amount of quantum amplification a frequency may take. A precise work based on minimal number of natural assumptions is required to work out the intensities, which is introduced in the rest.

5.10 Quantum amplification effect

In general, transitions fall into two categories: (i) *the generational transitions*, quantum jumps from a level to a lower level of the same generation, and (ii) *the inter-generational transitions*, quantum jumps from a level into a lower level of different generation. The frequency corresponding to the first type of emissions is proportional to the fundamental frequency of the generation to which both the initial and final levels belong, $\omega_n := n\varpi(\zeta)$ for integer positive n. These frequencies are called *harmonic frequencies* of the generation ζ. What ever frequency that is not of this type is of *non-harmonics*.

The strategy of determining the intensity of radiation is as follows. The intensity of an emissive frequency is defined by the amount of energy radiating at that frequency per unit time and area. The energy corresponding to a frequency is proportional to the average number of its emissive quanta. Firstly, it is assumed that the emissions occur in sequences. Accordingly, the probability of emissions of a typical sequence is determined. Having this, one can calculate the probability of the sequence that contains a number of the same frequencies. The average number of emissive quanta at different frequencies are determined. Thus, the intensity of frequencies are found. We calculate the intensity and the natural width of lines and the corresponding temperature to a black hole in this section. For the matter of clarifying the hidden assumption behind this strategy we give main axioms individually.

Axiom 1: Emissions occur in a sequential order.

This was first proposed by Ulrich Gerlach at the surface of a collapsing star in (75). From a black hole, as a possible ultimate state of a collapsing star, a quantum of energy may be emitted between two classical stationary states. Describing the decay of the black hole during any interval of observer time Δt, a set of j individual decays are emitted in the sequence $\{\omega_1, \omega_2, \cdots, \omega_n\}$, successively. The probability of a typical sequence is determined in this section.

In generational transitions, many copies of a harmonic frequency can be produced from different pairs. However, this is not the case for non-harmonics, because the irrational numbers $\sqrt{\zeta}$ that area eigenvalues are proportional to, cannot be decomposed into a sum of other irrational numbers. Accordingly, Lemma 2 approves that the difference $\Delta a = a(\zeta) - a'(\zeta')$ between two levels of different generations, $\zeta \neq \zeta'$, is 'unique' and cannot be produced by considering other pairs. Therefore, a non-harmonic transition is emitted only from *one* pair of levels.

On the other hand, from the classical relation between the horizon and the black hole mass (5.1), it is easy to verify $A(\mathrm{m}^2) = 2.77 \times 10^{-53} M(\mathrm{kg})^2$. The temperature of such a black hole is $T(\mathrm{k}) = 1.23 \times 10^{23}/M(\mathrm{kg})$. For instance, the horizon area corresponding to the black hole of mass 10^{12} kg is $2.77 \times 10^{-29}(\mathrm{m}^2)$ and its temperature is 1.228×10^{11}k. Such a horizon is 40 order of magnitude larger than the quanta of area! This gives the confidence that the number of levels that contribute to the radiation procedure is enormous.

This fact make the difference between harmonics and non-harmonics important. Namely, the population of harmonics exceed the population of non-harmonics. This

effect in quantum mechanics is called *Quantum Amplification Effect*. This effect has a strong root in the symmetry of area.

To determine how much the difference of the population is important and if it is visible a precise analysis is necessary. Let us start off the analysis with the probability of some decay in a sequential order.

5.10.1 The probability of time-ordered decays

The probability of one jump (no matter of what frequency) in the course of time Δt is indicated by $P_{\Delta t}(1)$. Similarly, the probability of no jump is $P_{\Delta t}(0)$. During the time interval $2\Delta t$, the probability of no jump (the failure of decaying) is equal to the probability of the failure in each one of its two fragment of time intervals, $P_{2\Delta t}(0) = [P_{\Delta t}(0)]^2$. The general solution of this functional equation is $P_{\Delta t}(0) = \exp(-\Delta t/\tau)$, where τ is the survival timescale of the black hole from decaying.

We let the horizon decay in a sequence of frequencies successively. Using the same argument, the probability of one jump (of any frequency) in time interval $2\Delta t$ is $P_{2\Delta t}(1) = 2P_{\Delta t}(0)P_{\Delta t}(1)$. Therefore, $P_{\Delta t}(1) = (\Delta t/\tau')\exp(-\Delta t/\tau)$.

The probability of 2 jumps in the time interval $2\Delta t$ can be written as $P_{2\Delta t}(2) = 2P_{\Delta t}(0)P_{\Delta t}(2)+[P_{\Delta t}(1)]^2$. This formula can be extended to the probability of emission of 'even' number (j) quanta in the time interval $2\Delta t$,

$$P_{2\Delta t}(j) = 2\sum_{i=0}^{i=\frac{j}{2}-1} P_{\Delta t}(i)P_{\Delta t}(j-i) + [P_{\Delta t}(j/2)]^2. \tag{5.14}$$

On the other hand, the probability of 3 jumps in the time interval $2\Delta t$ can be written as $P_{2\Delta t}(3) = 2P_{\Delta t}(0)P_{\Delta t}(3) + 2P_{\Delta t}(1)P_{\Delta t}(2)$. This formula can deduce to the probability of emission of 'odd' number (j) quanta in the time interval $2\Delta t$,

$$P_{2\Delta t}(j) = 2\sum_{i=0}^{i=\frac{j-1}{2}} P_{\Delta t}(i)P_{\Delta t}(j-i). \tag{5.15}$$

Generating all the probabilities starting from $P_{\Delta t}(0)$ up to $P_{\Delta t}(j-1)$ consecutively from the recursive formula (5.14) and (5.15), one can generate the probability of j emissions as a function of j and Δt. The general solution for the probability of j decays is

$$P_{\Delta t}(j) = \frac{1}{j!}\left(\frac{\Delta t}{\tau'}\right)^j \exp(-\Delta t/\tau), \tag{5.16}$$

in which by normalization $\tau' = \tau$.

This formula can be easily checked if the answer (5.16) is substituted into (5.15) or (5.14) or any other similar equations that can be made for any number of emissions in any time interval.

5.10.2 The probability of a decay

Consider a sequence of radiance frequencies $\{\omega_1, \omega_2 \cdots\}$. These frequencies might be harmonics or non-harmonics. For the purpose of determining the probability of this sequence let us begin with one jump $(j = 1)$ in the course of time Δt.

Since the emissions are supposed to occur in time order, the probability of a sequence of decays is the product of conditional probability and the probability distribution of time ordering. Thus, the probability of one emission is $P_{\Delta t}(\{\omega\}) = P_{\Delta t}(\{\omega \mid 1\})P_{\Delta t}(j=1)$. This probability is not difficult to determine. Before this the second axiom is introduced.

Axiom 2: The entropy of a Schwarzschild black hole is $A/4\ell_P^2$, where A is its horizon area and ell_P is the Planck's length.

Note that we have assumed this as an axiom first when we published the relevant paper on this subject. However, later on we noticed this axiom itself can be proven in the form of a theorem and it can be derived from within the generic degeneracy of area operator and thus no axiom is necessary to be assumed. For the rest of this thesis, in this chapter and next one we discuss this axiom as a theorem time to time and bring some modifications to the original text.

Entropy is defined as the logarithm of the number of microstates of a macroscopic state. Since the macroscopic state of a Schwarzschild black hole is determined by one parameter, the horizon area, the entropy associated to a black hole of horizon area A is determined by the number of quantum states associated to such a horizon. This degeneracy, $g(A)$, is dominantly $g(A) = \exp(A/4\ell_{\rm P}^2)$. The horizon area of a loop quantum black hole is made of N patches of area eigenvalues, $A = \sum_{i=1}^{N} a_i$. Therefore the black hole degeneracy is in fact $g(A) = \exp(\sum_{i=1}^{N} a_i/4\ell_{\rm P}^2)$. On the other hand, the overall degeneracy g corresponding to a system that is made of N subsystems each with individual degeneracy g_i, is $g = \prod_{i=1}^{N} g_i$. Due to the Lemma 2, the contribution of each generation in the horizon area A cannot be replaced by the combination of area levels of the other generations. Therefore, the macroscopic horizon area is split into its ingredient area contribution of each generation, $g(A) = \prod_{\zeta} \exp(\sum_i a_i(\zeta)/4\ell_{\rm P}^2)$. Therefore, the degeneracy associated to the generation τ is $g(\zeta) = \exp(\sum_i a_i(\zeta)/4\ell_{\rm P}^2)$, where i indicates the levels of the generation that contribute in the horizon area. Since each generation is equidistant, all levels that contribute in the horizon area from one generation sum into a level inside the same generation, say the level n. In other words, $\sum_i a_i(\zeta) =: a_n(\zeta)$. Consequently, the degeneracy $g(\zeta)$ can be thought of being the degeneracy associated to the level n of the generation, $g(n;\zeta) = \exp(a_n(\zeta)/4\ell_{\rm P}^2)$. By the use of equation (5.12), the degeneracy of a typical level $a_n(\zeta)$ is

$$g(n;\zeta) := e^{\pi\gamma\chi\sqrt{\zeta}\ n}. \tag{5.17}$$

where ζ is the representative number of the generation, n is the level of the frequency in the generation ladder. [8]

An area patch of level n of the generation ζ may decay into the level n'-th of the generation ζ', where $\sqrt{\zeta}n > \sqrt{\zeta'}n'$. In this process, the degeneracy $g(n;\zeta)$ changes into $g(n';\zeta')$. By the use of (5.17), the transition into a lower level changes the degeneracy by a factor of $\exp(-\pi\gamma\chi|\sqrt{\zeta}n - \sqrt{\zeta'}n'|)$ corresponding to the emission of the frequency $\omega = (\gamma\chi c^3/8GM)(\sqrt{\zeta}n - \sqrt{\zeta'}n')$.

[8] This degeneracy can also be determined exactly by considering the fact that a typical area level $a_n(\zeta)$ can be made of some smaller area patches (of the same generation) in some different configurations. Considering the degeneracy of each level, the exponentially growing degeneracy of a level is immediately reproduced, (71).

The 'population' of a quantum of area is the number of different pairs of levels that produce it. This number can be normalized to one by the use of the maximum population number, N_o, which is in fact nothing but the number of level pairs that produce the fundamental frequency of the first generation (the generation whose corresponding gap between levels is minimal). Therefore, the *population weight* of the frequency ω is defined as $\rho(\omega) = N/N_o$, where N is the number of pairs that produce the frequency ω. It is also clear that the population weight of non-harmonics is $1/N_o$.

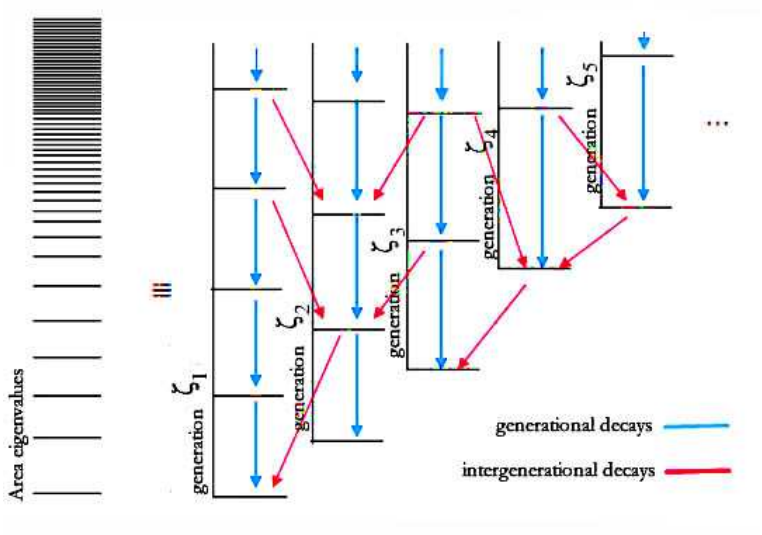

Figure 5.4: A schematic diagram of generational emissions (the vertical black arrows) and intergenerational emissions (the slanted red arrows) for a few generations.

In our navigation for determining the probability of a specific frequency emission the third axiom is introduced:

> *Axiom 3: The density matrix elements for quantum transitions between near levels are uniform.*

Having assumed this, the probability of a jump is proportional to the change of degeneracy as well as the population weight of the frequency. Therefore, the conditional probability of a typical frequency ω by the use of (5.17) is

$$P_{\Delta t}(\{\omega\} \mid 1) = \frac{1}{C}\rho(\omega)\ e^{-\Lambda\omega}, \tag{5.18}$$

where

$$\Lambda := 8\pi GM/c^3. \tag{5.19}$$

The normalization relation of the probability determines C. It is defined to be $C := \sum_\omega \rho(\omega)\ e^{-\Lambda\omega}$.

Since the probability of a typical frequency ω is determined from $P_{\Delta t}(\{\omega\}) = P_{\Delta t}(\{\omega\} \mid 1)\ P_{\Delta t}(1)$. By the use of (5.16) and (5.18) for $j = 1$,

$$P_{\Delta t}(\{\omega\}) = \frac{\Delta t}{C\tau}e^{-\Delta t/\tau}\ \rho(\omega)\ e^{-\Lambda\omega} \tag{5.20}$$

In the case of generational decays, the decay condition $\sqrt{\zeta}n > \sqrt{\zeta'}n'$ is reduced into $n > n'$. The conditional probability of a typical frequency $\omega_m := m\varpi(\zeta)$ emission, where $m = n - n'$, by the use of (5.13) and (5.18) reads

$$P_{\Delta t}(\{\omega_m(\zeta)\} \mid 1) = \frac{1}{C}\ \rho(\zeta)\ q(\zeta)^{-m}, \tag{5.21}$$

where $q(\zeta) := e^{\Lambda\varpi(\zeta)}$ is independent of mass and dependent to the generational representative number ζ. In fact it is [9]

$$q(\zeta) := e^{\pi\gamma\chi\sqrt{\zeta}}. \tag{5.22}$$

Given a black hole of horizon area A, it is discussed in section (5.10) a generation with smaller gap between levels produces more copies of each one of its corresponding harmonic frequencies. Since the gap between the levels is $(4\pi\gamma\chi\sqrt{\zeta})\ \ell_{\rm P}^2$ by the use of (5.12) the number of levels below the horizon area is $N := A/(4\pi\gamma\chi\sqrt{\zeta})\ell_{\rm P}^2$, which is a huge number (about 10^{40} levels). On the other hand, the number of m-level jumps down a ladder of total N levels is $N-m$. In a classical black hole N is extremely large, henceforth the population weight of the harmonics of frequency $\omega_m(\zeta)$ for $m \ll N$ is $\rho(\zeta) = N/N_o = \sqrt{\zeta_o/\zeta}$, where ζ_o is the generation with the minimal gap between levels.[10] Dropping the constant coefficient $\sqrt{\zeta_o}$ from the definition, the population weight of small harmonics is

$$\rho(\zeta) := \frac{1}{\sqrt{\zeta}}. \tag{5.23}$$

Since the probability of the harmonic frequency $\omega_n(\zeta)$ is defined by $P_{\Delta t}(\{\omega_n(\zeta)\}) = P_{\Delta t}(\{\omega_n(\zeta)\} \mid 1)\ P_{\Delta t}(1)$. By the use of (5.21) and (5.16) for $j = 1$, one can write the probability of the harmonic frequency

$$P_{\Delta t}(\{\omega_n(\zeta)\}) = \frac{\Delta t}{C\tau}e^{-\Delta t/\tau}\ \rho(\zeta)\ q(\zeta)^{-n} \tag{5.24}$$

What is C? In fact after a moment of analytical calculation the normalization coefficient C is found

$$C = \sum_{\text{all }\zeta}\ \frac{\rho(\zeta)}{q(\zeta) - 1} \tag{5.25}$$

It is easy to prove that C is a finite number of the order $O(1)$. A curious reader is encouraged to read the detail of the derivation of C and testing its finiteness in Appendix (D).

Next step is to generalized this probability for a sequence of j successive emissions of different frequencies.

5.10.3 The probability of a sequence of emissions

Following the Axiom 1, the generalized probability of a sequence of harmonics is $P_{\Delta t}(\{\omega_1, \omega_2, \cdots, \omega_j\})$, where the frequencies can be harmonics or non-harmonics. Let us assume the time interval is made of S fragments of smaller time intervals, $\Delta t = S\epsilon$,

[9] Comparing (5.22) with the degeneracy of a level (5.17) shows the simple relation: $g(n;\zeta) = q(\zeta)^n$.
[10] ζ_o in $SU(2)$ version is 3 and in $SO(3)$ version is 1.

where $S \gg j$ and each one of the j decays occurs in one fragment of time ϵ. There are $S!/j!(S-j)!$ number of ways for selecting j jumping intervals out of total S time intervals. This number of ways for the case of $S \gg j$ is approximated to $S^j/j!$. In the overall $j\epsilon$ moment intervals out of S ones, the black hole successfully decays and in the rest of time, $(S-j)\epsilon$, it fails to decay. The probability of j emissions is thus $(S^j/j!)P_\epsilon(0)^{S-j}\ \prod_{i=1}^{j} P_\epsilon(\{\omega_i\})$. Substituting $P_\epsilon(\{\omega_i\})$'s from (5.24), the probability is:

$$P_{\Delta t}(\{\omega_1, \omega_2, \cdots, \omega_j\}) = \frac{1}{j!}\left(\frac{\Delta t}{C\tau}\right)^j\ e^{-\Delta t/\tau}\ \prod_{i=1}^{j} \rho(\zeta_i)\ e^{-\Lambda\omega(\zeta_i)}. \tag{5.26}$$

In the presence of r non-harmonics in a sequence of frequencies decreases the probability of the sequence by a factor of $(1/N_o)^r$, which is negligible for classic black holes. In fact, only the harmonics take a major contribution to determining the intensities.

Let us consider now a sequence of harmonic emissions of different generations, $\{\omega_{n_1}(\zeta_1), \omega_{n_2}(\zeta_2), \cdots, \omega_{n_j}(\zeta_j)\}$. According to (5.21) and (5.26) the probability of the sequence is

$$P_{\Delta t}(\{\omega_{n_1}(\zeta_1), \omega_{n_2}(\zeta_2), \cdots, \omega_{n_j}(\zeta_j)\}) = \frac{1}{j!}\left(\frac{\Delta t}{C\tau}\right)^j\ e^{-\Delta t/\tau}\ \prod_{i=1}^{j} \rho(\zeta_i)\ q(\zeta_i)^{-n_i}. \tag{5.27}$$

By the use of the probability of j decays in the course of time Δt from (5.16), the generalized conditional probability of a sequence of harmonics is found

$$P_{\Delta t}(\{\omega_{n_1}(\zeta_1), \omega_{n_2}(\zeta_2), \cdots, \omega_{n_j}(\zeta_j)\} \mid j) = \left(\frac{1}{C}\right)^j\ \prod_{i=1}^{j} \rho(\zeta_i)\ q(\zeta_i)^{-n_i}. \tag{5.28}$$

This conditional probability turn out to be independent of time.

Since the intensity of a harmonic frequency depends on the average number of the emission in the course of time. This average number depends on the probability of k emissions of the emissive frequency in any sequence of dimension $j \geq k$.

5.10.4 The probability of k quanta of the same frequency

Let us assume that among the j emissions there exist k quanta of the frequency $\omega_{n_k}(\zeta_k)$ and the rest $j-k$ frequencies belong to other frequencies. Consider the j dimensional sequence $\{\omega_{n_1}(\zeta_1), \omega_{n_2}(\zeta_2), \cdots, \omega_{n_k}(\zeta_k), \cdots, \omega_{n_k}(\zeta_k), \cdots, \omega_{n_j}(\zeta_j)\}$ in which there are k quanta of the same frequency $\omega_{n_k}(\zeta_k)$. If the black hole makes j decays such that k of them are of the same frequency $\omega_{n_k}(\zeta_k)$, (for $k \leq j$), there are $k!/j!(j-k)!$ ways to select these k quanta. The probability of each selection due to (5.28) is

$$\left(\frac{1}{C}\right)^j\ \left(\rho\left(\zeta_k\right) q\left(\zeta_k\right)^{-n_k}\right)^k \prod_{i=1}^{j-k} \rho(\zeta_i)\ q(\zeta_i)^{-n_i}. \tag{5.29}$$

where in the product part of it the frequencies are any frequency except $\omega_{n_k}(\zeta_k)$.

For the purpose of determining the probability of k emissive quanta of the frequency $\omega_{n_k}(\zeta_k)$ in a j dimensional string included all possible accompanying frequencies, $P_{\Delta t}(k \mid \omega_{n_k}(\zeta_k), j)$, we should sum over the probabilities (5.29) for all possible frequencies associated to the accompanying frequencies, all frequency values except

$\omega_{n_k}(\zeta_k)$. Since the non-harmonic emissions are continuous sum over non-harmonics is effectively evaluated by integral. We must consider different cases for the $j-k$ accompanying emissions: the case that none of the $j-k$ frequencies is non-harmonic, the case that only one of them is non-harmonic, etc.. Therefore the conditional probability is

$$\begin{aligned}
P_{\Delta t}(k|\omega_{n_k}(\zeta_k),j) = \quad & \frac{j!}{k!(j-k)!}\left(\frac{1}{C}\right)^j \left(\rho\left(\zeta_k\right) q\left(\zeta_k\right)^{-n_k}\right)^k \times \\
& \Bigg[\prod_{i=1}^{j-k} \sum_{\text{all }\zeta} \sum_{\omega\neq\omega_{n_k}} \rho(\zeta_i)\ q(\zeta_i)^{-n_i} \\
& + \prod_{i=1}^{j-k-1} \sum_{\text{all }\zeta} \sum_{\omega\neq\omega_{n_k}} \rho(\zeta_i)\ q(\zeta_i)^{-n_i} \left(\int_{0,\omega\neq\omega_k}^{\infty} \rho e^{-\Lambda\omega}\Lambda d\omega\right) \\
& + \prod_{i=1}^{j-k-2} \sum_{\text{all }\zeta} \sum_{\omega\neq\omega_{n_k}} \rho(\zeta_i)\ q(\zeta_i)^{-n_i} \left(\int_{0,\omega\neq\omega_k}^{\infty} \rho e^{-\Lambda\omega}\Lambda d\omega\right)^2 + \cdots \\
& + \sum_{\text{all }\zeta} \sum_{\omega\neq\omega_{n_k}} \rho(\zeta_i)\ q(\zeta_i)^{-n_i} \left(\int_{0,\omega\neq\omega_k}^{\infty} \rho e^{-\Lambda\omega}\Lambda d\omega\right)^{j-k-1} \\
& + \left(\int_{0,\omega\neq\omega_k}^{\infty} \rho e^{-\Lambda\omega}\Lambda d\omega\right)^{j-k}\Bigg].
\end{aligned}$$

Substituting ρ, the contribution of a non-harmonic emission becomes $(1/N_o)(1-e^{-\Lambda\omega_k})$. By the use of the equality (D.2) the sum $\sum_{\text{all }\zeta}\sum_{n\neq n_k}\rho(\zeta)q(\zeta)^{-n}$ gives rise to $C-\rho(\zeta_k)q(\zeta_k)^{-n_k}$.

In the classical limit, $1/N_o \to 0$, inside the bracket all terms with the factor $1/N_o$ are higher order corrections to the probability. For the purpose of determining the intensity, it is sufficient to consider only the first order term. Effectively this probability is

$$\begin{aligned}
P_{\Delta t}(k \mid \omega_{n_k}(\zeta_k),j) = \frac{j!}{k!(j-k)!}\left(\frac{1}{C}\right)^j & \left(\rho\left(\zeta_k\right) q\left(\zeta_k\right)^{-n_k}\right)^k \\
& \times \left(C-\rho\left(\zeta_k\right) q\left(\zeta_k\right)^{-n_k}\right)^{j-k}. \qquad (5.30)
\end{aligned}$$

We multiply this conditional probability by the absolute probability distribution $P_{\Delta t}(j)$ in equation (5.16) and sum over all $j \geq k$ in order to provide the probability of $P_{\Delta t}\left(k|n_k\varpi^{(\zeta)}\right)$,

$$\begin{aligned}
P_{\Delta t}(k \mid \omega_{n_k}(\zeta_k)) = \frac{1}{k!} \quad & \left(\rho\left(\zeta_k\right) q\left(\zeta_k\right)^{-n_k}\right)^k \left(C-\rho\left(\zeta_k\right) q\left(\zeta_k\right)^{-n_k}\right)^{-k} e^{-\Delta t/\tau} \\
& \times \sum_{j\geq k}^{\infty} \frac{1}{(j-k)!}\left(\frac{\Delta t}{C\tau}\right)^j \left(C-\rho\left(\zeta_k\right) q\left(\zeta_k\right)^{-n_k}\right)^j
\end{aligned}$$

Applying the equality $\sum_{a=b}^{\infty} z^a/(a-b)! = z^b \exp(z)$ by replacing a, b with j, k respectively in the second line, the probability distribution of the emission k quanta of frequency $\omega_{n_k}(\zeta_k)$ is determined,

$$P_{\Delta t}\left(k \mid \omega_{n_k}(\zeta_k)\right) = \frac{1}{k!}\left(x_{n_k}\left(\zeta_k\right)\right)^k e^{-x_{n_k}(\zeta)}, \tag{5.31}$$

where $x_n(\zeta) := (\Delta t/C\tau)\ \rho(\zeta) q(\zeta)^{-n}$. This probability turns out to be Poisson-like distribution.

5.11 Intensity

By definition, the intensity of $\omega_{n_k}(\zeta_k)$ is the total energy that is emitted at this frequency and unit time per unit area. Since the emissions of diverse frequencies are independent, the total energy of a frequency is the average number of quanta emitted at that frequency times the energy of the frequency.

Using (5.31), this average number of quanta of this frequency is

$$\overline{k} = \sum_{k=1}^{\infty} k\ P_{\Delta t}\left(k \mid \omega_{n_k}(\zeta_k)\right) = \left(\frac{\Delta t}{C\tau}\right)\ \rho(\zeta_k) q(\zeta_k)^{-n_k}.$$

Since the mean value of the number of quanta emitted at a typical harmonic frequency $\omega_n(\zeta)$ is proportional to Δt as well as $\rho(\zeta)q(\zeta)^{-n}$, the intensity of a typical line $\omega_n(\zeta)$ is

$$I(\omega_n) = I_o\ \omega_n(\zeta)\ \rho(\zeta) e^{-\Lambda\omega_n(\zeta)}. \tag{5.32}$$

where I_o is a constant.

5.12 Temperature

In the thermal radiation from a black body the number of quanta in a frequency is distributed by a Poisson function, according to (5.31). To see the consistency of the Poisson distribution with the thermal distribution of a black body consider the radiation from a black body at a given temperature T. According to the definition of black body, the number of a frequency ω those are emitted from within the body is determined by the Boltzmann function, $P_T(\omega) = B\exp(-\hbar\omega/k_BT)$, where B is a normalization constant, $B = 1/\sum_\omega \exp(-\hbar\omega/k_BT)$, (similar to (5.21)) and k_B is Boltzman constant. The probability of k quanta emissions of a specific frequency ω_k in a j dimensional sequence of decays is $\binom{j}{k} P_T(\omega_k)^k \prod_{i\neq k} P_T(\omega_i)$. Summing over all accompanying frequency except ω_k, the conditional probability is

$$P_T(k|\omega_k, j) = \binom{j}{k} B^k \exp(-k\hbar\omega_k/k_BT)(1 - B\exp(-\hbar\omega_k/k_BT))^{j-k}. \tag{5.33}$$

Comparing this conditional probability and the one of (5.30), they are the same for a frequency ω_n if the coefficients of the two exponents are equal $\hbar/k_BT = 8\pi GM/c^3$. From this analogy between a black body radiation and a black hole, one may conclude the radiation is indeed thermal and the temperature associated to the black hole is

$$T := \frac{\hbar c^3}{8\pi G M k_B} \tag{5.34}$$

This coincides with the classical definition of black hole temperature and simply indicate that a radiating black hole is hot.

5.13 Width of lines

Having the above information, specially the probabilities (5.18) and (5.21), the mean value of emissive frequencies is easily evaluated,

$$\langle \omega \rangle = \frac{\eta \gamma \chi \omega_o}{C}, \tag{5.35}$$

where $\eta := \sum_{\text{all } \zeta} \frac{q(\zeta)}{(q(\zeta)-1)^2}$. A curious reader is encouraged to follow up the easy calculation in Appendix (E).

By the use of the probability of decays in (5.16), the mean value of the dimension of the emission sequences j is $\Delta t/\tau$. Thus, the mean decrease of the mass of black hole during the course of Δt is

$$\frac{\Delta \overline{M}}{\Delta t} = -\frac{\hbar \langle \omega \rangle}{c^2 \tau}. \tag{5.36}$$

On the other hand, the Stefan-Boltzmann law of black-body radiation from a black hole of horizon area A and surface temperature (5.34) indicates that the radiance rate from the black hole is

$$\frac{\Delta \overline{M}}{\Delta t} = -\frac{\hbar c^4}{15360\pi\ G^2 M^2}. \tag{5.37}$$

Comparing these two radiance rates of (5.37) and (5.36) we can evaluate τ,

$$\tau = \frac{1920\pi\ \eta \gamma \chi}{C \omega_o}, \tag{5.38}$$

By definition in (5.16) τ is the survival time scale of the black hole from decaying. On average the time elapsed before a decay is

$$\bar{t} = \int_{t=0}^{\infty} t P_t(j=1) dt = 2\tau, \tag{5.39}$$

The uncertainty of the elapsing time before a decay is

$$(\Delta t)^2 = \int_{t=0}^{\infty} (t-\tau)^2 P_t(j=1) dt = 3\tau^2. \tag{5.40}$$

Due to the uncertainty principle $\Delta E \Delta t \geq \hbar/2$ and the definition of the frequency by energy, $E = \hbar\omega$, the uncertainty of the frequency turns out to be $\Delta\omega \simeq 1/\tau$. Therefore, the width of emission frequencies is proportional to $W = 1/\tau$,

$$W = \left(\frac{C}{1920\pi\ \eta \gamma \chi} \right)\ \omega_o, \tag{5.41}$$

To estimate the order of it, let us substitute the numerical values that are provided after $\gamma = \ln 3/\pi\sqrt{2}$. We apply the values of C and η from the Appendices (D) and (E). In $SU(2)$ representation, where $\chi = 0.5$, $\eta = 9.01$, and $C = 2$, the ratio becomes $W = 0.00029\omega_o$. In $SO(3)$ group representation, $\chi = \sqrt{2}$, $\eta = 4.7$, and $C = 0.93$ the ratio turns out to be $W = 0.00009\omega_o$. The order of lines width ratio is a few thousandth of the gap between the lines, thus the spectral lines are reasonably narrow.

5.14 The spectrum

In this section, the spectrum is reviewed.

Comparing the intensities corresponding to the frequencies $\omega_n(\zeta) = n\varpi(\zeta)$ and $\omega_m(\zeta') = m\varpi(\zeta')$, depending on whether the generations are the same or not, there exist two cases:

(i) In a generation, $\zeta = \zeta'$, the relative intensity of two harmonic frequencies is

$$\frac{I_n}{I_m} = \frac{n}{m} q(\zeta)^{m-n} \tag{5.42}$$

(ii) In different generations, $\zeta \neq \zeta'$, the relative intensities of the two modes $\omega_n(\zeta)$ and $\omega_{n'}(\zeta')$ is

$$\frac{I_n(\zeta)}{I_{n'}(\zeta')} = \frac{n}{n'}\, e^{-\Lambda[n\varpi(\zeta) - n'\varpi(\zeta')]}. \tag{5.43}$$

Graphically, in Fig. (5.5) the intensities of harmonic frequencies corresponding to two different generations are shown in two different colours. The spectrum of harmonic frequencies corresponding to the fundamental frequency $\varpi(\zeta)$ is in black and the ones corresponding to $\varpi(\zeta')$ (for $\omega(\zeta') > \omega(\zeta)$) is in red (the thicker set of bar lines). The envelope of each generation matches with the one of Hawking and Bekenstein semiclassical result.

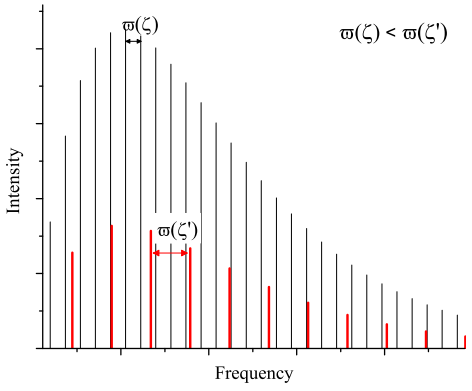

Figure 5.5: The intensities of harmonic frequencies of two generations ζ and ζ' subject to the condition $\varpi(\zeta) < \varpi(\zeta')$.

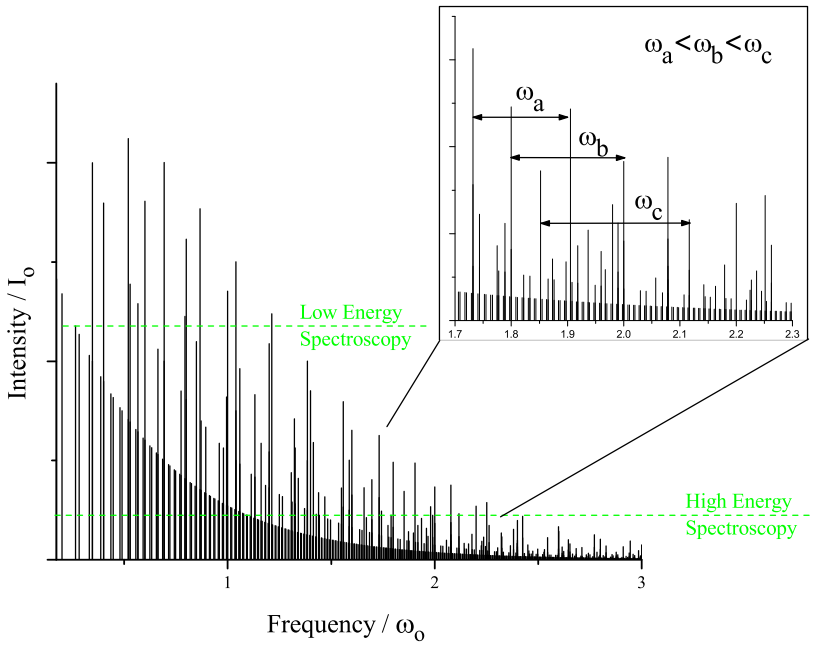

Figure 5.6: The radiation spectrum of a loop quantum black hole.

Let us explain the disordered intensities by the following example. Consider three *consecutive* harmonic frequency modes ω_1, ω_2 and ω_3 where $\omega_i = n_i \varpi(\zeta_i)$ for $i = 1, 2, 3$ and $\omega_1 < \omega_2 < \omega_3$. Since n_1, n_2, and n_3 are arbitrary integers in general, let us assume that the fundamental frequencies ϖ_1 and ϖ_3, associated to the frequencies ω_1 and ω_3 respectively, are equal and the double of the fundamental frequency ϖ_2 associated to ω_2; ($\varpi_1 = \varpi_3$ and $\varpi_1 = 2\varpi_2$). Since there is no other line between these three lines, $n_3 = n_1 + 1$ and $n_2 = 2n_1 + 1$. Comparing the intensities associated to these three lines from (5.42), it turns out that the intensity of ω_2 is doubled, thus the middle line is *much* brighter than the two nearby ones.

Figure (5.6) shows the intensities corresponding to the harmonic frequencies up to the maximum $3\omega_o$. It is easy to see only a countable number of the most bright line exist in any interval of the order of ω_o; those which belong to the first few generations. In fact the intensity formula (5.42) shows the intensities corresponding to the third generation on are highly suppressed relative to the first two generations.

Let us recall that in addition to these lines, there are non-harmonic lines too but since their intensities are extremely suppressed, they do not blend the discreteness of the most bright lines.

The maximum intensities in the spectrum belong to the frequencies of the condition $\omega_{\text{peak}} \sim 1/\Lambda = c^3/8\pi GM = \omega_o/\pi$. Therefore, the most bright lines are of the harmonics of integer valued number $n_{\text{peak}} \sim (\gamma\pi\chi\sqrt{\zeta})^{-1}$. Among all of the parameters, only the Barbero-Immirzi parameter is not certainly known and the dependency of the peak to the parameter is remarkable for the purpose of a possible way to determining it.

5.15 Discussion

The discreteness of area eigenvalues comes about the canonical quantization of 3-geometry because it is supposed that geometry has a distributional character with 1-dimensional excitations. Having this, the quantum geometrical operators are constructed by the canonical variables of loop quantum geometry. Among them, the area operator is the one whose corresponding eigenvalues are completely known.

In section 5.5 it was demonstrated that the area eigenvalues exhibits an unexpected symmetry. In fact, the spectrum of the numbers can be split into equidistant sequences of numbers. Each one of these evenly spaced sets of numbers is called a 'generation.' Each generation possesses an individual gap between levels, by which it is identified. The gap is proportional to the square root of a square-free number in $SO(3)$ representation, or the discriminant of a positive definite quadratic form in $SU(2)$ representation.

Consequently, the eigenvalues of area operator, instead of being labeled by three free numbers j_u, j_d and j_{u+d}, can be performed by fewer numbers; which can be the representative that specifies the generation and the level within a generation.

The relation between area and mass of a black hole (valid only on a black hole horizon), introduces quanta of energy by the use of the 'area' states of horizon. Having the symmetry of the quanta of horizon area, two different types of area transitions are possible: the transition either (i) between area levels within a generation (the so-called 'generational transitions') or (ii) between the area levels of different generations (the so-called 'inter-generational transitions'). One of the immediate consequences of this symmetry is there appears a discrimination between these two types of transitions. Those quanta emitting from generational transitions can be reproduced in many copies from many levels of a generation. However, there exists only one copy of each inter-generational transitions. This leads to a discrimination in the population of generational transitions motivated by the quantum amplification effect.

In section 5.9 the intensity of radiation for any frequency was worked out. It was illustrated that a black hole radiates a continuous spectrum of frequencies. The spectrum of the quanta frequencies ranges from zero to a maximum. Nonetheless, there exist some spectral lines which take *additional* intensities due to the quantum amplification effect. This 'amplification' is a feature of loop quantization of area. Following this, black hole radiation is dominated by the amplified area fluctuations and some discrete bright lines appear.

The smaller a fundamental frequency is, the more bright the harmonics are. Due to the γ-dependency of the intensity function and according to figure (5.6) the most bright lines in various energy scales of the spectrum belong to the first (or a few of the first) generation. Since the spectral lines are sufficiently narrow and apart from each other, they unlikely blend. In fact, the width of the lines are expected to be of the order of a thousandth of the frequency scale factor ω_o, while the gap between intensity peaks are of the order of this factor. Thus it is expected that such a quantum black hole radiates in a *visually discrete* pattern.

The precise spectroscopy depends on the exact value of the Barbero-Immirzi parameter as well as the group representation of spin network states.

Among the possible predictions of a canonically quantized black holes there are some features: 1) the radiation is effectively is visually discrete to observation, and

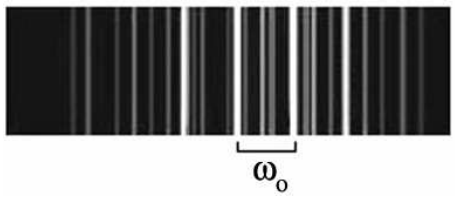

Figure 5.7: A typical spectrum of a canonically quantized black hole radiation for the low energy spectroscopy of Fig (5.6).

2) the intensities of consecutive lines are not orderly distributed.

Figure (5.7) is a typical expected radiance spectrum of a canonically quantized black hole is generated in low energy spectroscopy of figure (5.6). If the actual spectrum of black radiation is effectively discrete, the detection of a few of the most bright lines will be adequate to justify experimentally this prediction. The most bright lines in the spectrum belong to the first generation and the gap is of the order of the frequency scale $\omega_o \sim 10^{16}/M_{(\mathrm{kg})}$ (eV).

Recently, a number of efforts have been put on the discovery of the radiance patterns of different types of black holes, the primordial holes (76; 77) and the one of higher dimensions (78). One way to detect primordial black holes is by their Hawking radiation. The prediction of a canonically quantum black hole is also amenable to experimental check if the primordial black holes are founded. For instance, if the primordial black holes constitute an essential part of dark matter in the galactic distant, the observation of a few of their most bright radiance lines can be within the modern sensitivity and can be possibly distinguished from the radiation of other objects.

It should also be noted that this radiation, if associated to the primordial black holes, is far beyond the Trans-Planckian problem of inflationary cosmology. The Trans-Planckian problem refers to the derivation of physical quantities from quantum field theory beyond the Planck scale. However, the proposed spectroscopy is based on a version of quantum gravity in which the difficulties within the semiclassical approximation does not exist.

Among important questions that are asked about the developments of area operator and black hole physics, there remain some important questions.

From experimental point view,

- One of the most incredibly important questions is that how far are we from detecting this spectrum?
- Considering a tiny percentage of dark matter obtaining from primordial black holes, is it possible to verify the spectrum as an alternative instead of gamma-ray busters?
- In the case of a rotating black holes, how the spectral lines are shifted or widen?

From numerical point of view,

- What is the correlation between the Barbero-Immirzi parameter (γ) and the visual spectrum at different energy spectroscopies? In other words, considering

the γ-dependency of the intensities, what are the visual frequencies in a low energy spectroscopy?

From theoretical point of view,

- Under imposing what conditions the quantum dynamics of black hole spin network states are identified?
- What is the Planck scale corrections to the entropy of such a quantum black hole?

It will be also interesting to see if a similar pattern can be illustrated for near extremal black holes in supergravity and string theories.

Chapter 6

Area, ladder symmetry, degeneracy and entropy in loop quantum gravity

6.1 What is this about?

In the previous two chapters, we discuss two new properties in loop quantum gravity, the generic degeneracy of area operator and its ladder symmetry. During the time we were working on the complicated derivation of the radiance spectrum of a black hole we did not notice a weight factor in calculation. The absence of the factor does not change the physics and mathematics of what we have proposed before this at all. In fact, in this chapter we modify the intensity formula and revise the spectrum by the use of factor that makes a change in the appearance of the resulting intensities, yet the spectrum not only does not alter but also it reveals to be about ten times brighter at the brightest lines. We present the calculations in the most simple way that is possible and check the consistencies of the calculation with the thermodynamics of black hole in different spots in the text.

6.2 Area, ladder symmetry, degeneracy and entropy in loop quantum gravity

Loop Quantum Gravity admits a kind of area quantization that is characterized by three quantum numbers. We show the complete spectrum of area is the union of equidistant subsets and a universal reformulation with fewer parameters is possible. Associated with any area there is also another number that determines its degeneracy. One application is that a quantum horizon manifests harmonic modes in vacuum fluctuations. It is discussed the physical fluctuations of a space-time horizon should include all the excluded area eigenvalues, where quantum amplification effect occurs. Due to this effect the uniformity of transition matrix elements between near levels could be assumed. Based on these, a modification to the previous method of analyzing the radiance intensities is presented that makes the result one step further precise. A few harmonic modes appear to be extremely amplified on top of Hawking radiation. They are expected to form a few brightest lines with the wavelength not larger than

the black hole size.

6.3 Introduction

So far the main consequence of area quantization in loop quantum gravity has been the removal of classical gravitational singularities (10) as well as determining the isolated horizon entropy (45). The predicted generic exit of scale factor from an inflation sector into a Friedman universe in a loop quantized minisuperspace is at present in agreement with standard inflation models. This quantum phenomena, which comes from a quantum correction in the inhomogeneous Hamiltonian constraint, is through elementary area variable whose value should be determined by an underlying inhomogeneous state. Area is an elementary operator in Loop Quantum Gravity because in the classical limits it is directly related to the densitized triad as a canonical variable. In this thesis, we study two previously unknown properties of area quantization that further clarify the understanding of this operator. Firstly, the area eigenvalues possess a symmetry that its spectrum is the union of different evenly spaced subsets. Secondly, the eigenvalues are substantially degenerate such that in larger area the degeneracy increases. Due to the presence of a huge class of completely tangential excitations on a surface different regions of the surface are distinguishable. These together result in degeneracy increasing in a way that with any eigenvalue a finite exponentially proportional to area degeneracy is associated. One application is in area fluctuations of a collapsing star.

It is discussed the analysis of area fluctuations in a space-time horizon must include all those excluded quanta from a quantized isolated horizon (45). Having recognized the quantum amplification effect during transitions, the density matrix elements can be considered uniform in near levels. The black hole undergoes thermal fluctuations and harmonic modes resonate. Using these properties, a modification method to the previous analysis of the intensities (14) is introduced that makes the result more precise. The major result is that the fluctuations in the dominant configuration with minimal quantum of area is mostly amplified by the black hole such that a few sharp and bright lines appear on top of Hawking's radiation. These modes cannot be seen in the wavelength larger than the size of black hole. In summary, by the use of a few main assumptions from black hole studies, loop quantum gravity, a non-perturbative background independent approach to quantum gravity, becomes testable much above the Planck scales if quantum primordial black holes are ever found.

6.4 Area

In this thesis we choose to define a surface by a coordinate condition. The quantization of a 3-manifold is obtained by quantizing the holonomy configuration space on embedded graphs in a spatial manifold. The sub-graphs whose nodes lie on a surface are basis for defining the quantum state of the surface. Densitized conjugate momenta possess full information of the surface metric and consequently the surface area, (81).

Consider a vertex lying on a surface with total upper side spin j_u, bottom side spin j_d, and completely tangential edges of total spin j_t on the surface. The quantum of

area in this state depends on the upper and lower spins as well as the total tangent vector induced by these two on the surface, j_{u+d},

$$a = a_o\sqrt{2f(j_u) + 2f(j_d) - f(j_{u+d})}, \tag{6.1}$$

where $f(x) = x(x+1)$, $a_o := 4\pi\gamma\ell_P^2$, γ the Barbero-Immirzi parameter, and $j_{u+d} \in [|j_u - j_d|, \ldots, j_u + j_d - 1, j_u + j_d]$. Note that the completely tangential edges do not contribute in the area.

Consider a closed underlying surface dividing the 3-manifold into two completely disjoint sectors and not bounded by a boundary. A few additional vertices are needed in order to close this quantum state. This introduces two additional constraints on the states, namely: $\sum_\alpha j_u^{(\alpha)} \in \mathrm{Z}^+$ and $\sum_\alpha j_d^{(\alpha)} \in \mathrm{Z}^+$, where α labels all the residing vertices on the surface, (81).

6.5 Ladder symmetry

In SO(3) group representation spins are integers. Therefore in (6.1) the right side can be written as a positive integer number: $m \doteq f(j_u) + f(j_d) - \frac{1}{2}f(j_{u+d}) = \frac{1}{2}\,(a/a_o)^2$. This number due to the following proof is in fact *any* natural number. Suppose $j_u \geq j_d$ and the difference between them is a positive integer $n = j_u - j_d$. Restricting to the subset M^* of $j_{u+d} = j_u + j_d$, it is easy to verify the generator of this subset is $n(n+1)/2 + j_d$. The first term, a triangular number, is a positive integer. The second term is independent of n and in principle takes any positive integer value. Therefore the set of all M^* corresponding to the states with $j_d = \{1, 2, 3, 4, \cdots\}$ is equivalent to natural numbers; $\mathbb{N} \equiv \{\mathrm{M}^*\}/\mathcal{R}$, where $/\mathcal{R}$ stands for the modulation of repetition (or in a simple word different copies of one number are identified). Since m in general is a positive integer, any other subset fits into $\mathbb{N}$. Consequently, an irreducible reformulation of area when all copies of numbers are identified is possible by one quantum number, $a = a_o\sqrt{2n}$, where $n \in \mathbb{N}$.

The spectrum of area modulo repetitions in SU(2) group representations is impossible to reformulate by one parameter; however, it is possible by two in the following form: $a = \frac{1}{2}a_o\sqrt{\zeta}\ n$, for any discriminant of positive definite form ζ and any positive integer n, (13).

A universal reformulation is thus possible if one rewrites the SO(3) irreducible reformulation as a reducible one by two parameters. In the followings it is shown that any integer c can be represented uniquely by $c = \zeta n^2$ where ζ is a square-free number and $n \in \mathbb{N}$. A positive integer that has no perfect square divisors except 1 is called square-free (or quadratfrei) number. In other words it is a number whose prime decomposition contains no repeated factors; for instance 15 is square-free but 18 is not. Now consider an integer c containing s different prime factors $p_1, p_2, \cdots, p_s$ each repeated $n_1, n_2, \cdots, n_s$ times, respectively; $c = \prod_{i=1}^{s}(p_i)^{n_i}$. The exponents n_i are all positive integers and are either even or odd numbers. Consider the case that the exponents are all odd numbers, $n_i := 2m_i + 1$. Therefore c can be written in the form of $(\prod_{k=1}^{s} p_k).(\prod_{l=1}^{s}(p_l)^{m_l})^2$ which shows the integer c is a multiplication of a square-free part and a square part. This could be redone for any integer number and the result is the same decomposition. Since the prime factorization of every number is unique, its decomposition into square and square-free numbers is unique. Therefore, in SO(3) group the complete set of quantum area $\{m\}$, which fits into

natural numbers, is the multiplication of a square-free and a square number. In other words, the quantum of area can be reformulated into $a = a_o\sqrt{2\zeta}\ n$. This makes the universal reformulation of area as a function of ζ and n,

$$a_n(\zeta) = a_0\chi\sqrt{\zeta}\ n \tag{6.2}$$

for $\forall\ n \in \mathbb{N}$, where in SO(3) group ζ is any square-free number $\{1, 2, 3, 5, \cdots\}$ and $\chi := \sqrt{2}$; and in SU(2) group ζ is the 'discriminant of any positive definite form' $\{3, 4, 7, 8, 11, \cdots\}$ and $\chi := 1/2$. The parameters χ is 'the group characteristic parameter.' Fixing ζ a generation of evenly spaced numbers is picked out, thus the parameter ζ is the 'generational number.' For the purpose of making the rest of this thesis easier to read let us rename the first generational number whose gap between levels is minimal by $\zeta_{\min}$ and the minimal area $a_{\min}$.

Note that the term $\sqrt{\zeta}$ is an irrational number in both groups and in any generation it is unique. Therefore the sum or difference of any two quanta $a_{n_1}(\zeta_1)$ and $a_{n_2}(\zeta_2)$ for $\zeta_1 \neq \zeta_2$ is unique and belongs to none of generations.

6.6 Degeneracy

The spin network states of a surface under the action of area operator manifest a substantial degeneracy. Consider an N-valent vertex lying on a surface, some of the edges are contained in the upper side, some in the lower, and some lie completely tangential on the surface. Given the total spin of upper and lower sectors by j_u and j_d, respectively, a set of area eigenvalues are generated from a minimum where $j_{u+d} = j_u + j_d$ to a maximum where $j_{u+d} = |j_u - j_d|$ from eq. (6.1). Changing j_u and j_d a different finite subset of area is generated whose elements may or may not coincide with the elements of the other subset of area eigenvalues. Associated with any area eigenvalue there appears unexpectedly a finite number of completely *different* eigenstates. For instance, these states $|j_u = 1, j_d = 0, j_{u+d} = 1\rangle$, $|j_u = 0, j_d = 1, j_{u+d} = 1\rangle$, and $|j_u = 1, j_d = 1, j_{u+d} = 2\rangle$ correspond to the area $a = \sqrt{2}a_o$. Counting these states for every eigenvalue a power law correlation with the size of area appears such that a larger area possesses a higher degeneracy. This is studied for both SU(2) and SO(3) gauge groups in (13).

On a classical surface there are a finite number of area cells and a set of degenerate quantum states could be associated with it. However, this is essential for a background independent theory to identify only physical states after reducing the redundant gauge- and diffeomorphism-transformed ones. Gauge invariance by definition is satisfied in spin network state, but diffeomorphism invariance should be checked by its imposing on the states. Consider a surface containing a large number of the same area cell in different regions. Each cell is a degenerate eigenvalue of area. However, area operator does not 'see' the completely tangential edges of these degenerate states. By definitions, the number of completely tangential edges at each vertex could vary from zero to infinity and when there are many of these excitations at one vertex they accept a huge spectrum of spins. These various states make the identical cell configuration on different regions *distinguishable* under the measurements of other observable operators.

[1]

[1] Note that an isolated quantum horizon is diffeomorphism invariant under only a subset of diffeomorphism group

Note that the area of higher levels can be decomposed precisely into smaller fractions of the same generation (without any approximation). For example, $a_n = na_1 = (n-2)a_1 + a_2 = \cdots$. As it was explained above, these cells are all completely distinguishable. Therefore the degeneracy of the area eigenvalue a_n becomes $\Omega_n = g_n + g_{n-1}g_1 + \cdots + (g_1)^n$. Obviously the dominant term in the sum belongs to the configuration with maximum number of the area cell a_1. Therefore the total degeneracy of $a_n(\zeta)$ for $n \gg 1$ is:

$$\Omega_n(\zeta) = g_1(\zeta)^n. \tag{6.3}$$

In the classical limits, the dominant configuration of a large surface is the one occupying the highest possible level of area from the 'first' generation $\zeta_{\min}$; i. e. $A \approx na_{\min}$. This dominant degeneracy is $g_1(\zeta_{\min})^n$ and a kinematic entropy can be associated with it proportional to the area; $S = A(\ln g_1(\zeta_{\min})/a_{\min})$. Depending on the type of time evolution of the surface this entropy may vanish, decrease, increase or remains unchanged in the course of time. In other words, a classical surface characterized by its area at each time slice possesses a finite entropy-like parameter. Space-time horizons as a class of physical surfaces possess a non-decreasing entropy. In other words their kinematical entropy in the course of time, due to the second black hole thermodynamics law, are *physical* entropy. We will show in the next section such a horizon carries an entropy whose nature is the total degeneracy of vacuum fluctuation modes responsible for the thermal radiation of black hole. However, for the aim of this thesis on the study of kinematics of fluctuations we disregard here the issues of defining the Hamiltonian of a quantum horizon based on spin foam, which is still an open problem.

6.7 Fluctuations of a horizon

Having known a suitable definition for the information flow other than expansions of geodesic congruences used in general relativity, one can certainly define a quantum black hole. However, there are different definitions of quantum horizons with different properties, including causal ones. An event horizon is always a null surface by definition, thus it must satisfy one-way information transfer, (83). However an event horizon is not locally defined at all, not even in time. To define it classically, we need the information of the whole manifold. In canonical quantum gravity, we need a definition by which we can look at a place in space and say those photons reaching to us from there must come from a spatial slice that intersects a space-time horizon. Such local definitions are in fact those of apparent, trapping, and dynamical horizons, (11). On the other hand, the space-time horizons are *not* necessarily null. They would be so if we have vacuum and absence of gravitational radiation. Vacuum can easily be achieved for a spin network case, but we cannot prevent the local gravitational degrees of freedom to be excited in the neighborhood of a space-time horizon. With these gravitational radiation across the horizon and with positive energy conditions (or vacuum) the horizon will be *space-like* rather than null. Moreover, the energy conditions in quantum gravity could not be taken for granted, even for semiclassical

that map between a *sequence* of punctures. Complete diffeomorphism group elements when applied many of horizon states should be reduced from the counting of physical states since they are different copies of a fewer amount of physical states. This reduces horizon entropy such that it is unlikely that black hole entropy is satisfied.

states, as long as violations occur on small length scales, [2]. Thus, quantum space-time horizons can become even *time-like* with a two-way information transfer. As a consequence, one *cannot* restrict the quantum fluctuations of horizon area to the subset that is considered in the trapping-based theories of horizon because the basic assumption underneath those theories is that a quantum horizon is the extension of a classical null boundary of space-time in a quantum theory, (11). Physical fluctuations of space-time horizons, in fact, occurs in a wider spectrum that includes all excluded quanta of area.

Note that in the Hawking's conception of black hole radiation, those modes created in vacuum at past null infinity pass through the center of a collapsing star, hover around it and come out of it at future infinity. The outgoing quanta get a thermal statistics from this incipient (about-to-be-formed) black hole. Quantum fluctuations of the horizon change this simple picture because the Hawking quanta will not be able to hover at a nearly fixed distance from the fluctuating horizon. Bekenstein and Mukhanov postulated an equidistant spectrum for the horizon area fluctuations in (85) and showed concentrating of radiance modes in discrete lines. In loop quantum gravity as a fundamental candidate theory of quantum gravity, quantum of area is different and here its emissive pattern is work out.

During the latest stages of gravitational collapse of a neutral non-rotating spherical star, all radiatable multipole perturbations in the gravitational fields are radiated away such that its classical physics is described only by its horizon area. The energy associated with this object depends on the area by the relation $A = \frac{16\pi G^2}{c^4} M^2$. The energy fluctuations of a large space-time horizon are easy to find $\delta M = \gamma\chi \frac{M_{Pl}}{8M} \sqrt{\zeta}\delta n$. Ladder symmetry classifies the transitions between levels into: 1) 'generational transitions', those with both initial and final levels belonging to the same generation, or 2) 'inter-generational transitions', with initial and final levels belonging to two different generations. The generational transitions produce 'harmonic' frequencies proportional to a fundamental frequency by an integer. Inter-generational transitions produce 'non-harmonic modes'.

In generational transitions, the fundamental frequency is the jump between two consecutive levels with frequency $\varpi(\zeta) = (\gamma\chi\sqrt{\zeta})\ \omega_o$, where $\omega_o := \frac{c^3}{8GM}$ is the so-called 'frequency scale'. For instance, a black hole of mass $10^{-18} M_\odot$ has a horizon of area about $10^{-29}\mathrm{m}^2$ and a temperature about 10^{11} K. The frequency scale is thus of the order of ~ 10 keV. Such a typical hole has a horizon 40 order of magnitude larger than the Planck length area. Therefore from each harmonic mode there are many *copies* emitted in the different levels; or in other words these modes are amplified. On the other hand, since the difference of two levels of different generations is a unique number, there exists only *one* copy from each non-harmonic mode in all possible transitions. This *quantum amplification effect* makes a black hole condensate its particles production mostly on harmonic modes. One important consequence is the density matrix elements of non-harmonic modes can be regarded negligible and therefore the generational transitions matrix elements can be assumed to be uniform.

In a transition down the level of a generation, there are two weight factors: the transition and the population weights. Assume a hole of large area A. When the hole jumps f steps down the ladder of levels in the generation ζ, it emits a quanta of the

[2] There are also examples in quantum field theory on a curved background for how energy conditions can be violated locally.

frequency $f\varpi(\zeta)$. This much of radiance energy could also be emitted in the dominant configuration by radiating $f\frac{a_1(\zeta)}{a_{\min}}$ quanta of the fundamental frequency $\varpi(\zeta_{\min})$. These two transitions, although are of the same radiance frequency, appear with different possibilities. The degeneracy ratio of these two is $\Omega(f\varpi(\zeta))/\Omega(f\frac{a_1(\zeta)}{a_{\min}}\varpi(\zeta_{\min}))$ that gives rise to the definition of 'transition weight' $\theta(\zeta, f) = g_1(\zeta)^f g_1(\zeta_{\min})^{-fa_1(\zeta)/a_{\min}}$. The second weight is the population one that comes from a different root. Due to quantum amplification effect, from each harmonic frequency there produced many copies in different levels on the generation. This weight is in fact the number of possible quanta emitting from different levels with the same frequency. It is easy to verify this number is $N_{\varpi(\zeta)} - f + 1$ where $N_{\varpi(\zeta)}$ is the number of copies from the fundamental frequency, and for near level modes ($f \ll N_{\varpi(\zeta)}$) it is $\frac{A}{a_1(\zeta)}$. We absorb constants in normalization factors and the population weight in near levels becomes $\rho(\zeta) := 1/\sqrt{\zeta}$.

Finally notice that within one generation when a space-time hole jumps f steps down the ladder of levels, the degeneracy decreases by a factor of $g_1(\zeta)^f$. Having defined the transition and the population weights, the conditional probability of $\omega_f(\zeta)$ emission after using (6.2) becomes $P(\omega_f(\zeta)|1) = C^{-1}\rho(\zeta)g_1(\zeta_{\min})^{-f\sqrt{\zeta/\zeta_{\min}}}$, where C is the normalization factor, [3].

One can consider a successive emissions and associates a probability to it as the multiplication of the probability of each emission. The conditional probability of a j dimensional sequence of different frequencies becomes $\prod_{i=1}^{j} P(\omega_{f_i}(\zeta_i)|1)$. The probability of the sequences to include k emissions out of j to be of the frequency $\omega_{f^*}(\zeta^*)$ (in no matter what order) while the rest of accompanying emissions are of any value except this frequency, is $P(k, \omega_{f^*}(\zeta^*); \{\omega_{f_1}(\zeta_1), \cdots\}|j) = \binom{j}{k} [P(\omega_{f^*}(\zeta^*)|1)]^k \times \prod_{i=1;\ \zeta\neq\zeta^*}^{j-k} P(\omega_{f_i}(\zeta_i)|1)$. The accompanying modes are allowed to accept any frequency except $\omega_{f^*}(\zeta^*)$ and therefore the probabilities of any accompanying frequency should sum. From the definition of C, it is easy to find out in each sum over accompanying modes instead of $\sum_{\omega\neq\omega^*} P(\omega_{f_i}(\zeta_i)|1)$ we can replace $C - P(\omega_{f^*}(\zeta^*)|1)$ that simplifies the probability to $P(k, \omega_{f^*}(\zeta^*)|j) = \binom{k}{j} [P(\omega_{f^*}(\zeta^*)|1)]^k \times [C - P(\omega_{f^*}(\zeta^*)|1)]^{j-k}$.

Note that a black hole radiates in a 'time' sequential order, (87). The probabilities of zero and one jump (of no matter what frequency) in the time interval Δt are $P_{\Delta t}(0)$ and $P_{\Delta t}(1)$, respectively. In the time interval $2\Delta t$, the probabilities of zero, one, and two jumps are $P_{\Delta t}(0)^2$, $2P_{\Delta t}(0)P_{\Delta t}(1)$, and $2P_{\Delta t}(0)P_{\Delta t}(2) + P_{\Delta t}(1)^2$, respectively. By induction this is found for higher number of jumps in an interval and for longer time. A general solution for the equations the probability of j time-ordered decays in an interval of time Δt is $P_{\Delta t}(j) = \frac{1}{j!}(\frac{\Delta t}{\tau})^j \exp(\frac{\Delta t}{\tau})$. Multiplying this probability with $P(k, \omega_{f^*}(\zeta^*)|j)$ and then summing over all sequence dimensions $j \geq k$, it is easy to manipulate the total probability of k emissions with frequency $\omega_{f^*}(\zeta^*)$ to be $P_{\Delta t}(k, \omega_{f^*}(\zeta^*)) = \frac{1}{k!}(x_f^*)^k \exp(-x_f^*)$, where $x_f^* = \frac{\Delta t}{C\tau}\rho(\zeta^*)\ g_1(\zeta_{\min})^{-f\sqrt{\zeta/\zeta_{\min}}}$. This indicates the distribution of the number of quanta emitted in harmonic modes is Poisson-like.

Let us now look at the distribution of the number of quanta emitted from a black body radiation. The probability of one emission of frequency ω^* is Boltzmann-like; $\pi_{\omega^*} = B\exp(-\frac{\hbar\omega^*}{kT})$ where B is normalization factor $B = \sum_\omega \pi_\omega$. Successive emissions

[3] From normalization $C = \sum_\zeta \rho(\zeta)/|1 - g_1(\zeta_{\min})^{-\sqrt{\zeta/\zeta_{\min}}}|$.

occurs independently and therefore the probability of a j dimensional sequence in which p emissions are of the frequency ω^* is $\binom{j}{p}(\pi_{\omega^*})^k \prod_i^{j-p} \sum_{\omega_i \neq \omega *} \pi_{\omega_i}$. The last summation term can be replaced from the normalization relation by $B - \pi_{\omega^*}$. This makes the probability equivalent with the black hole emission probability $P(k, \omega_{f^*}(\zeta^*)|j)$ when $g_1(\zeta_{\min})^{-f^*}\sqrt{\zeta^*/\zeta_{\min}}$ (i.e. $\exp(-S)$) is replaced with $\exp(-\frac{\hbar\omega^*}{kT})$. The analogy indicates that the hole radiation is characterized by Planck's black body radiation and the temperature matches the black hole temperature when the Barbero-immirzi parameter is properly defined for getting the Bekenstein-Hawking entropy. In fact the black hole is hot and the thermal character of the radiation is entirely due to the degeneracy of the levels, the same degeneracy (6.3) that becomes manifest as black hole entropy.

By definition, the intensity of a mode is the total energy emitted in that frequency per unit time and area. The average number of emissive quanta at a typical harmonic frequency is $\overline{k} = \sum_{k=1}^{\infty} k P_{\Delta t}(k|\omega_f(\zeta))$. Calculating this summation gives rise to the intensity

$$\frac{I(\omega_f(\zeta))}{I_o} = f g_1(\zeta_{\min})^{-f}\sqrt{\zeta/\zeta_{\min}} \tag{6.4}$$

where I_o is constant.

To estimate the width of lines, we need to compare the average loss of collapsing star mass in late times with a black body. The average of time elapsing between two decays is $\bar{t} = \int dt\ t P_t(1) = 2\tau$ and its uncertainty is $(\Delta t)^2 = \int dt (t - \bar{t})^2 P_t(1) = 3\tau^2$. The average frequency emitted from a black hole can be shown to be $\bar{\omega} = \omega_o \gamma \chi$, [4] Moreover, the mean value of the number of jumps in Δt is $\bar{j} = \sum_j j P_{\Delta t}(j)$, which becomes $\frac{\Delta t}{\tau}$. As a consequence, a black hole losses the ratio of mass $\frac{\Delta \bar{M}}{\Delta t} = -\frac{\hbar \omega_o \gamma \chi}{c^2 \tau}$ on average. On the other hand, the nature of a black hole radiation is the same as a black body where the loss of mean energy is described by Stephan-Boltzman law, $\frac{\Delta \bar{M}}{\Delta t} = -\frac{\hbar c^4}{15360\pi G^2 M^2}$. Comparing these two, one finds $\tau = \frac{1920\pi\gamma\chi}{\omega_o}$. According to the uncertainty principle $\Delta E \Delta t \sim \hbar$, the frequency uncertainty becomes of the order of a thousandth of the frequency scale ω_o. This shows that the spectrum lines are indeed very narrow and the various black hole lines of one generation are unlikely to overlap.

The intensity envelope of the first three generations is plotted in Fig. (6.1), where the envelope (a), (b) and (c) belongs to the intensity of harmonics in the first, second and third generations, respectively. It becomes clear that in a generation with the least gap between levels, the strongest harmonic modes are amplified. The brightest lines belong to a few of the first harmonics of the generation $\zeta_{\min}$. Other than these lines, the intensity of the rest of harmonics in other generations are suppressed exponentially. We expect in a low energy spectroscopy a clear observation of only a few narrow and unblended lines highly on top of other harmonics. Also we expect these brightest lines appear in the wavelength not larger than the size of black hole M in Planck units.

In summary: we showed the quantum of area are substantially degenerate. The complete spectrum is possible to reformulate into a universal form with two parameters and more importantly it is the union of exactly equidistant subsets. The spectrum

[4] By definition $\bar{\omega} = \sum_\zeta \sum_f \omega_f P_{\Delta t}(\{\omega_f|1\})$. After using $\sum_n n x^n = x/(1-x)^2$ for $x < 1$ and approximating the sum by an integral with a high upper bound on ζ, the integral gives the same result when the sum in the definition of C is approximated sum by integral.

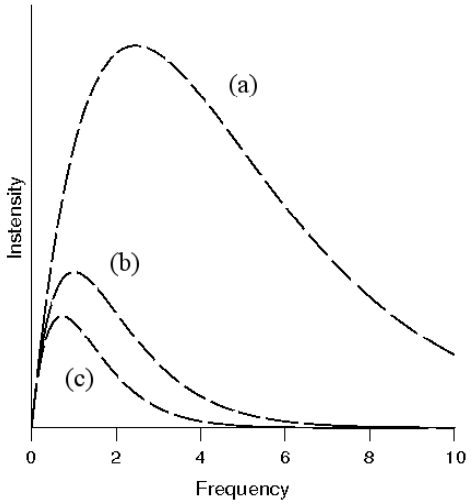

Figure 6.1: The intensity envelope of some generations.

of radiation due to these new properties reveals a clear discretization on a few brightest lines which cannot blend into one another. The most notable point is that Loop Quantum Gravity as one fundamental theory of quantum gravity is substantially testable with an observational justification if primordial black holes are ever found.

Appendix A

Area spectrum in $SO(3)$ version

Theorem 1: The set of numbers evaluated by the generating formula $\frac{1}{2}[2a(a+1)+2b(b+1)-c(c+1)]$, where a, b, and c are positive integers and $c \in \{|a-b|, \cdots, a+b-1, a+b\}$, is reduced into the whole $\mathbb{Z}^+$, modulo rematching.

Proof: Suppose $a \geq b$. Let us consider the two independent numbers are $a = b + n$, where n is a positive integer. The subset $c = a + b$ is generated by the formula $n(n+1)/2+b$. The first term is called Triangular numbers and are integers. The second term is independent from the first term and can be any positive integer. This subset generates all positive integers and since other subsets generate integers, all of them fit into the whole positive integer sets $\mathbb{Z}^+$. This set is a reduced set of the original one subject to identifying all repeated numbers.

The fundamental theorem of arithmetic states that every positive integer (except the number 1) can be represented in exactly one way as a product of one or more primes, apart from rearrangement. This theorem is also called 'the unique factorization theorem'. Thus, prime numbers are the 'basic building blocks' of the natural numbers.[1] Decomposing any natural number into its prime numbers, the primes are either repeated or not. Collecting the natural numbers whose prime factors are not repetitive the square-free sequence of numbers are produced.

▶ **Definition of Square-free Numbers:** an integer number is said to be square-free, if its prime decomposition contains no repeated factors. For example, 30 is square free since its prime decomposition $2\times3\times5$ contains no repeated factors. In this thesis, this sequence is indicated by the symbol $\mathbb{A}$. Some of the known square-free numbers are given in table (A.1).

$\mathbb{A} = \{1, 2, 3, 5, 6, 7, 10, 11, 13, 14, 15, 17, 19, 21, 22, 23, 26, 29, 30, 31, 33, 34, 35, 37, 38, 39, 41, 42, 43, 46, 47, 51, 53, 55, 57, 58, 59, 61, 62, 65, 66, 67, 69, 70, 71, 73, 74, 77, 78, 79, 82, 83, 85, 86, 87, 89, 91, 93, 94, 95, 97, 101, 102, 103, 105, 106, 107, 109, 110, 111, 113 , \cdots\}$.

Table A.1: Square-free numbers (Sloane's A005117)

[1] In number theory, the prime factors of a number are considered as indistinguishable building blocks of numbers and thus the ordering of numbers does not matter.

There is no known polynomial algorithm for recognizing square-free, (79). ◄

A natural number is the multiplication of a square-free number and a square number.

Theorem: The natural numbers can be rewritten as a mixture of square generations by the contribution of all square-free representatives,

$$\{\mathbb{N}\} \equiv \bigcup_{\zeta \in \mathbb{A}} \{\zeta \mathbb{N}^2\}. \tag{A.1}$$

Proof: Any natural number can be written in terms of its prime factors, say $p_1^{n_1} \times p_2^{n_2} \cdots \times p_i^{n_i}$, where p_1, p_2, $\cdots$, and p_i are different prime numbers and the exponents n_1, n_2, $\cdots$, n_i are positive integers. These exponents are either even or odd numbers. In the most general case all of the exponents are different odd numbers, $n_i = 2m_i+1$. Therefore, the above-mentioned number can be rewritten in the form $(p_1 \times p_2 \cdots \times p_i) \times (p_1^{m_1} \times p_2^{m_2} \cdots \times p_i^{m_i})^2$. Due to the assumption that the prime number p's are different, the first parenthesis is equivalent to a square-free number and the second parenthesis is nothing but n^2 for the natural number $n = p_1^{m_1} \times p_2^{m_2} \cdots \times p_i^{m_i}$. Therefore, $\forall\ x \in \mathbb{N},\ \ \exists\ y \in \mathbb{N}$ and $a \in \mathbb{A},\quad x \equiv a \times y^2$.

In Table A.2, having the first 12 square-free numbers of $\mathbb{A}$, the corresponding elements of the square generations $\zeta\mathbb{N}^2$ are tabulated up to the first five elements.

	$1\mathbb{N}^2$	$2\mathbb{N}^2$	$3\mathbb{N}^2$	$5\mathbb{N}^2$	$6\mathbb{N}^2$	$7\mathbb{N}^2$	$10\mathbb{N}^2$	$11\mathbb{N}^2$	$13\mathbb{N}^2$	$14\mathbb{N}^2$	$15\mathbb{N}^2$
m=1	1	2	3	5	6	7	10	11	13	14	15
m=2	4	8	12	20	24	28	40	44	52	56	60
m=3	9	18	27	45	54	63	90	99	117	126	135
m=4	16	32	48	80	96	112	160	176	208	224	240
m=5	25	50	75	125	150	175	250	275	325	350	375

Table A.2: The first fifteen elements of some $SO(3)$ based generations $\zeta\mathbb{N}^2$.

A column in the Table (A.2) indicates the elements of a square generation and consists of all natural number up to 21. By extending this Table, the consistency of the elements with natural numbers can be verified up to any order. There is no common element in different square generations,

$$\forall\ \zeta_1, \zeta_2 \in \mathbb{A},\ \ \text{if}\ \zeta_1 \neq \zeta_2, \quad \{\zeta_1\mathbb{N}^2\} \cap \{\zeta_2\mathbb{N}^2\} = \emptyset. \tag{A.2}$$

Consider the sequence of numbers that contain the same square-free ζ factor multiplied by all square numbers, $\zeta\mathbb{N}^2$. Taking square root from the elements of the square generation the *equidistant* sequence $\sqrt{\zeta}\mathbb{N}$ is produced.

Appendix B

Area spectrum in $SU(2)$ version

Theorem: The set of numbers evaluated by the generating formula $4[2a(a+1) + 2b(b+1) - c(c+1)]$, where a and b are positive integer or half-integer of $\frac{1}{2}\mathbb{Z}$ and $c \in \{|a-b|, \cdots, a+b-1, a+b\}$, is reduced into the congruent number unto 0 and 3 mode 4 modulo the degeneracies.

Proof: Suppose $a \geq b$. Let us consider the two independent numbers are $a = b + n$, where $n \in \frac{1}{2}\mathbb{Z}$. The subset $c = a + b$ is generated by the formula $4n(n+1) + 8b$. Let us consider $n = N/2$ and $b = B/2$ where N and B are independent natural numbers. Substituting them in the formula it becomes $N(N+2) + 4B$. The first term is the mixture of congruent numbers unto 0 or 3 mod 4. The second term is the congruent numbers unto 0 mod 4. In other words, a number that is generated by $N(N+2)$ is either $4m+3$ or $4m$ for some integers m. This is not changed when the term $4B$ is added to the numbers. Let us fix N unto either 0 or 1. The whole sequence of congruent numbers unto 0 and 3 mod 4 are obviously generated from $4B+3$ and $4B$ for any integer B. All other numbers fit to the whole sequence if one identifies all degeneracies.

Evaluating $4(m_{j_u, j_d, j_{u+d}})^2$ in $SU(2)$ group representation, the Skew Amenable numbers are produced.

► **Definition of Skew Amenable numbers**: in a simple definition these numbers are the page numbers of a book that is printed out only at the pages that come after each two leaves of sheets by face. This can be interpreted in a mathematical language as the congruent numbers to either 0 or 3 in mod 4. [1]

The Skew Amenable numbers smaller than 200 are 3, 4, 7, 8, 11, 12, 15, 16, 19, 20, 23, 24, 27, 28, 31, 32, 35, 36, 39, 40, 43, 44, 47, 48, 51, 52, 55, 56, 59, 60, 63, 64, 67, 68, 71, 72, 75, 76, 79, 80, 83, 84, 87, 88, 91, 92, 95, 96, 99, 100, 103, 104, 107, 108, 111, 112, 115, 116, 119, 120, 123, 124, 127, 128, 131, 132, 135, 136, 139, 140, 143, 144, 147, 148, 151, 152, 155, 156, 159, 160, 163, 164, 167, 168, 171, 172, 175, 176, 179, 180, 183, 184, 187, 188, 191, 192, 195, 196, 199, 200, etc. (Sloane's A014601)[2] ◄

It is known in number theory that any square integer number is the congruent to either 0 or 1 mod 4. On the other hand, there is a theorem that in the existence of

[1] There is also another definition that a number n is skew amenable if there exist a set of integers $\{m_i\}$ satisfying the relations: $n = \sum_{i=1}^{n} m_i = -\prod_{i=1}^{n} m_i$, (74). For instance, the number 8 is a skew amenable because is can be decomposed into an 8 term sum as well as the negated product of exactly the same numbers: $8 = 1+1+1+1+1+1-2+4 = -(1\times 1\times 1\times 1\times 1\times 1\times(-2)\times 4)$. Another example is 3, which satisfied the condition: $3 = 1+3-1 = -(1\times 3\times(-1))$.

[2] http://www.research.att.com/ njas/sequences/A014601

two equalities $x_1 \equiv x_2 \pmod{m}$ and $x_3 \equiv x_4 \pmod{m}$ of the same modular m, it can be it is easy to verify that $x_1 \times x_3 \equiv x_2 \times x_4 \pmod{m}$. Accordingly, having one of the two equality as $x_1 = 0$ or 3 (mod4) for a Skew Amenable number x_1, and the equality $x_2 = 0$ or 1 (mod4) for a square number x_2, the multiplication of these two produces a Skew Amenable number $x_1 \times x_2 = 0$ or 3 (mod4) is generated. In other words, multiplying the complete set of Skew Amenable numbers and the complete set of square numbers, the product a subset of the Skew Amenable numbers is generated.

Having this fact in mind, for any random Skew Amenable number b' there exists a corresponding Skew Amenable number b that satisfies the equality $b' = b \times n^2$ for $n \in \mathbb{N}$. In fact, the set of numbers b for all $n \in \mathbb{N}$ is a subset of Skew Amenable numbers. We represent this subset by the symbol $\mathbb{B}$. Now the question is: what is $\mathbb{B}$? To answer the questions, the Skew Amenable number can be generated and the elements of the set $\mathbb{B}$ are identified individually. The result is in the table (B.1).

$\mathbb{B} = \{3, 4, 7, 8, 11, 15, 19, 20, 23, 24, 31, 35, 39, 40, 43, 47, 51, 52, 55, 56, 59, 67, 68, 71, 79, 83, 84, 87, 88, 91, 95, 103, 104, 107, 111, 115, 116, 119, 120, 123, 127, 131, 132, 136, 139, 143, 148, 151, 152, 155, 159, 163, 164, 167, 168, 179, 183, 184, 187, 191, \cdots\}$.

Table B.1: The Discriminants of the Positive Definite Quadratic Forms (Sloane's A003657)

The negative of this sequence of numbers coincide with a well-known sequence of discriminants of *the Positive Definite Quadratic Forms*, (80). The definition of the positive definite quadratic forms is explained in the Appendix (C) of this thesis.

Consequently, an Skew Amenable sequence of number, which is generated from the evaluation of $4(m_{j_u,j_d,j_{u+d}})^2$ in $SU(2)$ representation, can be rewritten as an element of the set $\mathbb{B}$ multiplied by an integer squared. In other words, the elements of the set $4(m_{j_u,j_d,j_{u+d}})^2$ can be represented as square generations with representative elements of the set $\mathbb{B}$. In table B.2 sixteen elements of the square generations whose representatives are the first five elements of the set $\mathbb{B}$, is tabulated.

	$3\mathbb{N}^2$	$4\mathbb{N}^2$	$7\mathbb{N}^2$	$8\mathbb{N}^2$	$11\mathbb{N}^2$	$15\mathbb{N}^2$	$19\mathbb{N}^2$	$20\mathbb{N}^2$	$23\mathbb{N}^2$
m=1	3	4	7	8	11	15	19	20	23
m=2	12	16	28	32	44	60	76	80	92
m=3	27	36	63	72	99	135	171	180	207
m=4	48	64	112	176	240	304	320	368	384
m=5	75	100	175	200	275	375	475	500	575

Table B.2: The first sixteen elements of some $SU(2)$ based generations $\zeta\mathbb{N}^2$.

In the table (B.2), all elements of the Skew Amenable numbers up to 44 are present and any extension of the table will produce all of the others up to any order.

There is no common element in different square generations,

$$\forall\ \zeta_1, \zeta_2 \in \mathbb{B}, \quad \text{if } \zeta_1 \neq \zeta_2, \quad \{\zeta_1\mathbb{N}^2\} \cap \{\zeta_2\mathbb{N}^2\} = \emptyset. \tag{B.1}$$

Appendix C

Positive definite quadratic forms

A quadratic form is a two-variable integer-valued function $f(x, y) = ax^2 + bxy + cy^2$, with $a, b, c \in \mathbb{Z}$. This form 'primitive' if a, b, c are relatively 'prime'. The 'discriminant' of this form is defined as $\Delta := b^2 - 4ac$.

Substituting integers values in two variables x and y respectively, the form is evaluated by an integer m, $f(x_0, y_0) = m$. This problem can be restated as follows, the 'representation' of the form $f(a, b, c) = m$ is elements of the solution space of the equation (x_0, y_0). A representation is called 'primitive' if $\gcd(x_0, y_0)$=1.

Given a form f, the transformation $x = \alpha x' + \beta y'$ and $y = \gamma x' + \delta y'$ transforms f into f'. The new form f' remains as an integer if and only if $\alpha\delta - \beta\gamma = \pm 1$. The interesting fact is that in such a transformation that preserves the integer character of the form the discriminant Δ remains *invariant*.

If f is a form of integer m, we can rewrite the definition of a form as $4am = (2ax + by)^2 - \Delta y^2$. In the case that Δ is a perfect square number the right hand side is written in the form $(2ax + by + y\sqrt{\Delta})(2ax + by - y\sqrt{\Delta})$. In this case the different representations of solutions are *degenerate* and thus indistinguishable. These forms are of this thesis.

In the case of $\Delta < 0$, it is clear from $4am = (2ax + by)^2 - \Delta y^2$ that for any representation (x, y), m and a (and c) are of the same sign. A forms whose corresponding discriminant is negative is called a 'definite form' and if m is positive, it is called a 'positive definite form'.[1]

By substituting the positive a and c in $f(x, y) = ax^2 + bxy + cy^2$, if the form for any representation (x, y) become positive and the discriminant becomes negative, the form is a definite positive quadratic form. Evaluating the negated values of the discriminants of such forms produces the following sequence of numbers 3, 4, 7, 8, 11, 15, 19, 20, 23, 24, 31, 35, 39, 40, 43, 47, 51, 52, 55, 56, 59, 67, 68, 71, 79, 83, 84, 87, 88, 91, 95, 103, 104, 107, 111, 115, 116, 119, 120, 123, 127, 131, 132, 136, 139, 143, 148, 151, 152, 155, 159, 163, 164, 167, 168, 179, 183, 184, 187, 191, $\cdots$, which is the same elements of the set $\mathbb{B}$ in table (B.1).

For instance, $(a = 1, b = 1, c = 1)$ defines a positive definite form whose corresponding discriminant is -3 and its negated value is the first element of $\mathbb{B}$. The second element is produced after $(a = 1, b = 0, c = 0)$.

To verify that this sequence is the congruent to either 0 or 3 mod4, it is enough

[1] In the case that $\Delta > 0$, a and c are of opposite signs and thus both positive an negative integers m may be represented on f. This case is called indefinite form and is not of our interest of study.

check the consistency of the negated discriminant $-\Delta = 4ac - b^2$ with this congruent. It is clear that b^2 is congruent to 0 or 1 (mod4). Also, $4ac$ is the congruent to 0 mod4. Therefore, $-\Delta$ is congruent to 0 or 3 (mod4).

Appendix D

The normalization coefficient C

To calculate this coefficient, it should be noticed the spectrum of non-harmonics is almost continuous except at zero and the harmonics, $\omega' \in \mathbb{R}^+ - \{0\} - \{\text{harmonics}\}$. These frequencies are all uniformly weighted by $\rho = 1/N_o$. Since the population of harmonics is much more than the non-harmonics, we can approximate the population of a harmonics to be $N-1$ instead of N and add the one copy of each harmonic into the above mentioned set of frequencies in order to fill the gaps. Doing so, the equally weighted set of frequencies $\omega' \in \mathbb{R}^+ - \{0\}$ is provided. By the use of (5.18) and (5.21), in the classical limits ($N_o \gg 1$), the normalization coefficient reads

$$\begin{aligned} C &= \lim_{N\to\infty} \sum_{\text{all } \zeta} \sum_{n=1}^{N} \frac{N-1}{N} \rho(\zeta)\ q(\zeta)^{-n} + \int \frac{1}{N_o}\ e^{-\Lambda\omega'} \Lambda d\omega' \\ &\simeq \sum_{\text{all } \zeta} \sum_{n=1}^{\infty} \rho(\zeta)\ q(\zeta)^{-n}. \end{aligned} \tag{D.1}$$

By the use of the algebraic relation $\sum_{n=1}^{\infty} x^{-n} = 1/(x-1)$, the internal sum in C is summarized. Consequently, the normalization coefficient becomes

$$C = \sum_{\text{all } \zeta} \frac{\rho(\zeta)}{q(\zeta) - 1} \tag{D.2}$$

It is useful to check the finiteness of the normalization coefficient C.

The finiteness of C: for the purpose of simplicity the definition $q(\zeta) = \exp(\pi\gamma\chi\sqrt{\zeta})$ can be rewritten $q(\zeta) := h^{\sqrt{\zeta}}$, where $h := \exp(\pi\gamma\chi)$ is in both groups greater than 1.

The Cauchy root method of convergence test is such that for series like $\sum_n a_n$, if the value of $\lim_{n\to\infty} |a_n|^{1/n}$ is smaller than one, the series converges. In the series sum of C, this condition reads

$$\lim_{\sqrt{\zeta}\to\infty} \left| \frac{1}{\sqrt{\zeta}}\ \frac{1}{h^{\sqrt{\zeta}} - 1} \right|^{\frac{1}{\sqrt{\zeta}}} \sim \lim_{\sqrt{\zeta}\to\infty} \left(\frac{h^{-\sqrt{\zeta}}}{\sqrt{\zeta}} \right)^{\frac{1}{\sqrt{\zeta}}} = \frac{1}{h} < 1. \tag{D.3}$$

Therefore C is a finite number.

Numerical work can estimate the range of C. Substituting ρ from (5.23) and Barbero-Immirzi parameter from (13), $\gamma = \ln 3/\pi\sqrt{2}$, in $q(\zeta)$ the coefficient C is simplified to $\sum_\zeta \zeta^{-1/2}(3^\chi\sqrt{\zeta/2} - 1)$. In the $SU(2)$ representation, where $\zeta \in \mathbb{B}$ and $\chi = 1/2$, turn out to be $C = 2.01$, whilst in the $SO(3)$ representation group, where $\zeta \in \mathbb{A}$ and $\chi = \sqrt{2}$, it is $C = 0.93$.

Appendix E

Average of frequency $\langle\omega\rangle$

Since the probabilities of (5.18) and (5.21) are normalized, the mean value of the emitting frequencies is

$$\langle\omega\rangle := \sum_{\zeta}\sum_{n=1}^{\infty}\omega_n(\zeta)\ P_{\Delta t}(\{\omega_n(\zeta)\}\mid 1) + \left(\frac{1}{N_o}\right)\int_0^{\infty}\omega e^{-\Lambda\omega}\Lambda d\omega.$$

The second term for a classical black hole is negligible comparing to the first term. Using (5.21) and the algebraic formula $\sum_{n=1}^{\infty} nx^n = x/(1-x)^2$, where $x<1$, the mean value of the frequency of a generation ζ turns out to be $(1/C)\ \varpi(\zeta)\ \rho(\zeta)q(\zeta)/\left(q(\zeta)-1\right)^2$ and therefore the mean value of all frequencies becomes

$$\langle\omega\rangle \sim \frac{1}{C}\sum_{\zeta}\varpi(\zeta)\ \frac{\rho(\zeta)\ q\left(\zeta\right)}{\left(q(\zeta)-1\right)^2} \tag{E.1}$$

Using (5.13) and (5.23), we can rewrite the equation in the from

$$\langle\omega\rangle \sim \frac{\omega_o\gamma\chi}{C}\ \sum_{\zeta} q\left(\zeta\right)/\left(q(\zeta)-1\right)^2. \tag{E.2}$$

Convergence of $\langle\omega\rangle$: To check the convergence of the sequence $\sum_{\zeta} q(\zeta)/(q(\zeta)-1)^2$ via the Cauchy's convergence test, since the real free index in the function $q(\zeta)$ is $\sqrt{\zeta}$ the test function $\lim_{\sqrt{\zeta}\to\infty}\ |q(\zeta)/(q(\zeta)-1)^2|^{1/\sqrt{\zeta}}$ should be considered. By the use of the definition of $q(\zeta) := h^{\sqrt{\zeta}}$, where $h := \exp(\pi\chi\gamma) > 1$,

$$\lim_{\sqrt{\zeta}\to\infty}\left|\frac{1}{\sqrt{\zeta}}\ \frac{h^{\sqrt{\zeta}}}{(h^{\sqrt{\zeta}}-1)^2}\right|^{\frac{1}{\sqrt{\zeta}}} \sim \frac{1}{h} < 1. \tag{E.3}$$

This summation converges.

Let us rewrite the sum by the use of the definition $\eta := \sum_{\zeta} q(\zeta)/(q(\zeta)-1)^2$ as $\langle\omega\rangle = \eta\gamma\chi\omega_o/C$. Having the parameter from Appendix (D), and by substituting $\gamma = \ln 3/\pi\sqrt{2}$ the coefficient η in the $SU(2)$ representation turns out to be $\eta = 9.0$, while it is $\eta = 1.7$ in the $SO(3)$ group representation. By the use of the numerical values of C, the mean value of frequency $\langle\omega\rangle$ is either about $11\omega_o$ in $SU(2)$ group or about $15\omega_o$ in $SO(3)$ group.

Bibliography

[1] Veltman, M.J., *"Quantum theory of Gravitation"*, in Balian, R., and Zinn- Justin, J., eds., *Methods in Field Theory*, Proceedings of the Les Houches Summer School 1975, 265-327, (North-Holland, Amsterdam, 1976).

[2] 't Hooft, G., and Veltman, M.J., *One loop divergencies in the theory of gravitation*, Ann. Inst. Henri Poincare, A, 20, 69-94, (1974).

[3] K. S. Stelle, *"Renormalization of Higher-derivative Quantum Qravity"* Phys. Rev. D 16, No 4, 953 (1977).

[4] M. Ansari, MS Thesis, *"S-Matrix in Quantum Gravity"*, Physics department, University of Isfahan, Iran, 2000.

[5] D. Johnston, *"Nilsen Identities in the 't Hooft Gauge"* Nucl. Phys. B. 253, 687 (1985); D. A. Johnston, *"Sedentary Ghost Poles in Higher-derivative Gravity"*, Nucl. Phys. B. 297, 721 (1988).

[6] Utiyama, R., *"Invariant Theoretical Interpretation of Interaction"*, Phys. Rev., 101, 1597-1607, (1956); Maldacena, J., *"The Large N Limit of Superconformal Field Theories and Supergravity"*, Adv. Theor. Math. Phys., 2, 231-252, (1998); Aharony, O., Gubser, S.S., Maldacena, J., Ooguri, H., and Oz, Y., *"Large N Field Theories, String Theory and Gravity"*, Phys. Rep., 323, 183-386, (2000); Hehl, F.W., McCrea, J.D., Mielke, E.W., and Neeman, Y., *"Metric Affine Gauge Theory Of Gravity: Field Equations, Noether Identities, World Spinors, And Breaking Of Dilation Invariance",* Phys. Rep., 258, 1-171, (1995).

[7] Singleton, D., *"General relativistic analog solutions for Yang-Mills theory",* Theor. Math. Phys., 117, 1351-1363, (1998).

[8] H. Kawai, D.C. Lewellen, and S. H Tye, *"A relation between tree amplitudes of closed and open strings"*, Nucl. Phys. B, 269, 1-23, (1986).

[9] M. Bojowald, *"Inflation from quantum geometry,"* Phys. Rev. Lett. **89**, 261301 (2002) [arXiv:gr-qc/0206054].

[10] M. Bojowald, *"Absence of singularity in loop quantum cosmology,"* Phys. Rev. Lett. **86**, 5227 (2001) [arXiv:gr-qc/0102069].

[11] A. Ashtekar, J. C. Baez and K. Krasnov, *"Quantum geometry of isolated horizons and black hole entropy,"* Adv. Theor. Math. Phys. **4**, 1 (2000) [arXiv:gr-qc/0005126]; A. Ashtekar, *"Interface of general relativity, quantum physics and statistical mechanics: Some recent developments,"* Annalen Phys. **9**, 178 (2000) [arXiv:gr-qc/9910101]; A. Ashtekar, J. Baez, A. Corichi and K. Krasnov, *"Quantum geometry and black hole entropy,"* Phys. Rev. Lett. **80**, 904 (1998) [arXiv:gr-qc/9710007]; A. Ashtekar and B. Krishnan, *"Isolated and dynamical horizons and their applications,"* Living Rev. Rel. **7**, 10 (2004) [arXiv:gr-qc/0407042].

[12] V. Husain and O. Winkler, "Flat slice Hamiltonian formalism for dynamical black holes," Phys. Rev. D **71**, 104001 (2005) [arXiv:gr-qc/0503031]; V. Husain, "Gravitational collapse in quantum gravity," arXiv:0801.1317 [gr-qc]; V. Husain

and O. Winkler, "Quantum black holes from null expansion operators," Class. Quant. Grav. **22**, L135 (2005) [arXiv:gr-qc/0412039].

[13] M. Ansari, *"Genericness of degeneracy and entropy in loop quantum gravity,"* arXiv:gr-qc/0603121.

[14] M. H. Ansari, *"Spectroscopy of a canonically quantized horizon,"* Nucl. Phys. B **783**, 179 (2007) [arXiv:hep-th/0607081].

[15] S. Bilson-Thompson, J. Hackett, L. Kauffman and L. Smolin, *"Particle Identifications from Symmetries of Braided Ribbon Network Invariants,"* arXiv:0804.0037 [hep-th]; S. O. Bilson-Thompson, F. Markopoulou and L. Smolin, *"Quantum gravity and the standard model,"* Class. Quant. Grav. **24**, 3975 (2007) [arXiv:hep-th/0603022].

[16] K. Wilson, *The Renormalization Group: Critical Phenomena And The Kondo Problem*, Journal-ref: Rev. Mod. Phys. 47 (1975) 773; K Wilson and J. Kogut, *The Renormalization Group And Critical Phenomena*, Rev. Mod. Phys. 55 (1983) 583.

[17] C. Rovelli, Quantum Gravity. ISBN: 0521837332, Cambridge University Press; L. Smolin *An invitation to loop quantum gravity*, hep-th/0408048.

[18] J. Ambjorn, J. Jurkiewicz and R. Loll, Phys. Rev. D64 (2001) 044011 [hep-th/0011276]; J. Ambjorn, J. Jurkiewiczcy and R. Loll, *Emergence of a 4D World from Causal Quantum Gravity*, hep-th/0404156. J. Ambjorn, Z. Burda, J. Jurkiewicz and C. F. Kristjansen, "Quantum gravity represented as dynamical triangulations," Acta Phys. Polon. B **23**, 991 (1992); J. Ambjorn, "Quantum Gravity Represented As Dynamical Triangulations," Class. Quant. Grav. **12**, 2079 (1995); M. E. Agishtein and A. A. Migdal, "Simulations of four-dimensional simplicial quantum gravity," Mod. Phys. Lett. A **7**, 1039 (1992).

[19] Herbert W. Hamber, Ruth M. Williams, *Non-Perturbative Gravity and the Spin of the Lattice Graviton* , hep-th/0407039 and references contained therein.

[20] P. Bak, C. Tang and K. Wiesenfeld, Phys. Rev. Lett. **59** (1987) 381; L. Pietronero, P. Tartaglia and Y. C. Zhang, Physica A **173** (1991) 22-44.

[21] P. Bak, How Nature Works, Springer-Verlag, New York 1996.

[22] D. L. Turcotte, Rep. Prog. Phys. **62** (1999) 1377-1429

[23] F. Markopoulou and L. Smolin, Nucl. Phys. **B508** (1997) 409

[24] Fotini Markopoulou, "Dual formulation of spin network evolution", gr-qc/9704013.

[25] C. Rovelli, Phys. Rev. **D48** (1993) 2702

[26] J. Baez, Adv. Math. **117** (1996) 253-272 (gr-qc/941107); in "The Interface of Knots and physics", ed. L. Kauffman, A.M.S., Providence, (1996) 167-203

[27] C. Rovelli and L. Smolin, Phys. Rev. **D52** (1995) 5743-5759

[28] R. Borissov and S. Gupta, Phys. Rev. D **60** (1999), 024002

[29] J. W. Harris and H. Stocker, Handbook of Mathematics and Computational Science. New York: Springer-Verlag, **113**, 1998.

[30] M. Baiesi and C. Maes, cond-mat/0505274

[31] M. Paczuski and P. Bak, (cond-mat/9906077)

[32] B. A. Carreras, V. E. Lynch, D. E. Newman and R. Sanchez, Phys. Rev. **E66** (2002) 011302

[33] S. F. Nrrelykke and P. BakPhys. Rev. E 65, 036147 (2002).

[34] S. Boettcher and M. Paczuski, Phys. Rev. Lett. 79, 889-892 (1997).

[35] J Ambjorn and R Loll, Nucl. Phys. B **536** (1998) 407, [hep-th/9805108].

[36] J. Ambjorn, A. Dasgupta, J. Jurkiewicz and R. Loll, it A Lorentzian cure for Euclidean troubles, [hep-th/0201104]; J. Ambjorn, J. Jurkiewicz and R. Loll, Phys. Rev. Lett. 85 (2000) 924, [hep-th/0002050]; Nucl. Phys. B610 (2001) 347, [hep-th/0105267]; *Emergence of a 4D World from Causal Quantum Gravity*, [hep-th/0404156]. R. Loll, Nucl. Phys. B (Proc. Suppl.) 94 (2001) 96, [hep-th/0011194]; J. Ambjorn, J. Jurkiewicz, R. Loll and G. Vernizzi, *Lorentzian 3d gravity with wormholes via matrix models*, JHEP **0109**, 022 (2001), [hep-th/0106082]; B. Dittrich (AEI, Golm), R. Loll, *A Hexagon Model for 3D Lorentzian Quantum Cosmology*, [hep-th/0204210]; C. Teitelboim, Phys. Rev. Lett. **50** (1983) 705.

[37] P. Di Francesco, E. Guitter and C. Kristjansen, *Integrable 2D Lorentzian gravity and random walks*, Nucl. Phys. B **567**, 515 (2000) [hep-th/9907084]; P. Di Francesco, E. Guitter and C. Kristjansen, *Generalized Lorentzian gravity in (1+1)D and the Calogero Hamiltonian*, Nucl. Phys. B **608**, 485 (2001) [hep-th/0010259]; P. Di Francesco and E. Guitter, *Critical and Multicritical Semi-Random (1+d)-Dimensional Lattices and Hard Objects in d Dimensions*, J. Phys. A **35**, 897 (2002) [cond-mat/0104383].

[38] J. Ambjorn, B. Durhuus and T. Jonsson: *Quantum Geometery*, Cambridge Monographs on Mathematical Physics, Cambridge University Press, Cambridge, 1997.

[39] R. Sorkin, Phys. Rev. D 12 (1975) 385-396; Err. ibid. 23 (1981) 565.

[40] F. Markopoulou, L. Smolin, [hep-th/0409057]

[41] V.B. Andreichenko, Vi.S. Dotsenko, W. Selke and J.-S. Wang, "Monte Carlo study of the 2D Ising model with impurities", Nucl.Phys.B344 (1990) 531-556.

[42] *"Black Hole Entropy from Loop Quantum Gravity"*, Carlo Rovelli, Physical Review Letter **14**, 3288 (1996); "Loop Quantum Gravity" by Carlo Rovelli, Cambridge University Press 2005.

[43] B. K. Berger, D. M. Chitre, Y. Nutku, V. E. Moncrief, Phys. Rev. D**5**, 2467-2470 (1971); S. W. Hawking, Commun. Math. Phys. **43** (1975) 199; W. Unruh, Phys. Rev. D**14**, 870 (1973); P. Hajicek, Phys. Rev. D**30** 1178 (1984); T. Thiemann and H. A. Kastrup, Nucl. Phys. B**425**, 665 (1994); K. Kuchar, Phys. Rev. D**50**, 3961 (1994).

[44] S. A. Hayward, *'General laws of black hole dynamics'* Phys. Rev. D 49, 6477, (1994).

[45] A. Ashtekar, J. Baez, A. Corichi and K. Krasnov, *"Quantum geometry and black hole entropy,"* Phys. Rev. Lett. **80**, 904 (1998) [arXiv:gr-qc/9710007]. ; A. Ashtekar, J. C. Baez and K. Krasnov, *"Quantum geometry of isolated horizons and black hole entropy,"* Adv. Theor. Math. Phys. **4**, 1 (2000) [arXiv:gr-qc/0005126] ; L. Smolin, *"Linking topological quantum field theory and nonperturbative quantum gravity,"* J. Math. Phys. **36** (1995) 6417. [arXiv:gr-qc/9505028]; K. V. Krasnov, *"Counting surface states in the loop quantum gravity,"* Phys. Rev. D **55**, 3505 (1997) [arXiv:gr-qc/9603025]; K. V. Krasnov, *"On statistical mechanics of gravitational systems,"* Gen. Rel. Grav. **30**, 53 (1998) [arXiv:gr-qc/9605047].

[46] E. Livine et. al. *"Quantum black holes: Entropy and entanglement on the horizon,"* [arXiv:gr-qc/0508085]; E. Livine et. al. *"Reconstructing quantum geometry from quantum information: Area renormalisation, coarse-graining and entanglement on spin networks,"* [arXiv:gr-qc/0603008]; D. R. Terno, *"From qubits to black holes: Entropy, entanglement and all that,"* Int. J. Mod. Phys. D **14**, 2307 (2005) [arXiv:gr-qc/0505068].

[47] O. Dreyer, *"Quasinormal modes, the area spectrum, and black hole entropy,"* Phys. Rev. Lett. **90**, 081301 (2003) [arXiv:gr-qc/0211076]; L. Motl, *"An analytical computation of asymptotic Schwarzschild quasinormal frequencies,"* Adv. Theor. Math. Phys. **6**, 1135 (2003) [arXiv:gr-qc/0212096]; J. Natario and R. Schiappa, *"On the Classification of Asymptotic Quasinormal Frequencies for d–Dimensional Black Holes and Quantum Gravity,"* Adv. Theor. Math. Phys. **8**, 1001 (2004) [arXiv:hep-th/0411267]; M. R. Setare, Class. Quant. Grav. **21**, 1453 (2004) [arXiv:hep-th/0311221]; M. R. Setare, "Area spectrum of extremal Reissner-Nordstroem black holes from Phys. Rev. D **69**, 044016 (2004) [arXiv:hep-th/0312061].

[48] A. Perez, *"Spin foam models for quantum gravity,"* Class. Quant. Grav. **20**, R43 (2003) [arXiv:gr-qc/0301113].

[59] C. Rovelli and L. Smolin, *"Discreteness of area and volume in quantum gravity,"* Nucl. Phys. B **442**, 593 (1995) [Erratum-ibid. B **456**, 753 (1995)]. [arXiv:gr-qc/9411005].

[50] A. Ashtekar and J. Lewandowski, *"Quantum theory of geometry. I: Area operators,"* Class. Quant. Grav. **14**, A55 (1997). [arXiv:gr-qc/9602046]; S. Frittelli, L. Lehner and C. Rovelli, *"The complete spectrum of the area from recoupling theory in loop quantum gravity,"* Class. Quant. Grav. **13**, 2921 (1996) [arXiv:gr-qc/9608043].

[51] J. F. Barbero, *"Real Ashtekar variables for Lorentzian signature space times,"* Phys. Rev. D **51**, 5507 (1995) [arXiv:gr-qc/9410014]; G. Immirzi, *"Real and complex connections for canonical gravity,"* Class. Quant. Grav. **14**, L177 (1997) [arXiv:gr-qc/9612030].

[73] R. Sorkin, Stud. Hist. Philos. Mod. Phys. **36**, 291 (2005); R. Wald, Living Rev. Rel. **4**, 6 (2001).

[53] H. P. Nollert, *"TOPICAL REVIEW: Quasinormal modes: the characteristic 'sound' of black holes and neutron stars,"* Class. Quant. Grav. **16** (1999) R159; K. D. Kokkotas and B. G. Schmidt, *"Quasi-normal modes of stars and black holes,"* Living Rev. Rel. **2** (1999) 2 [arXiv:gr-qc/9909058]; S. Hod, *"Bohr's correspondence principle and the area spectrum of quantum black holes,"* Phys. Rev. Lett. **81** (1998) 4293 [arXiv:gr-qc/9812002]; A. Alekseev, A. P. Polychronakos and M. Smedback, *"On area and entropy of a black hole,"* Phys. Lett. B **574**, 296 (2003) [arXiv:hep-th/0004036].

[54] A. D. Helfer, *"Do black holes radiate?,"* Rept. Prog. Phys. **66**, 943 (2003) [arXiv:gr-qc/0304042].

[55] R. M. Wald, *"The thermodynamics of black holes,"* Living Rev. Rel. **4**, 6 (2001) [arXiv:gr-qc/9912119]; T. Padmanabhan, *"Gravity and the thermodynamics of horizons,"* Phys. Rept. **406**, 49 (2005) [arXiv:gr-qc/0311036].

[85] Bekenstein et. al. *"Spectroscopy of the quantum black hole,"* Phys. Lett. B **360**, 7 (1995) [arXiv:gr-qc/9505012].

[57] L. Smolin, *"Generic predictions of quantum theories of gravity,"* [arXiv:hep-th/0605052]; A. Ashtekar and J. Lewandowski, *"Background independent quantum gravity: A status report,"* Class. Quant. Grav. **21**, R53 (2004) [arXiv:gr-qc/0404018].

[58] F. Markopoulou, *"Towards gravity from the quantum,"* arXiv:hep-th/0604120; J. Ambjorn, J. Jurkiewicz and R. Loll, *"Quantum gravity, or the art of building spacetime,"* arXiv:hep-th/0604212.

[59] C. Rovelli and L. Smolin, *"Discreteness of area and volume in quantum gravity,"* Nucl. Phys. B **442**, 593 (1995) [Erratum-ibid. B **456**, 753 (1995)] [arXiv:gr-qc/9411005];

[60] A. Ashtekar et. al., *"Quantum theory of geometry. I: Area operators,"* Class. Quant. Grav. **14**, A55 (1997). [arXiv:gr-qc/9602046].

[61] Barreira, et. al. *"Physics with nonperturbative quantum gravity: Radiation from a quantum black hole,"* Gen. Rel. Grav. **28**, 1293 (1996) [arXiv:gr-qc/9603064].

[62] M. Bojowald and R. Swiderski, *"Spherically symmetric quantum horizons,"* Phys. Rev. D **71**, 081501 (2005) [arXiv:gr-qc/0410147].

[63] D. Beckman, D. Gottesman, M. A. Nielsen and J. Preskill, Phys. Rev. A **64**, 052309 (2001), B. Schumacher, M. Westmoreland, arXiv.org:quant-ph/0406223.

[64] K. Fredenhagen and R. Haag, *"On The Derivation Of Hawking Radiation Associated With The Formation Of A Black Hole,"* Commun. Math. Phys. **127**, 273 (1990).

[65] K. V. Krasnov, *"Counting surface states in the loop quantum gravity,"* Phys. Rev. D **55**, 3505 (1997) [arXiv:gr-qc/9603025], K. V. Krasnov, *"On statistical mechanics of gravitational systems,"* Gen. Rel. Grav. **30**, 53 (1998) [arXiv:gr-qc/9605047].

[66] V. Husain and O. Winkler, *"Quantum black holes from null expansion operators,"* Class. Quant. Grav. **22**, L135 (2005), V. Husain and O. Winkler, Phys. Rev. D **73**, 124007 (2006) [arXiv:gr-qc/0601082], V. Husain and O. Winkler, Class. Quant. Grav. **22**, L127 (2005) [arXiv:gr-qc/0410125].

[67] B. Dittrich and R. Loll, *"Counting a black hole in Lorentzian product triangulations,"* [arXiv:gr-qc/0506035].

[68] J Ambjorn and R Loll, *"Non-perturbative Lorentzian Quantum Gravity, Causality and Topology Change,"* Nucl. Phys. B **536** (1998) 407, [hep-th/9805108].

[69] M. Ansari and F. Markopoulou, *"A statistical formalism of causal dynamical triangulations,"* Nucl. Phys. B **726**, 494 (2005) [arXiv:hep-th/0505165].

[70] S. Frittelli, L. Lehner and C. Rovelli, *"The complete spectrum of the area from recoupling theory in loop quantum gravity,"* Class. Quant. Grav. **13**, 2921 (1996) [arXiv:gr-qc/9608043].

[71] M. Ansari, *"The action of semi-causality"*, in preparation.

[72] J. Ambjorn, J. Jurkiewicz and R. Loll, *"Dynamically triangulating Lorentzian quantum gravity,"* Nucl. Phys. B **610**, 347 (2001) [arXiv:hep-th/0105267].

[73] R. D. Sorkin, *"Ten theses on black hole entropy,"* Stud. Hist. Philos. Mod. Phys. **36**, 291 (2005) [arXiv:hep-th/0504037].

[74] S. F. Barger, *"Solution to problem 10454, Amenable Numbers"*, Amer. Math. Monthly Vol. 105 No. 4 April 1998 MAA Washington DC.

[75] U. Gerlach, preceding thesis, Phys. Rev. D 14, 1479 (1976).

[76] D. B. Cline, C. Matthey and S. Otwinowski, *"Evidence for a Galactic Origin of Very Short Gamma Ray Bursts and Primordial Black Hole Sources,"* Astropart. Phys. **18**, 531 (2003) [arXiv:astro-ph/0110276]; D. B. Cline, B. Czerny, C. Matthey, A. Janiuk and S. Otwinowski, *"Study of Very Short GRB: New Results from BATSE and KONUS,"* Astrophys. J. **633**, L73 (2005) [arXiv:astro-ph/0510309]; B. J. Carr, *"Primordial Black Holes: Do They Exist and Are They Useful?,"* [arXiv:astro-ph/0511743]; A. Rau, A. v. Kienlin, K. Hurley and G. G. Lichti, *"The 1st INTEGRAL SPI-ACS Gamma-Ray Burst Catalogue,"* Astron. Astrophys. **438**, 1175 (2005) [arXiv:astro-ph/0504357].

[77] P. H. Frampton and T. W. Kephart, *"Primordial black holes, Hawking radiation and the early universe,"*
Mod. Phys. Lett. A **20**, 1573 (2005) [arXiv:hep-ph/0503267]; I. B. Khriplovich and N. Produit, *"Is Radiation of Black Holes Observable?,"* [arXiv:astro-ph/0604003]; G. Bertone, *"Dark matter: The connection with gamma-ray astrophysics,"* [arXiv:astro-ph/0608706]; P. Sizun, M. Casse and S. Schanne, *"Continuum gamma-ray emission from light dark matter positrons and electrons,"* [arXiv:astro-ph/0607374]; F. Ferrer and T. Vachaspati, *"511-keV photons from superconducting cosmic strings,"* Phys. Rev. Lett. **95**, 261302 (2005) [arXiv:astro-ph/0505063]; G. Bertone, A. Kusenko, S. Palomares-Ruiz, S. Pascoli and D. Semikoz, *"Gamma ray bursts and the origin of galactic positrons,"* Phys. Lett. B **636**, 20 (2006) [arXiv:astro-ph/0405005].

[78] C. Barcelo, S. Liberati and M. Visser, *"Towards the observation of Hawking radiation in the Bose-Einstein condensates,"* Int. J. Mod. Phys. A **18**, 3735 (2003) [arXiv:gr-qc/0110036]; S. Hossenfelder, M. Bleicher, S. Hofmann, H. Stoecker and A. V. Kotwal, *"Black hole relics in large extra dimensions,"* Phys. Lett. B **566** (2003) 233 [arXiv:hep-ph/0302247].

[79] Niven et. al., *"An Introduction to the Theory of Numbers"*, 2nd ed., Wiley, NY, 1966, p. 251; S. Ramanujan, *"Irregular numbers"*, J. Indian Math. Soc. 5 (1913) 105-106.

[80] D. A. Buell, *"Binary Quadratic Forms"*. Springer-Verlag, NY, 1989; H. Cohen, *"Course in Computational Alg. No. Theory"*, Springer, 1993, p. 514; P. Ribenboim, *"Algebraic Numbers"*, Wiley, NY, 1972, p. 97.

[81] A. Ashtekar and J. Lewandowski, *"Quantum theory of geometry. I: Area operators,"* Class. Quant. Grav. **14**, A55 (1997). [arXiv:gr-qc/9602046]; S. Frittelli, L. Lehner and C. Rovelli, *"The complete spectrum of the area from recoupling theory in loop quantum gravity,"* Class. Quant. Grav. **13**, 2921 (1996) [arXiv:gr-qc/9608043]; C. Rovelli and L. Smolin, *"Discreteness of area and volume in quantum gravity,"* Nucl. Phys. B **442**, 593 (1995) [Erratum-ibid. B **456**, 753 (1995)]. [arXiv:gr-qc/9411005].

[82] C. Rovelli, *"Black hole entropy from loop quantum gravity,"* Phys. Rev. Lett. **77**, 3288 (1996) [arXiv:gr-qc/9603063].

[83] D. Beckman, D. Gottesman, M. A. Nielsen and J. Preskill, *"Causal and localizable quantum operations,"* Phys. Rev. A **64**, 052309 (2001) [arXiv:quant-ph/0102043]; T. Eggeling, D. Schlingemann, and R. F. Werner, *"Semicausal operations are semilocalizable,"* [arXiv.org:quant-ph/0104027]; B. Schumacher, M. D. Westmoreland, *"Locality and information transfer in quantum operations,"* Quant. Info. Proc. 4, 13 (2005) [arXiv.org:quant-ph/0406223].

[84] R. D. Sorkin, *"Ten theses on black hole entropy,"* Stud.Hist. Philos. Mod. Phys. **36**, 291 (2005)

[85] Bekenstein et. al. *"Spectroscopy of the quantum black hole,"* Phys. Lett. B **360**, 7 (1995) [arXiv:gr-qc/9505012].

[86] S. Hawking, Nature **248**, 30 (1974), S. W. Hawking, Commun. Math. Phys. **43**, 199 (1975).

[87] U. Gerlach, preceding paper, Phys. Rev. D **14**, 1479 (1976).

Bibliography of chapters

Chapter 2:
Mohammad Ansari and Lee Smolin,
"Self-organized criticality in quantum gravity,"
Class. Quant. Grav. **25**, 095016 (2008)
[arXiv:hep-th/0412307].

Chapter 3:
Mohammad Ansari and Fotini Markopoulou,
"A Statistical formalism of causal dynamical triangulations.
Nucl. Phys. B 726: 494-509,2005
[arXiv:hep-th/0505165]

Chapter 4:
Mohammad Ansari,
"Generic degeneracy and entropy in loop quantum geometry."
Nucl. Phys. B 795, 635-644,2008
[arXiv:gr-qc/0603121]

Chapter 5:
Mohammad Ansari,
"Spectroscopy of a canonically quantized horizon."
Nucl. Phys. B 738:179-212, 2007
[arXiv:hep-th/0607081]

Chapter 6:
Mohammad Ansari,
"Area, ladder symmetry, degeneracy, and fluctuations of a horizon"
[arXiv:0711.1879 hep-th]

Index